# COORDINATED REGULATION OF THE SNAIL FAMILY OF TRANSCRIPTION FACTORS BY THE NOTCH AND TGF-β PATHWAYS DURING HEART DEVELOPMENT

by

**KYLE NIESSEN**

B.Sc. Molecular Biology and Biochemistry, Simon Fraser University, 2001

THESIS SUBMITTED IN PARTIAL FULFILLMENT OF
THE REQUIREMENTS FOR THE DEGREE OF

DOCTOR OF PHILOSOPHY

in

THE FACULTY OF GRADUATE STUDIES

(Experimental Medicine)

THE UNIVERSITY OF BRITISH COLUMBIA,
VANCOUVER, BC, CANADA

December 2007

## ABSTRACT

The Notch and TGFβ signaling pathways have been shown to play important roles in regulating endothelial-to-mesenchymal transition (EndMT) during cardiac morphogenesis. EndMT is the process by which endocardial cells of the atrioventricular canal and the outflow tract repress endothelial cell phenotype and upregulate mesenchymal cell phenotype. EndMT is initiated by inductive signals emanating from the overlying myocardium and inter-endothelial signals and generate the cells that form the heart valves and atrioventricular septum. The Notch and TGFβ pathway are thought to act in parallel to modulate endothelial phenotype and promote EndMT. Vascular endothelial (VE) cadherin is a key regulator of cardiac endothelial cell phenotype and must be downregulated during EndMT. Accordingly, VE-cadherin expression remains stabilized in the atrioventricular canal and outflow tract of Notch1-deficient mouse embryos, while activation of the Notch or TGFβ pathways results in decreased VE-cadherin expression in endothelial cells. However, the downstream target gene(s) that are involved in regulating endothelial cell phenotype and VE-cadherin expression remain largely unknown.

In this thesis the transcriptional repressor *Slug* is demonstrated to be expressed by the mesenchymal cells and a subset of endocardial cells of the atrioventricular canal and outflow tract during cardiac morphogenesis. *Slug* is demonstrated to be required for cardiac development through its role in regulating EndMT in the cardiac cushion. Data presented in Chapter 6 further suggests that *Slug*-deficiency in the mouse is compensated for by a increase in *Snail* expression after embryonic day (E) 9.5, which restores EndMT in the cardiac

cushions. Additionally, the Notch pathway, via CSL, directly binds and regulates expression of the *Slug* promoter, while a close *Slug* family member, *Snail* is regulated by the TGFβ pathway in endothelial cells. While Notch does not directly regulate *Snail* expression, Notch and TGFβ act synergistically to regulate *Snail* expression in endothelial cells. It is further demonstrated that *Slug* is required for Notch mediated EndMT, binds to and represses the *VE-cadherin* promoter, and induces a motile phenotype. Collectively the data demonstrate that Notch signaling directly regulates *Slug*, but not *Snail*, expression and that the combined expression of *Slug* and *Snail* are required for cardiac cushion morphogenesis.

## TABLE OF CONTENTS

## LIST OF TABLES

## LIST OF FIGURES

CHAPTER 1



CHAPTER 2



CHAPTER 3



CHAPTER 4

CHAPTER 5



CHAPTER 6

## LIST OF ABBREVIATIONS

| | |
|---|---|
| ActR | activin type receptor |
| AGS | alagille syndrome |
| Alk | activin receptor-like kinase |
| AV canal | atrioventricular canal |
| bHLH | basic helix-loop-helix |
| BMP | bone morphogenetic protein |
| BrdU | 5-bromo-2'deoxyuridine |
| CADASIL | cerebral autosomal dominant arteriopathy with subcortical infarcts and leukoencephalopathy |
| CDK | cyclin dependent kinase |
| ChIP | chromatin immunoprecipitation |
| CIR | CBF1-interacting co-repressor |
| Co-Smad | common smad (Smad4) |
| CSL | CBF1, Suppressor of Hairless, Lag-1, also known as Recombination Signal-Binding Protein 1 for J-Kappa (RBP-Jκ) and C Promoter-Binding Factor 1 (CBF1) |
| CycC | Cyclin C |
| DAPI | 4',6-diamidino-2-phenylindole |
| DAPT | N-[N-(3,5-Difluorophenacetyl-L-alanyl)]-S-phenylglycine *t*-Butyl Ester |
| Dll | delta-like |
| Dlk | delta homology-like |
| DSL | delta/serrate/lag-2 |
| EGF | epidermal growth factor |
| EMT | epithelial-to-mesenchymal transition |
| EndMT | endothelial-to-mesenchymal transformation |
| ESMA | electrophoretic mobility shift assays |
| Ets | v-ets erythroblastosis virus E26 oncogene homolog |
| Fbw | F-box and WD repeat domain containing |
| GFAP | glial fibrillary acidic protein |
| HA | hyaluronic acid |
| HAEC | human aortic endothelial cell |
| HAT | histone acetyltransferase |
| HDAC | histone deacetylase |
| Hes | hairy enhancer of split |
| Hey | hairy/enhancer of split-related with YRPW motif |
| HMEC | human microvascular endothelial cell |
| HUVEC | human umbilical vein endothelial cell |
| ILK | integrin-linked kinase |
| I-Smad | inhibitory smad (Smad6/7) |
| LNR | lin-12/Notch |
| MAML | mastermind-like |
| MESP | mesoderm posterior |
| MH | mad-homology |

| | |
|---|---|
| MMP | matrix metalloproteinase |
| NcoR | nuclear receptor co-repressor |
| NLS | nuclear localization signal |
| Notch1IC | notch1 intracellular domain |
| Notch4IC | notch4 intracellular domain |
| OFT | outflow tract |
| PAK1 | p21-activated kinase |
| PEST | praline-glutamine-serine-threonine |
| RAM | RBP-Jκ-associated molecule |
| R-Smad | receptor smad (Smad1/2/3/5/8) |
| SAP30 | sin3A-associated protein 30kDa |
| SARA | smad anchor for receptor activation |
| shRNA | short-hairpin RNA |
| SMA | smooth muscle α-actin |
| Smad | sma and mothers against decapentaplegic |
| SMRT | silencing mediator of retinoid and thyroid hormone receptors |
| TACE | tumor necrosis factor-α converting enzyme |
| TAD | transactivation domain |
| TGF | transforming growth factor |
| TGFβRI | transforming growth factor beta receptor type I |
| TGFβRII | transforming growth factor beta receptor type II |
| TGFβRII | transforming growth factor beta receptor type III |
| TSS | transcriptional start site |
| VE-cadherin | vascular endothelial cadherin |
| VEGF | vascular endothelial growth factor |
| VEGFR | vascular endothelial growth factor receptor |

## ACKNOWLEDGEMENTS

First and foremost I would like to thank my family, my parents Peter and Dicky Niessen, my sister Sherry Niessen-Kroon, and my partner Kristen McKnight. Their belief in me and my abilities was the motivation I required to complete this thesis. Special thank you to Kristen for reading and contributing to the endless versions of manuscripts and this thesis during my PhD.

I would like to acknowledge all members of the Karsan Lab, both past and present, who have influenced my academic career. Special thank you to YangXin Fu for providing knowledge and technical expertise on the TGFβ pathway, his work contributed to Figures 5.4 and 5.5 of this thesis, to Kristen McKnight and Pavle Vrljicak for providing technical expertise on developmental biology, to Jennifer Baker and Alastair Kyle for technical expertise on data analysis and immunohistochemistry, and to Fred Wong for help with the apoptosis studies, his work contributed to Figure 4.15 of this thesis. Thank you to Bruno Larrivee, Graeme McLean, and Michela Noseda for teaching me laboratory techniques when I first started my PhD. To my graduate committee members, Drs. Pamela Hoodless, Calvin Roskelley, and Gerald Krystal, thank you for your dedication and insight into my research project.

To my research supervisor Dr. Aly Karsan, thank you for bringing me into your lab and providing me with the opportunity to learn and discover. This experience has provided me with an extensive knowledge of both work at the lab bench and the scientific writing process.

Financial support for my graduate career was provided by a Senior Graduate Studentship Award from the Michael Smith Foundation for Health Research.

*Chapter 1*

# INTRODUCTION

## 1.1 The Notch Pathway

### 1.1.1 Notch pathway components

The Notch pathway was first identified in the early 1900's in a *Drosophila* strain characterized by notches in the wing margins. The gene responsible was not identified until 60 years later when a transmembrane receptor "Notch" was cloned in the mid-1980's (Wharton et al. 1985). Since then Notch orthologues have been identified in organisms from *C. elegans* to humans (Mumm and Kopan 2000). In mammals the Notch receptor family consists of four type-I transmembrane receptors (Notch 1 to Notch 4) that regulate cell fate decisions through interaction with Notch ligand expressing cells (Fleming 1998). Decades of research have demonstrated that the Notch pathway regulates cell fate decisions through trans-activation, where a ligand expressing cell (signaling cell) activates a neighboring receptor expressing cell (receiving cell). Activation of the Notch pathway in turn reinforces expression of the ligand in the signaling cell and the receptor in the receiving cell. Trans-activation leads to the processes of lateral-inhibition or boundary formation, where ligand and receptor expressing cells become segregated and adopt unique cell fates (Artavanis-Tsakonas et al. 1999). Cis-interaction of Notch receptors and ligands in the same cell has also been identified, although cis-interactions are non-signaling events and lead to inhibition of the Notch pathway by sequestering the ligand-receptor complexes in the cytoplasm (Li and

Baker 2004; Glittenberg et al. 2006). Notch receptors are translated as a large (~200 to 300 kDa) precursor protein comprising an extracellular, a transmembrane, and an intracellular domain each consisting of numerous protein modification and protein interaction motifs (Figure 1.1) (Fleming 1998). Under certain conditions Notch receptors are capable of being expressed on the cell surface as large unprocessed proteins but more frequently the Notch proteins are processed in the trans-Golgi network by Furin and expressed on the cell surface as noncovalently linked heterodimers (Blaumueller et al. 1997; Bush et al. 2001) (Logeat et al. 1998). Furin cleavage occurs at the S1 cleavage site and generates an extracellular fragment (NotchEC) and an extracellular-transmembrane-intracellular fragment (NotchTM) that is expressed on the cell surface as a noncovalently linked heterodimer stabilized by a $Ca^{2+}$ ion (Blaumueller et al. 1997) (Figure 1.1 and 1.2).

The extracellular domain of the Notch receptor is comprised of 29 to 36 epidermal growth factor (EGF)-like repeats, depending upon the specific Notch receptor, and 3 lin-12/Notch (LNR) motifs (Figure 1.1). The EGF-like motifs are responsible for ligand interaction while the LNR motifs are responsible for preventing receptor activation in the absence of receptor-ligand engagement (Greenwald and Seydoux 1990; Rebay et al. 1991; Rand et al. 2000; Sanchez-Irizarry et al. 2004). The intracellular domain of the Notch receptor is comprised of an RBP-Jκ-associated molecule (RAM) domain, 7 cdc10/ankyrin repeats of which only the C-terminal 6 assume the proper ankyrin fold, and a transactivation domain (TAD) that is present in Notch1, Notch2 and Notch3 (Figure 1.1) (Kurooka et al. 1998; Beatus et al. 2001; Zweifel et al. 2003; Ehebauer et al. 2005; Ong et al. 2006). In addition, there are two nuclear localization signals (NLS), a glutamine-rich stretch, and a

PEST domain in the Notch intracellular domain (Figure 1.1) (Kurooka et al. 1998). The RAM domain is involved in potentiating Notch signaling through interaction with the transcription factor CSL (CBF1, Suppressor of Hairless, Lag-1, also known as Recombination Signal-Binding Protein 1 for J-Kappa (RBP-Jκ) and C Promoter-Binding Factor 1 (CBF1)) (Tamura et al. 1995). The ankyrin repeats are involved in protein-protein interactions including interaction with CSL, however the 7$^{th}$ ankyrin repeat in cooperation with the TAD domain recruits transcriptional activators such as mastermind-like (MAML) and the histone acetyltransferase (HAT) complex (Kurooka et al. 1998; Tani et al. 2001). The PEST domain is involved in regulating the protein half-life of the Notch receptors (Oberg et al. 2001; Fryer et al. 2004). (Figure 1.1)

In mammals there are five well characterized Notch ligands, Jagged1, Jagged2, Delta-like (Dll) 1, Dll3 and Dll4, collectively referred to as the DSL (Delta/Serrate/Lag-2) family (Figure 1.1). There are two additional Notch ligands, F3/contactin (Hu et al. 2003) and Delta homology-like 1 (Dlk1) (Baladron et al. 2005), however these two receptors do not function in a similar manner as the DSL family. F3/contactin is capable of activating Notch receptors but results in downstream signaling independent of CSL (Hu et al. 2003), while Dlk1 has been suggested to block activation of the Notch pathway (Baladron et al. 2005; Nueda et al. 2007).

The DSL family of proteins is itself composed type-I transmembrane proteins, with an extracellular domain comprised of 7 to 16 EGF-like repeats and a DSL domain, which is unique to Notch ligands (Figure 1.1). Jagged1 and Jagged2 have an additional cysteine-rich

domain and a von Willebrand factor Type C domain in the extracellular region (Fleming 1998). The EGF-like repeats are thought to stabilize receptor-ligand interaction while the DSL domain is responsible for Notch receptor activation through interaction with EGF-like repeats 11 and 12 of the Notch receptors (Rebay et al. 1991). The cysteine-rich domain of Jagged ligands is thought to control Notch receptor binding specificity while the von Willebrand factor Type C domain is thought to be involved in ligand dimerization (Fleming 1998). The intracellular regions of the DSL ligands are relatively short. However, Jagged1 and Dll1 contain a PDZ domain, which is thought to be involved in activating downstream signaling through mechanisms that are currently not well understood (Ascano et al. 2003; Six et al. 2003).

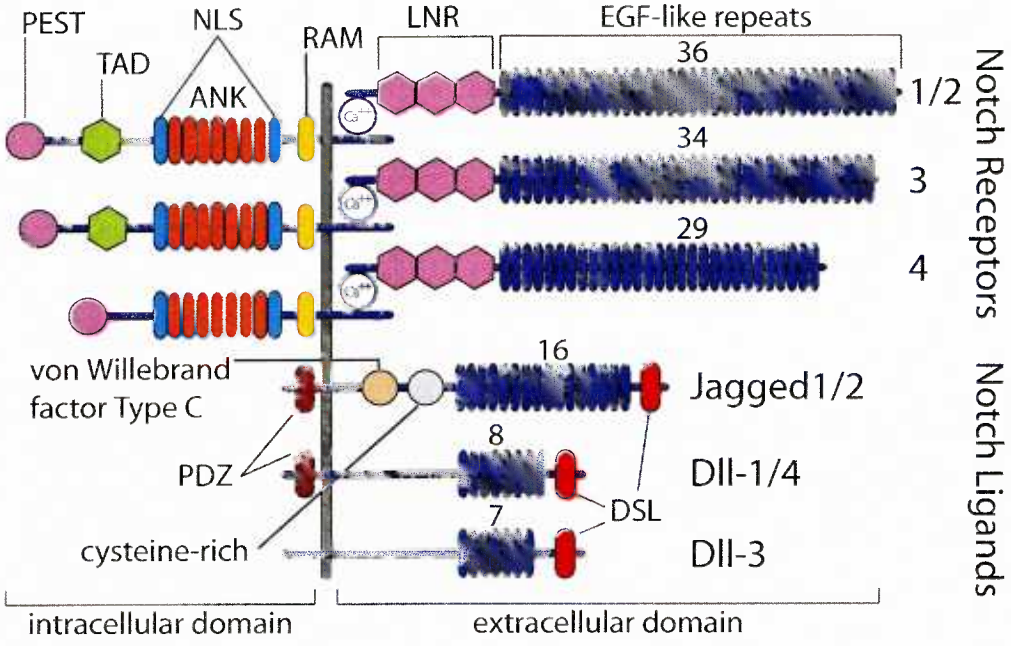


**Figure 1.1 Notch receptors and ligands.**
In mammals there are four Notch receptors (Notch1-4) and five ligands (Jagged1/2, Delta-like (Dll) 1/3/4). Notch receptors are expressed on the cell surface as heterodimers stabilized through calcium dependent interactions. The Notch receptor extracellular domain contains 29-36 epidermal growth factor-like (EGF) repeats involved in ligand binding (human Notch receptors), 3 Lin-12/Notch (LNR) repeats involved in regulating receptor activity, and a heterodimerization domain. The Notch receptor intracellular domain contains an RBP-jκ–associated molecule (RAM) domain involved in interaction with CSL, seven ankyrin (ANK) repeats involved in protein-protein interactions, two nuclear localization signals (NLS), a transactivation (TAD) domain, and a PEST domain involved in protein stability. Notch ligands are also expressed on the cell surface. The Notch ligand extracellular domain contains a Delta/Serrate/Lag2 (DSL) domain involved in receptor activation and is unique to Notch ligands; it also contains multiple EGF repeats involved in receptor-ligand interaction. Jagged1/2 also contains a cysteine-rich domain and a von Willebrand factor Type C domain. The intracellular domains of Jagged1 and Dll1 have also been shown to contain a PDZ domain.

### 1.1.2 Notch receptor-ligand activation

Activation of the Notch pathway by receptor-ligand interaction is a multi-step process that ultimately results in liberation of the active intracellular domain of the Notch receptor. Notch receptor-ligand interaction is thought to result in a conformational change in the Notch extracellular domain exposing the S2 cleavage site, a motif that is recognized and cleaved by the disintegrin-metalloprotease tumor necrosis factor-α converting enzyme (TACE/ADAM17) (Figure 1.2) (Brou et al. 2000). S2 cleavage occurs just extracellular to the plasma membrane, resulting in the release of the Notch extracellular fragment. S2 cleavage is followed by two intramembrane cleavage steps mediated by the γ-secretase complex, comprised of presenilin1, presenilin2, Pen-2, Aph-1, and nicastrin (De Strooper et al. 1999; Struhl and Greenwald 2001; Francis et al. 2002; Hu et al. 2002). The γ-secretase complex has been shown to cleave Notch receptors at two distinct sites, the S4 site between Ala1731-Ala1732 and the S3 site at the conserved Val1744, in the mouse Notch1 protein (Figure 1.2) (Schroeter et al. 1998; Okochi et al. 2002). γ-secretase cleavage ultimately releases the intracellular domain of Notch (NotchICD), which subsequently translocates to the nucleus to effect gene transcription (De Strooper et al. 1999; Okochi et al. 2002) (Figure 1.2). Recently it has been shown that the Notch ligand Dll1 is also cleaved by the γ-secretase complex following receptor-ligand interaction, resulting in the release of the Dll1-intracellular domain (Hiratochi et al. 2007). The Dll1-intracellular domain was further shown to interact with Smad2, Smad3, and Smad4 and enhanced Smad-dependent transcription downstream of the TGFβ pathway (Hiratochi et al. 2007). However, the extent that this pathway is involved in development or disease has not been established.

The most thoroughly investigated downstream component in Notch signaling is the CSL transcription factor. In the absence of NotchICD, CSL recruits either the silencing mediator of retinoid and thyroid hormone receptors/nuclear receptor co-repressor/histone deacetylase 1 (SMRT/NcoR/HDAC1) or the CBF1-interacting co-repressor/histone deacetylase 2/Sin3A-associated protein 30kDa (CIR/HDAC2/SAP30) complex to negatively regulate target gene expression (Kao et al. 1998; Hsieh et al. 1999). Binding of NotchICD to CSL in the nucleus converts CSL from a transcriptional repressor to a transcriptional activator by releasing the repressor complexes and recruiting activator complexes (Hsieh et al. 1996). CSL has been shown to bind preferentially to the consensus sequence defined by (C/T)(A/G)TG(A/G/T)GA(A/G/T) (Pursglove and Mackay 2005), however, most of the identified direct CSL target genes have a less permissive (C/T)(A/G)TGGGAA binding sequence. The basic helix-loop-helix transcription factors hairy enhancer of split (HES) family, comprised of Hes1 through Hes7, and the hairy/enhancer of split-related with YRPW motif (Hey, also called HESR, CHF, Hrt) family, comprised of Hey1, Hey2, and HeyL, are the most thoroughly investigated direct Notch-CSL targets (Davis and Turner 2001; Iso et al. 2002). Other direct targets include *Cyclin D1* (Ronchini and Capobianco 2001), *p21* (Rangarajan et al. 2001), *glial fibrillary acidic protein* (GFAP) (Ge et al. 2002), *Nodal* (Krebs et al. 2003a), *Myc* (Klinakis et al. 2006), *PTEN* (Whelan et al. 2007), *Ephrin B2* (Iso et al. 2006; Grego-Bessa et al. 2007), and *smooth muscle α-actin* (SMA) (Noseda et al. 2006).

The exact composition of transcriptional activators and the temporal sequence of their recruitment to the CSL-NotchICD complex remain to be elucidated. However, it has been demonstrated that the CSL-NotchICD complex includes the Ski interacting protein (SKIP), a protein that can interact with CSL, Notch, or SMRT but promotes NotchICD-CSL interaction over CSL-SMRT interaction (Zhou et al. 2000; Leong et al. 2004). Additionally, the co-activator MAML binds the NotchICD-CSL complex, but is not capable of binding NotchICD or CSL when not in a complex (Petcherski and Kimble 2000; Nam et al. 2003; Nam et al. 2006). MAML itself has transactivation potential and in combination with the NotchICD TAD domain, activates gene transcription (Fryer et al. 2002). The p300-HAT complex is also recruited to NotchICD, which, in cooperation with MAML, is necessary for activation of gene transcription (Fryer et al. 2002) (Figure 1.2).

MAML also negatively regulates NotchICD activity by recruiting the nuclear kinase complex Cyclin C (CycC) and Cyclin dependent kinase 8 (CDK8), which hyperphosphorylate the TAD and PEST domains of NotchICD (Fryer et al. 2004). Phosphorylation of NotchICD at conserved serine residues in the PEST domain by CycC:CDK8 recruits the ubiquitin ligase F-box and WD repeat domain containing 7 (Fbw7/Sel10), resulting in ubiquitin-mediated proteasome degradation (Figure 1.2) (Fryer et al. 2004). Negative regulation of Notch signaling has also been shown to occur by GSK-3β phosphorylation of NotchICD, and ubiquitination of NotchICD by the E3-ubiquitin ligases Itch and c-Cbl, which results in NotchICD degradation (Qiu et al. 2000; Foltz et al. 2002; Jehn et al. 2002; Espinosa et al. 2003).

In addition to the Notch interacting proteins discussed above, Deltex binds the NotchICD ankyrin repeats and positively regulates Notch signaling independent of CSL. The exact mechanism is unclear but involves targeting NotchICD to the late-endosome where it accumulates (Izon et al. 2002; Matsuno et al. 2002; Hori et al. 2004). Other post-translational events also affect various aspects of Notch signaling including receptor and ligand stability (Qiu et al. 2000) and receptor-ligand specificity (Hicks et al. 2000), and have been extensively reviewed but are not within the scope of this thesis (Kadesch 2000; Cayouette and Raff 2002; Haltiwanger 2002; Nickoloff et al. 2003; Hansson et al. 2004).

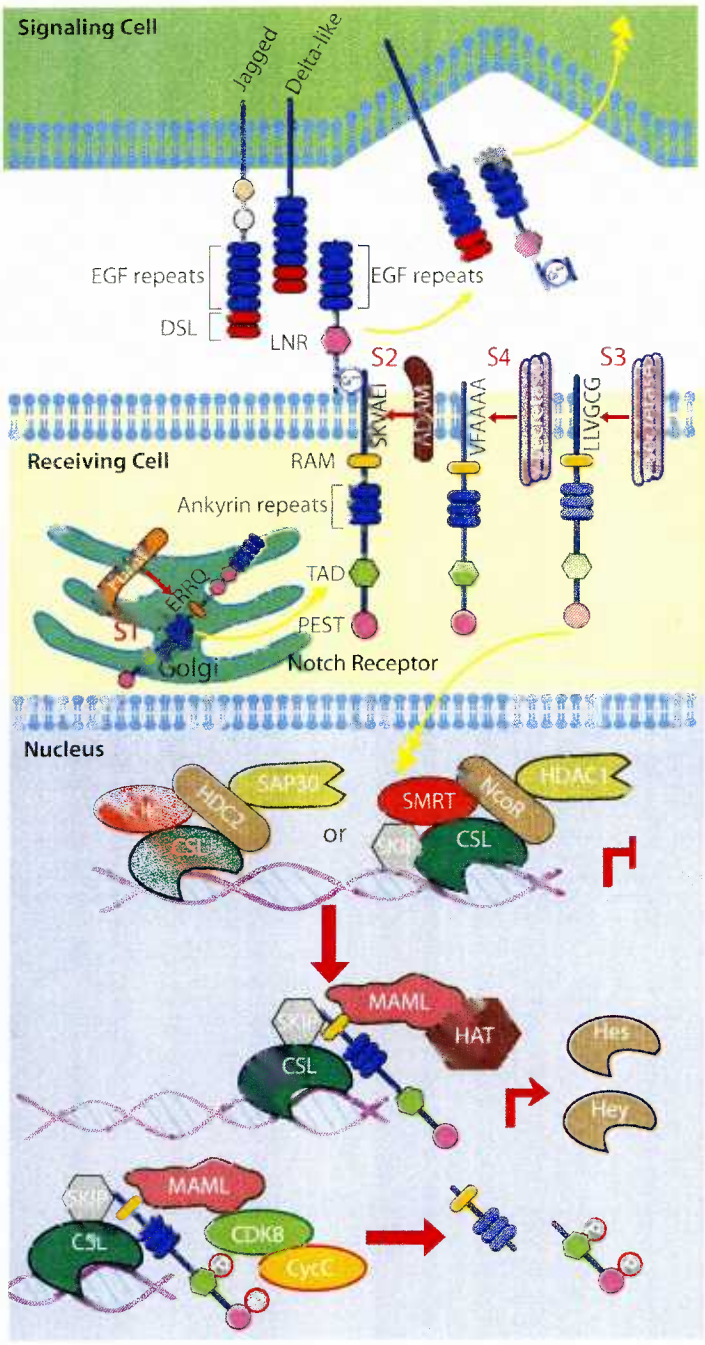


**Figure 1.2 The Notch signaling pathway.**
Notch receptors undergo processing in the trans-Golgi network by Furin and are expressed on the cell surface as a heterodimer. Receptor-ligand interaction results in three additional cleavage events that release the intracellular region of the Notch receptor (NotchICD). The ectodomain of the Notch receptor and the ligand are thought to be endocytosed by the signaling cell. NotchICD then translocates to the nucleus where it binds and converts CSL from a transcriptional repressor to a transcriptional activator of the Hes and Hey family of genes. Notch signaling is negatively regulated by hyperphosphorylation of NotchICD by the nuclear kinase CycC:CDK8 complex, which is recruited by the coactivator MAML. Hyperphosphorylation of NotchICD by CycC:CDK8 complex results in degradation of NotchICD.

## 1.2 The TGFβ Signaling Pathway

### 1.2.1 TGFβ pathway components

The transforming growth factor beta (TGFβ) signaling pathway controls a diverse array of cellular processes and plays a pivotal role during development and cancer progression (Shi and Massague 2003; Massague and Gomis 2006). The TGFβ pathway is comprised of a large superfamily of structurally similar polypeptide ligands, including the TGFβs, the activins, and the bone morphogenetic proteins (BMPs) (Azhar et al. 2003; Feng and Derynck 2005). The TGFβ and BMP class of ligands is of particular importance to this thesis due to their known role in heart development. The TGFβ and BMP ligands are secreted from the cell as latent complexes that undergo processing by proteases such as plasmin (Lyons et al. 1990b), thrombospondin (Schultz-Cherry and Murphy-Ullrich 1993), calpain (Abe et al. 1998), and matrix metalloproteinases (Yu and Stamenkovic 2000) resulting in active signaling molecules that are capable of forming both hetero- and homodimers (Tam and Philip 1998). TGFβ and BMP ligands contain ordered set of six or seven cysteine residues that form three intra-subunit disulfide bonds and one inter-subunit disulfide bond that regulate structural integrity and dimer stability, respectively (Lin et al. 2006a).

The TGFβ family of receptors are single-span transmembrane serine-threonine kinase receptors that are divided into three classes, the type I (TGFβRI), type II (TGFβRII), and type III (TGFβRIII) families. The type I family is comprised of seven receptors, termed the activin receptor-like kinase (ALK)-1 to ALK-7. TGFβRI is characterized by a conserved

TTSGSGSG (GS domain) motif in the cytoplasmic region, which regulates receptor kinase activity (Figure 1.3) (ten Dijke et al. 1993; Tsuchida et al. 1993; ten Dijke et al. 1994; Tsuchida et al. 1996). The type II family is comprised of five receptors, Activin type II Receptor (ActRII) (Mathews and Vale 1991), ActRIIB (Attisano et al. 1992), anti-Mullerian Hormone Receptor type-II (AMHR-II) (Baarends et al. 1994), TGFβ Receptor II (TGFβRII) (Lin et al. 1992), and BMP Receptor II (BMPRII) (Kawabata et al. 1995). While the type III family is comprised of β-glycan (Wang et al. 1991) and Endoglin (Cheifetz et al. 1992). β-glycan and Endoglin are capable of ligand binding, but lack serine-threonine kinase domains, and participate in TGFβ signaling as accessory receptors, presenting ligands to the type I and type II receptors (Lopez-Casillas et al. 1991; Wang et al. 1991). TGFβ receptors primarily exist on the cell surface as homodimers but also have been shown to form heterotetramer complexes comprised of TGFβRI and TGFβRII homodimers (Wells et al. 1999). In the absence of ligand these heterotetramer complexes are not capable of activating downstream signaling (Wells et al. 1999).

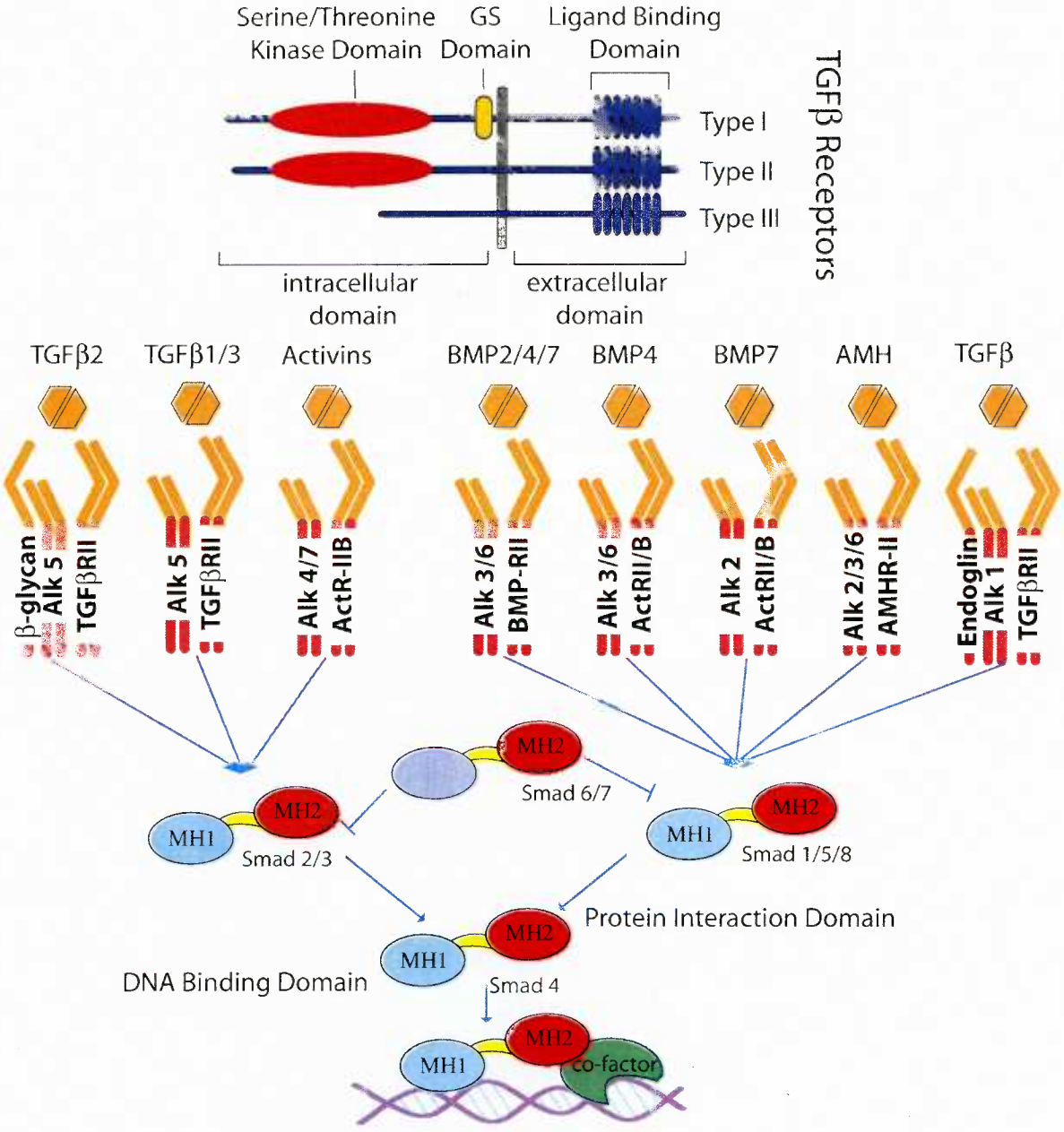


**Figure 1.3 The TGFβ Superfamily.**
The TGFβ receptor family consists of the type I class which has a ligand binding domain, a serine/threonine kinase domain and a GS domain that regulates receptor kinase activity and is unique to the type I class. The type II class lacks a GS domain while the type III class lacks a GS domain and a serine/threonine kinase domain and participates in signaling as an accessory receptor. TGFβ ligands from the TGFβ, activin, and BMP family activate unique receptor complexes consisting of a type I homodimer and a type II homodimer and in some situations a type III accessory receptor. Following receptor-ligand interaction the TGFβ and Activin family of ligands mainly signaling through the Smad2/3 proteins while the BMP family mainly signal though Smad1/5/8. The other Smad proteins are divided into Smad6/7 which are inhibitory Smads and Smad4 which participates in Smad1/2/3/5/8 signaling. The Smad proteins contain two Mad-homology (MH) domains, the MH1 domain is involved in DNA binding while the MH2 domain is involved in protein-protein interactions.

### 1.2.2 TGFβ receptor-ligand activation

TGFβ receptors and ligands are expressed in tissue specific patterns and form unique binding complexes (Azhar et al. 2003; Zavadil and Bottinger 2005; Lin et al. 2006a). These biochemical properties allow for selective activation of one receptor-ligand complex which results in similar but non-overlapping physiological functions (Shi and Massague 2003; Massague and Gomis 2006). Upon receptor-ligand interaction, the formation of a ligand-bound heterotetramer receptor complex, comprised of the ligand and a homodimer of both the TGFβRI and TGFβRII, results in the transphosphorylation of the GS domain of TGFβRI by the TGFβRII (Willis et al. 1996). The phosphorylated-TGFβRI is then capable of phosphorylating the downstream Sma and mothers against decapentaplegic (Smad) proteins (Willis et al. 1996). In humans there are eight Smad proteins, five of which (Smad 1, 2, 3, 5, and 8) act as substrates for the TGFβRI and are collectively referred to as receptor Smads (RSmads) (Chen et al. 1996; Eppert et al. 1996; Hoodless et al. 1996; Lechleider et al. 1996; Liu et al. 1996; Yingling et al. 1996; Zhang et al. 1996; Imamura et al. 1997; Nakao et al. 1997a; Nakao et al. 1997c). The remaining three Smad proteins are divided into Smad4 (co-Smad) which participates with the RSmads in TGFβ signaling (Lagna et al. 1996; Zhang et al. 1996; Kretzschmar et al. 1997), and Smad6 and Smad7 (inhibitory-Smads) which interfere with RSmad signaling (Figure 1.3) (Imamura et al. 1997; Nakao et al. 1997a). Of the five RSmad proteins, Smad 1, 5, and 8 typically function in a receptor complex that contains the BMP and anti-Muellerian receptors while Smad 2 and 3 typically function in a receptor complex that contain the TGFβ and Activin receptors (Figure 1.3) (Baker and

Harland 1996; Hoodless et al. 1996; Liu et al. 1996; Thomsen 1996; Kretzschmar et al. 1997; Nakao et al. 1997b).

Smad proteins consist of two Mad-homology domains (MH1 and MH2) coupled by a linker sequence, except for the inhibitory-Smads which only contain an MH2 domain (Baker and Harland 1996; Liu et al. 1996). The MH1 domain has been shown to be responsible for DNA binding while the MH2 domain is a protein-interaction domain (Figure 1.3) (Baker and Harland 1996; Liu et al. 1996). In the unphosphorylated state the RSmad proteins predominantly exist in the cytoplasm, while Smad4 is distributed throughout the cell (Hoodless et al. 1996; Liu et al. 1996; Pierreux et al. 2000; Inman and Hill 2002). RSmad accumulation in the cytoplasm is the result of cytoplasmic Smad binding proteins, the most well characterized example is the Smad Anchor for Receptor Activation (SARA) protein which binds Smad2 and Smad3 (Tsukazaki et al. 1998). In addition to a Smad interacting domain the SARA protein contains a FYVE phospholipid-binding domain, which targets the SARA/Smad complex to the membrane and promotes interaction with TGFβRI (Tsukazaki et al. 1998; Di Guglielmo et al. 2003). Phosphorylation of Smad2 or Smad3 by TGFβRI results in a decreased affinity of the SARA/Smad complex and its subsequent dissociation (Wu et al. 2001). The phosphorylated RSmad proteins then translocate to the nucleus and at some point, either in the cytoplasm or nucleus, interact with Smad4 which promotes nuclear retention of the RSmad/co-Smad complex (Figure 1.3) (Hoodless et al. 1996; Liu et al. 1996; Inman and Hill 2002).

In the nucleus the RSmad/co-Smad complex is capable of directly binding DNA, however the Smad MH1 domain has low DNA binding affinity and minimal sequence requirements (Shi et al. 1998; Seoane et al. 2004). Therefore, the Smad proteins require other DNA binding co-factors, through interaction with the MH2 domain, to achieve high affinity and to provide sequence specificity (Seoane et al. 2004). Over 45 different Smad binding co-factors have been identified which provide diverse target gene specificity (Feng and Derynck 2005). Depending upon the co-factors involved, formation of the RSmad/co-Smad/co-factor transcriptional complex results in either the activation or repression of target gene expression. For example, Smad 2/3-Smad4 complexes bind the co-factor FoxH1, which then recruits the coactivators p300, CBP, p/Caf to activate *Mix2* expression (Chen et al. 1997; Feng et al. 1998; Itoh et al. 2000). In another situation the Smad3-Smad4 complex binds the co-factor E2F4 or E2F5, which then recruit the corepressor p107 and represses *c-Myc* expression (Chen et al. 2002). Dephosphorylation of the RSmads by PPM1A, for example, results in dissociation of the transcriptional complex and nuclear export of RSmads, effectively terminating signaling (Inman and Hill 2002; Lin et al. 2006b).

### 1.3 Notch and TGFβ Pathway Crosstalk

Until 2003 the Notch and TGFβ pathways were thought to carry out their physiological roles independently from one another, however, in the past several years a series of manuscripts have been published demonstrating an integration of these two pathways (Blokzijl et al. 2003; Dahlqvist et al. 2003; Itoh et al. 2004; Zavadil et al. 2004). These manuscripts demonstrate that components of the Notch pathway act as DNA binding

co-factors for the Smad proteins, and when the TGFβ pathway is activated, regulate genes most commonly considered Notch target genes.

Using a myogenic differentiation model Dahlqvist et al. demonstrated that activation of the BMP pathway, using exogenous BMP4, blocks differentiation of muscle stem cells (Dahlqvist et al. 2003). In this same system, when the Notch pathway was blocked with a chemical γ-secretase inhibitor, BMP4 was no longer capable of blocking muscle stem cell differentiation, suggesting an active Notch pathway is required for the ability of BMP4 to block differentiation (Dahlqvist et al. 2003). It was additionally demonstrated that the intracellular domain of Notch1 and Smad1 physically interact and regulate the Hey1 promoter, a classical Notch target gene (Dahlqvist et al. 2003). The Smad-NotchICD complex was further shown to bind the Hey1 promoter in a region that contains both CSL and Smad binding sites, suggesting DNA binding of both CSL and Smad is involved (Dahlqvist et al. 2003).

Using an endothelial migration model Itoh et al. demonstrated that activation of the BMP pathway, using exogenous BMP6, in confluent endothelial cells resulted in increased *Hey1* expression. Similar to Dahlqvist et al., BMP6 induction of *Hey1* was due to an interaction of Smad1 with the intracellular domain of Notch1 (Itoh et al. 2004). In addition, Itoh et al. demonstrated that the Smad1/Notch1ICD complex requires the Notch pathway component CSL and recruitment of the coactivator p/CAF for stabilization and activation of the *Hey1* promoter (Itoh et al. 2004). These data lead to a model where under conditions without cell-cell contacts (during migration) the Notch pathway is not active and BMP6

activation of Smad1 results in increased migration (Itoh et al. 2004). However, under confluent conditions when the Notch pathway is active, BMP6 activation of Smad1 results in its interaction with the NotchICD/CSL complex and activation of Hey1 expression. Hey1 expression in turn blocks the migratory effects of BMP6 (Itoh et al. 2004).

Using an *in vitro* cell culture system Blokzijl et al. demonstrated that activation of the TGFβ pathway, using exogenous TGFβ1, in C2C12 mouse myoblasts resulted in increased *Hes1* expression, a Notch target gene (Blokzijl et al. 2003). Induction of *Hes1* by TGFβ1 was further shown to be the result of Smad3, but not Smad2, interaction with the Notch1ICD/CSL complex on the *Hes1* promoter (Blokzijl et al. 2003).

While the above three papers demonstrate a physical interaction of the Smad proteins with NotchICD and CSL, Zavadil et al. demonstrated an alternate mechanism for integration of the Notch and TGFβ pathways. In this manuscript it was demonstrated that TGFβ1 treatment of epithelial cells resulted in the upregulation of *Hey1* mRNA and protein expression (Zavadil et al. 2004). It was further demonstrated that a Smad3/4 complex directly binds to a distinct Smad-binding site in the *Hey1* promoter independent of NotchICD or CSL following TGFβ1 treatment (Zavadil et al. 2004). Simultaneously, TGFβ1 treatment resulted in the activation of the ERK MAPK pathway, which in turn resulted in the upregulation of Jagged1 and activation of the Notch pathway (Zavadil et al. 2004). This resulted in a biphasic activation of the Hey1 promoter, the initial direct binding of the Smad3/4 complex to the promoter and a secondary Jagged1/Notch receptor activation of the *Hey1* promoter.

These manuscripts suggest that the Notch and TGFβ pathways functionally interact to regulate Notch target gene expression, through at least two different mechanisms. In the first, BMP4 or BMP6 treatment results in a Smad1-Notch1ICD-CSL complex to regulate *Hey1* expression and TGFβ1 treatment results in a Smad3-Notch1ICD-CSL complex to regulate *Hes1* expression. In the second mechanism, TGFβ1 treatment results in formation of a Smad3/4 complex and an upregulation of Jagged1, both of which activate the *Hey1* promoter independently (Figure 1.4).

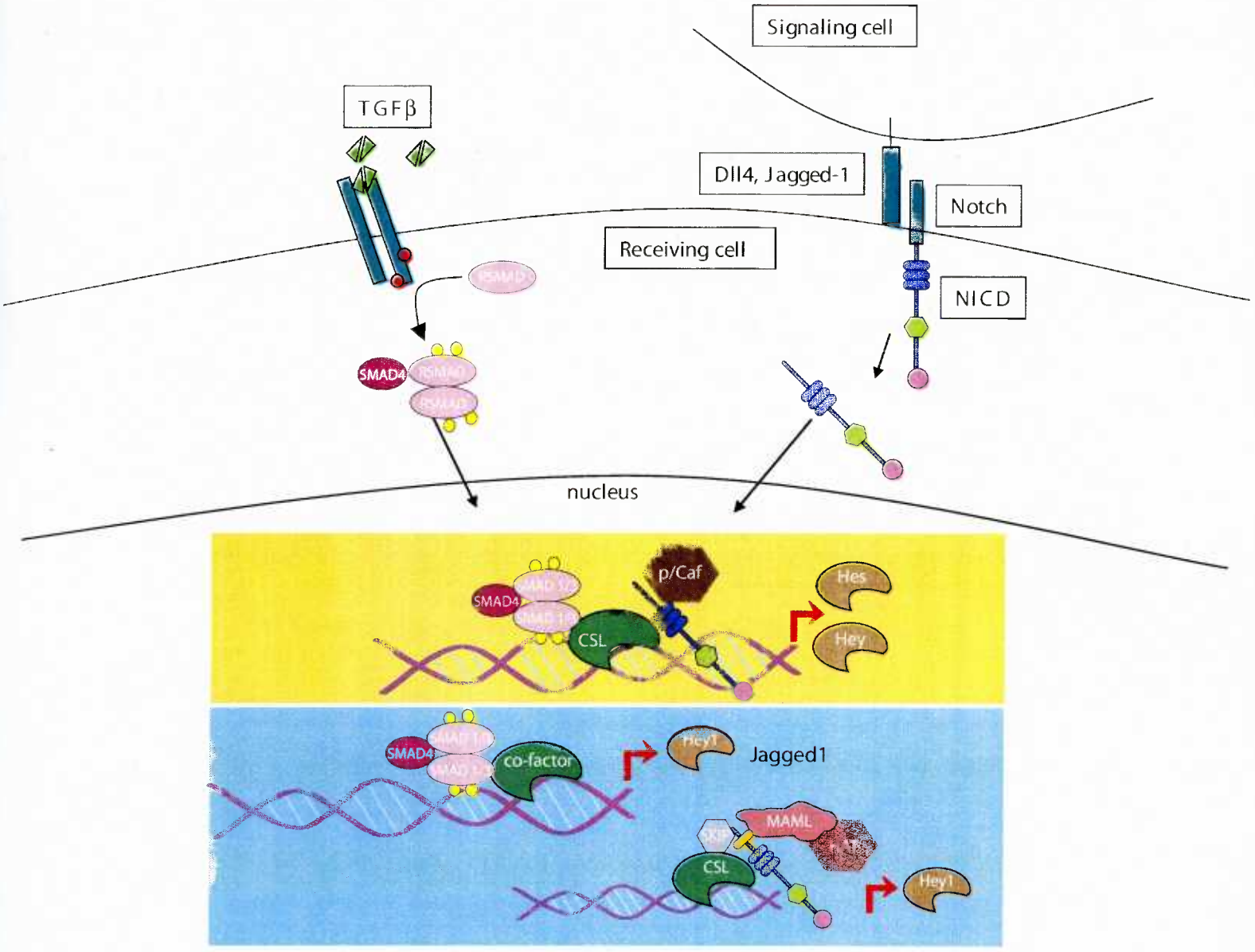


**Figure 1.4 Notch and TGFβ crosstalk.**
The Notch and TGFβ pathways functionally interact to regulate Notch target gene expression. Two mechanisms for co-regulation of Notch target genes has been identified, in the first situation the Smad proteins interact with the Notch\CSL complex and directly activates Notch target gene expression (Yellow box). In the second situation the Smad complex binds to the Hey2 promoter independent of the Notch\CSL complex activating its expression, in addition TGFβ activation results in upregulation of Jagged1 which activates the Notch pathway. Following activation of the Notch pathway by increased Jagged1 expression the Notch pathway directly regulates Hey2 expression independent of the Smad proteins (Blue box).

## 1.4 Snail Family of Transcription Factors

The Snail family of transcription factors was first identified in a mutant strain of *Drosophila* that displayed defects in mesoderm formation. The gene responsible was later identified as *Snail* (Grau et al. 1984). In mammals three Snail family members have been identified, *Snail* (also known as Snai1), *Slug* (also known as Snai2), and *Snai3* (Locascio et al. 2002; Katoh and Katoh 2003). The Snail family of genes encode zinc finger-containing transcriptional repressors that trigger epithelial-to-mesenchymal transition (EMT) during embryonic development and tumour progression by regulating expression of junction proteins, most notably E-cadherin (Nieto 2002). The expression patterns of the Snail family members *Snail* and *Slug* have suggested an inversion in function between chick and mouse (Jiang et al. 1998; Sefton et al. 1998), while the expression pattern of *Snai3* has not been investigated. In the chick, *Slug* is expressed in tissues that require EMT such as the pre-migratory neural crest cells and the primitive streak, while *Snail* is absent from these tissues but expressed in the migratory neural crest cells (Jiang et al. 1998; Sefton et al. 1998). By comparison in the mouse, *Snail* is expressed in the pre-migratory neural crest cells and primitive streak, while *Slug* is absent from these tissues but is expressed in the migratory neural crest cells (Jiang et al. 1998; Sefton et al. 1998). Furthermore, incubation of chick embryos with *Slug* antisense oligonucleotides inhibits neural crest and mesoderm formation, while targeted deletion of the *Snail* gene in the mouse results in embryonic lethality at E8.5, due to defects in mesoderm formation (Nieto et al. 1994; Carver et al. 2001). In comparison, *Slug*-deficient mice are viable and fertile but exhibit defects in pigmentation, palate development, hematopoiesis, and are growth-retarded (Jiang et al. 1998; Inoue et al. 2002;

Murray et al. 2007). These data, and others, have suggested that the role of *Slug* during EMT in the chick is performed by *Snail* in the mouse.

Regulation of Snail family member expression has been linked to several signaling pathways. The TGFβ pathway has been shown to regulate *Snail* expression in hepatocytes, epithelial cells, and during several developmental processes (Spagnoli et al. 2000; Wang et al. 2005). Activation of the FGF pathway has been shown to result in increased *Slug* expression in rat-bladder-carcinoma cells (Savagner et al. 1997), while *FGFR1*-deficiency in the mouse results in the absence of *Snail* expression in the primitive streak during gastrulation (Ciruna and Rossant 2001). In addition, activation of the integrin-linked kinase (ILK) pathway has been shown to result in upregulation of *Snail* in colon carcinoma cells (Tan et al. 2001). During chick heart development *Slug* is a direct target of TGFβ2 signaling (Romano and Runyan 2000). However, due to the possible inversion of function between the chick and mouse it may indicate that *Snail* is the direct target of TGFβ2 in the mouse. Finally, activation of the Notch pathway has been proposed to regulate *Snail* expression in porcine endothelial cells (Timmerman et al. 2004). However, the signaling pathway(s) involved in regulating Snail family expression during mammalian heart development is currently not well understood.

The Snail family of proteins are zinc finger containing transcription repressors that negatively regulate gene transcription by recruiting the Sin3A/HDAC1/2 complex (Peinado et al. 2004). There is not much information regarding structure-function relationship of the Snail family. However, phosphorylation of Snail, at two distinct sites, by GSK-3β results in

its nuclear export and protein degradation, resulting in the inactivation of Snail activity (Zhou et al. 2004; Yook et al. 2005). It is unclear whether Slug contains similar phosphorylation sites or is regulated in a similar manner by GSK-3β. In addition, it has been demonstrated that GSK-3β negatively regulates *Snail* mRNA expression by repressing NFκB activity, suggesting that GSK-3β regulates both *Snail* transcription and Snail protein activity (Bachelder et al. 2005). The p21-activated kinase (PAK1) also has been shown to phosphorylate Snail but, in contrast to GSK3β, PAK1 induces Snail nuclear localization and activity (Yang et al. 2005). Collectively, the Snail family of transcriptional repressors have been demonstrated to be involved in two main processes: first for regulation of adherens and tight junction protein(s) expression, and second as a survival factor (Nieto 2002; Barrallo-Gimeno and Nieto 2005). Regulation of adherens and tight junctions during EMT is critical during multiple stages of development, including gastrulation, neural crest migration, and cardiac development. As discussed above, expression and gene-targeting studies of Snail family members has demonstrated that they play an important role during EMT. Furthermore, during neural crest cell migration Slug and Snail have been shown to be functionally equivalent and promote the formation and migration of neural crest cells (del Barrio and Nieto 2002).

## 1.5 Introduction to Cardiac Development

### 1.5.1 Early cardiac progenitors

The heart is the first functional organ to form during vertebrate development. Based on expression of cardiac markers, cells fated to form the heart are first identifiable in the anterior third of the primitive streak during gastrulation (E7.0) (excluding the node) (Figure 1.5 Yellow and Blue). The transcriptional coactivator *CITED2* is expressed in the primitive streak by the cells that will go on to form the heart, and represents one of the earliest known markers of cardiac progenitors (Schlange et al. 2000). The prospective heart precursors undergo epithelial-to-mesenchymal transition and migrate bilaterally from the primitive streak forming the left and right heart fields, also referred to as the primary heart field (Figure 1.5, E7.5). Formation of the primary heart field is dependent upon expression of the basic helix-loop-helix (bHLH) transcription factors *Mesp1* and *Mesp2* (Kitajima et al. 2000). *Mesp1* and *Mesp2* double-deficient embryos have a specific defect in the development of the cardiac and anterior-cephalic mesoderm (Kitajima et al. 2000). Using *Mesp1*- and *Mesp2*-deficient ES cells in chimeric embryo studies, it was further shown that *Mesp1* and *Mesp2* are redundantly required for EMT and migration of cardiac and anterior-cephalic mesoderm from the primitive streak (Kitajima et al. 2000). In addition, lineage analysis of the *Mesp1* derived cells demonstrated that the majority of cells in the myocardium and endocardium are derived from *Mesp1* expressing mesoderm (Saga et al. 1999; Saga et al. 2000).

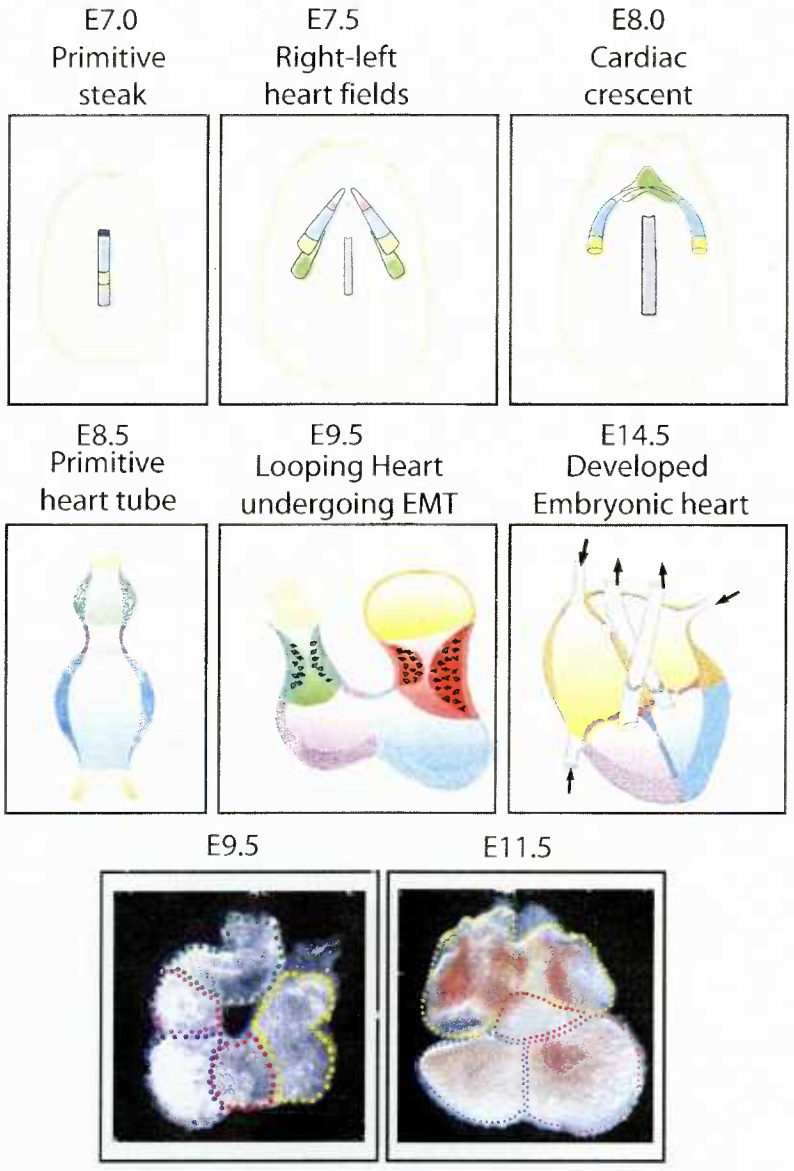


**Figure 1.5 Cardiac development.**
Heart precursors are identifiable in the anterior third of the primitive streak (blue and yellow), but not in the node (dark grey) at the primitive streak stage (E7.0). As embryonic development progresses the heart precursors undergo EMT and migrate bilaterally from the primitive streak forming the left and right primary heart fields (E7.5). The primary and secondary (green) heart fields undergo anterior-medial migration and fusion forming the cardiac crescent (E8.0). The primitive heart tube is formed by fusion of the cardiac crescent at the embryonic midline at E8.5. The primary heart field gives rise to the left ventricle (blue), and atria (yellow), while the secondary heart field give rise to cells of the outflow tract (green) and right ventricle (purple). The heart tube undergoes elongation at the atrial and ventricular ends, and looping to form a C-shaped structure is initiated shortly after formation of the heart tube at E8.5. At E9.5 EndMT is initiated in the AV canal (red) and OFT (green), and the cardiac cushions become cellularized by EndMT. EndMT-derived cells from the AV canal contribute to the membranous atrial septum and mitral and tricuspid valves, while OFT EndMT-derived cells combined with neural crest-derived cells contribute to the aortic and pulmonary valves. Panels at E9.5 and E11.5 represent images of mouse embryonic hearts at the respective stages. Original images can be found at (www.mouseatlas.org/morgen/content).

Cardiac specification involves inductive and repressive cues from all three germ layers. The endoderm underlying the primary heart field plays an important role in specifying the cardiogenic phenotype. Using transplantation studies of mesoderm from a non-cardiogenic source transplanted into the cardiogenic field, Inagaki and colleagues demonstrated that non-cardiogenic mesoderm can be reprogrammed to the cardiac fate (Inagaki et al. 1993). This reprogramming was further shown to be in part due to secreted factors from the endoderm, such as members of the BMP family, sonic hedgehog, fibroblast growth factor (FGF) 8, and Crescent (Brand 2003). In addition to the endoderm, the ectoderm secretes Wnt inhibitors that are required for induction of a cardiogenic fate (Brand 2003).

Even at this early stage (E7.5 in the mouse) in heart development, cell fate analysis reveals that compartmentalization of heart chambers has occurred. Atrial precursors are present in the posterior region and ventricular progenitors in the anterior region of the primary heart field (Figure 1.5) (Redkar et al. 2001). The most frequently used primary heart field markers are *Nkx2.5* (homologue of Drosophila Tinman), *BMP2*, *Tbx20*, *GATA4*, *GATA5* and *GATA6*. Although these markers are expressed in the primary heart field, the exact boundaries of the primary heart field are not precisely delineated by the expression of these genes. The heart field extends both laterally and medially of *Nkx2.5* and *BMP2* expression while *BMP2* expression extends posterior and anterior of the heart field (Redkar et al. 2001).

The cardiac crescent is formed when the right and left heart fields undergo anterior-medial migration, and subsequently fuse at the anterior end (Figure 1.5). Initially all cells of

the cardiac crescent have cardiomyogenic potential, however signals from the prospective myocardium and neurogenic tissue subdivide the cardiac crescent into a ventral myogenic and a dorsolateral nonmyogenic domain (Raffin et al. 2000). The ventral myogenic domain of the cardiac crescent gives rise to the myocardium of the heart tube while the dorsolateral nonmyogenic domain gives rise to the mesocardial and pericardial roof cells (Raffin et al. 2000).

Endocardial precursors are first identifiable at the cardiac crescent stage as a population of $Flk1^{+}/TAL1^{+}$ positive cells distributed throughout the cardiac crescent (Drake and Fleming 2000). Lineage analysis of Mesp1 derived mesoderm reveals that the endocardium is derived from the same mesoderm as the myocardium, thereby demonstrating that the endocardium and myocardium are of the same origin (Saga et al. 1999; Saga et al. 2000). During subsequent development of the embryo the cardiac crescent fuses into a linear tube-like structure that starts beating at E8.0 in the mouse and about 3 weeks of gestation in humans (Figure 1.5) (Sissman 1970).

In addition to the primary heart field, the existence of a secondary heart field has been identified in both the developing chick and mouse heart. The secondary heart field is located in the splanchnic mesoderm that underlies the floor of the caudal pharynx and expresses many of the same markers as the primary heart field such as *Nkx2.5* and *GATA4*, but also expresses unique makers such as *FGF-10* and *Nkx3.1* (Schneider et al. 2000; Kelly and Buckingham 2002). The extent of the contribution of cells from the secondary heart field to the adult heart is not fully understood. In the chick the secondary heart field generates the

smooth muscle cells of the conus and truncus only (de la Cruz et al. 1977; Waldo et al. 2001). In the mouse, cells from the secondary heart field migrate into the arterial pole between E8.25 and E10.5, and in addition to the smooth muscle cells of the conus and truncus, a population of the myocardial cells of the right ventricle are also generated from the secondary heart field (Kelly and Buckingham 2002). (Figure 1.5)

### 1.5.2 Heart looping

The primitive heart tube is composed of an outer myocardial cell layer and an inner endocardial cell layer separated by a layer of extracellular matrix called the cardiac jelly, which is secreted by the myocardial cells. As heart development progresses, the linear heart undergoes several morphological changes that align and fuse the chambers of the heart. Of particular importance to this thesis is the process of endothelial-to-mesenchymal transformation (EndMT). EndMT is involved in formation of the heart valves and membranous septa that divide the heart into chambers which regulate blood flow.

### 1.5.3 Endothelial-to-mesenchymal transformation

Beginning at E9.0, in the mouse, localized acellular swellings of the cardiac jelly appear in the atrioventricular (AV) canal and cardiac outflow tract (OFT) as a result of increased extracellular matrix protein synthesis by the myocardium (Eisenberg and Markwald 1995). The ErbB signaling pathway and hyaluronic acid (HA) play a key role in regulating cardiac jelly formation. HA is a glycosaminoglycan and a key component of the

cardiac jelly (Day and Prestwich 2002). *HA-synthetase (Has) 2*-deficient mice display a complete absence of cardiac jelly formation and subsequent block in EndMT (Camenisch et al. 2000). However, *Has2*-deficiency can be rescued by exogenous addition of the ErbB3 ligand, heregulin, suggesting HA modulates ErbB signaling (Camenisch et al. 2002b). The exact mechanism by which HA regulates ErbB signaling is unknown, however, it is thought to function by regulating ErbB ligand availability (McDonald and Camenisch 2002).

At E9.5 endocardial cells of the AV canal and OFT are activated by signals emanating from the myocardium and by inter-endothelial signaling pathways to undergo EndMT. EndMT is a specific form of epithelial-to-mesenchymal transition required for mesenchymal cell formation from endothelial cells of the endocardium during cardiac cushion development. It is a critical process characterized by phenotypic and morphological alterations resulting in loss of apical-basolateral polarity, disruption of intercellular junctions, and acquisition of the ability to degrade the basement membrane and migrate away from the confines of the endothelial sheet to invade the underlying cardiac jelly. As heart development proceeds, the mesenchymal cells undergo proliferation and the expansion of the cardiac cushions results in their fusion within the lumen of the heart tube, forming the initial septa. In addition to the Notch and TGF-β pathways, the focus of this thesis, the vascular endothelial growth factor (VEGF) pathway is an important regulator of EndMT during heart development. *VEGF* is expressed throughout the endocardium prior to EndMT but becomes restricted to a subpopulation of endocardial cells of the AV canal and OFT endocardium at E9.5 (Miquerol et al. 1999). Enforced expression of VEGF in endocardial or myocardial cells of the AV canal results in excessive endocardial cell proliferation, decreased EndMT, and

delayed cardiac cushion fusion (Miquerol et al. 2000; Dor et al. 2001). These findings suggest that VEGF expression in the subpopulation of endothelial cells is necessary to maintain endothelial phenotype, and VEGF signaling must be blocked for EndMT to occur. Accordingly, we previously demonstrated that activation of the Notch pathway results in EndMT and blocks activation of the VEGF pathway by downregulating expression of VEGF receptor 2 (Noseda et al. 2004).

Following EndMT and subsequent fusion of the cardiac cushion, the very poorly understood process of heart valve remodeling is initiated. Remodeling of the cardiac cushion results in the formation of thin protruding leaflets comprised of endocardial and mesenchymal cells and extracellular matrix protein (ECM) that go on to develop into the heart valves. Of the four mature heart valves, the mitral and tricuspid valves are solely formed from EndMT-derived cells of the AV canal while the aortic and pulmonary valves are formed from EndMT-derived cells of the OFT and neural crest-derived cells. Remodeling is known to involve further differentiation of the mesenchyme to support cells of the mature valve. In addition, an excess of mesenchymal cells are generated by EndMT and through apoptosis the excess mesenchymal cells are eliminated and mature valves are formed. The molecular mechanisms underlying the differentiation and apoptotic processes during cushion remodeling remain largely unknown.

### 1.5.4 Expression of Notch and TGFβ components during heart development

Expression patterns of the Notch and TGFβ pathway components and gain- and loss-of-function studies have revealed critical roles for these pathways in regulating EndMT during heart development. Studies in *Xenopus laevis* have demonstrated that the Notch ligand *Jagged1,* but not *Delta1* or *Delta2*, is expressed in the dorsolateral nonmyogenic domain of the cardiac crescent, while the dorsal-most region of the cardiac crescent myogenic domain expresses both *Jagged1* and *Notch1* in an overlapping pattern (Rones et al. 2000). At the cardiac crescent stage of heart development in the mouse, *Hey1* is expressed in the precursor cells that will give rise to the atria and sinus venosus, while *Hey2* is expressed in the precursor cells that will give rise to the ventricles (Nakagawa et al. 1999). By E11.5 *Hey2* expression becomes restricted mainly to the compact myocardial layer of the ventricles, and *Hey1* expression becomes restricted mainly to the atrial myocardium (Leimeister et al. 1999). Expression of *HeyL* remains unclear. There have been several studies failed to identify *HeyL* expression in the heart, but recently *HeyL* was found to be expressed in the AV canal endocardium at E11.5 (Leimeister et al. 2000; Fischer et al. 2007a). As both Hey1 and Hey2 are direct target genes of Notch signaling, the mechanism by which *Hey1* and *Hey2* become differentially expressed remains to be resolved. In the atrial myocardium there is high expression of *Jagged1*, which could potentially regulate the atrial expression of *Hey1* (Loomes et al. 1999; Villa et al. 2001). However, no Notch receptors have been detected in the chamber myocardium and no Notch ligands have been detected in the ventricular myocardium, suggesting that in this context *Hey1* and *Hey2* may be regulated by a pathway other than Notch (Loomes et al. 1999; Villa et al. 2001). In the mouse *Notch1*, *Notch2*, *Notch4, Jagged1,* and *Dll4* are all expressed in the AV canal and OFT endocardial cells from the onset of EndMT (E9.5) (Loomes et al. 1999; Loomes et al. 2002; Fischer et al. 2007a). At

E9.5 *Hey1/2/L* are also highly expressed at the onset of EndMT in the AV canal endocardial cells (Wang et al. 2005; Fischer et al. 2007a). However, Notch activity and expression of *Hey1/2/L* are not sustained in the AV canal mesenchymal cells, suggesting Notch activity is required for initiation of EndMT, but not for maintaining a mesenchymal phenotype.

The TGFβ ligand *TGFβ1* is expressed by endocardial cells in all chambers of the heart throughout early heart development (Shull et al. 1992). In contrast, *TGFβ2* is exclusively expressed by the myocardium overlying the cardiac cushions of the AV canal and OFT (Dickson et al. 1993). *TGFβ3* is not expressed in the heart until E12.5 when it is expressed by the mesenchymal cells in the cardiac cushions (Molin et al. 2003). The TGFβ2 receptor *β-glycan* is expressed by the endocardial cells of the AV canal and OFT region (Brown et al. 1999), suggesting that TGFβ2 secreted from the myocardium activates a β-glycan-dependent pathway in the underlying endothelial cells. The BMP ligands also are expressed in a manner which suggests their importance during EndMT. *BMP2*, *BMP4*, *BMP5*, *BMP6*, *BMP7* are all strongly expressed by the myocardium overlying the cardiac cushions (Lyons et al. 1990a; Jones et al. 1991; Dudley and Robertson 1997; Solloway and Robertson 1999; Kim et al. 2001). However, *BMP2* displays higher expression in the AV canal myocardium while *BMP4* displays higher expression in the OFT myocardium. The main BMP receptors *Alk2*, *Alk3*, and *BMPRII* are widely expressed with no tissue specific pattern in the heart (Roelen et al. 1997a; Roelen et al. 1997b). Overlapping expression patterns of the Notch and TGFβ components during heart development highlight their potential importance during heart development. Expression pattern of Notch and TGFβ pathway components are summarized in Table 1.

Table 1.1 Expression of Notch and TGFβ pathway components during murine heart development.

| *Notch pathway component* | *Expression pattern* |
|---|---|
| Notch1 | Expressed in the cardiac crescent (E7.5). At E8.0 to E11.5 expression is limited to the entire endocardium and highly expressed in the AV canal and outflow tract endocardium (Williams et al. 1995; Timmerman et al. 2004). |
| Notch2 | Expressed in the AV canal endocardium (E12.5) and the outflow tract (E11.5 and 14.5). Expressed in atrial and ventricular myocardium (E13.5) (McCright et al. 2001; Loomes et al. 2002; McCright et al. 2002). |
| Notch3 | Expressed in the cardiac crescent (E7.5) but not detected after heart tube formation (E8.0) (Williams et al. 1995). |
| Notch4 | Expressed in the endocardium (E10.5) (Noseda et al. 2004). |
| Jagged1 | Expressed in the AV canal and outflow tract endocardium and atrial myocardium (E10.5-E12.5) (Loomes et al. 1999). |
| Jagged2 | Expression has not been analyzed |
| Dll1 | Not expressed in the heart (Bettenhausen et al. 1995) |
| Dll3 | Expression has not been analyzed |
| Dll4 | Expressed in the cardiac crescent (E8.0) and the endocardium from E8.5 onward. Expression is further restricted to the ventricular endocardium after E11.5 (Duarte et al. 2004; Benedito and Duarte 2005). |
| Hey1 | Expressed in the lateral portion of the heart tube (E8.5) and the endocardium and septum transversum (E9.5). Expressed exclusively in the atrial myocardium at E10.5 (Leimeister et al. 1999; Timmerman et al. 2004). |
| Hey2 | Expressed in the anterior portion of the heart tube (E8.5) and the AV canal and OFT endocardium (E11.0). Highly expressed in the subcompact ventricular myocardium (E10.5) (Leimeister et al. 1999; Chin et al. 2000). |
| HeyL | It has been reported that HeyL is not expressed in the embryonic heart (Leimeister et al. 2000), but combined targeting of Hey1 and HeyL results in cardiovascular defects related to EndMT (Fischer et al. 2007b). |
| *TGFβ pathway components* | *Expression pattern* |
| TGFβ1 | Endocardium throughout the heart (Shull et al. 1992) |
| TGFβ2 | AV canal and OFT myocardium from the onset of EndMT (Dickson et al. 1993) |
| TGFβ3 | Epicardium and cardiac cushion mesenchyme after E12.5 (Molin et al. 2003) |
| β-glycan | Endocardium of AV canal and OFT from the onset of EndMT (Brown et al. 1999) |
| BMP2 | Restricted to the AV canal myocardium from the onset of EndMT (Lyons et al. 1990a) |
| BMP4 | Restricted to the OFT myocardium from the onset of EndMT (Jones et al. 1991) |
| BMP5/6/7 | Restricted to the AV canal and OFT myocardium from the onset of EndMT (Dudley and Robertson 1997; Solloway and Robertson 1999; Kim et al. 2001) |

## 1.6 Insights into Cardiac Development from Gain and Loss of Function Studies

### 1.6.1 Prior to EndMT

In *Xenopus laevis* activation of the Notch pathway in the cardiac crescent by Jagged1/Notch1 interaction reinforces *Jagged1* expression in the dorsolateral region and suppresses the myogenic potential of cells residing in this region (Rones et al. 2000). Although Notch activation suppresses myogenic potential, expression of primary heart field markers *Nkx2.5* and *GATA4* are unaffected (Rones et al. 2000). In addition, in *Notch1*- and *CSL*-deficient mouse embryos the heart field specification and the heart tube development appear normal, suggesting Notch acts after the specification of the heart field. (Oka et al. 1995; Souilhol et al. 2006).

Mouse embryos that are null for *CSL* or embryos that are *Notch1*-null and have a *Notch2*-hypomorphic mutation exhibit randomized heart looping and axial rotation defects (Krebs et al. 2003a; Raya et al. 2003). However, this phenotype is not reproduced in Notch1-deficient or Notch2-deficient embryos (Hamada et al. 1999; Krebs et al. 2003a). Additionally, embryos deficient for the Notch ligand, *Dll1*, display randomized heart looping and axial rotation (Krebs et al. 2003a; Przemeck et al. 2003). Defects in heart looping in the *Dll1*-deficient embryos are due to loss or misexpression of *Nodal*, *Lefty2*, and *Pitx2,* which are part of the evolutionarily-conserved signaling cascade that controls left-right morphogenesis. Krebs and colleagues have found that in *Dll1*-deficient embryos *Nodal* and *Lefty2* expression is absent from the left lateral plate mesoderm (LPM), and *Pitx2* expression was randomized in the LPM or not expressed at all (Krebs et al. 2003a). However,

Prezemeck et al. have found that *Nodal* and *Lefty2* expression is absent from only 50% and 25% of *Dll1*-deficient embryos, respectively. In the remaining embryos, *Nodal* and *Lefty2* are expressed in the left, right or both LPM (Przemeck et al. 2003). The specific reasons for the discrepancy between these two groups of investigators remain to be elucidated, but maybe due to the difference in genetic backgrounds of the two *Dll1*-deficient strains. *Nodal* expression appears dependent on two CSL binding sites in a node specific enhancer located -9.5 to -8.7 kb 5' of the *Nodal* gene (Krebs et al. 2003a). In addition, ectopic misexpression of active NotchICD in early zebrafish embryos results in *Nodal* and *Pitx2* expression in the right LPM and ultimately left-right patterning defects (Raya et al. 2003). The above findings suggest that Notch signaling controls left-right patterning of the embryonic heart and controls cardiac cell fate following specification of the heart field.

### 1.6.2 Onset of EndMT and heart valve formation

#### 1.6.2.1 The Notch pathway

The atrioventricular (AV) canal is the first structure that regulates flow of blood between the atria and ventricles, and gives rise to the tricuspid and mitral valves and the atrioventricular septum (Armstrong and Bischoff 2004). When the primitive heart tube forms at E8.0, no identifiable AV canal is present, but as a result of the growth of the heart tube by E9.0, a morphologically identifiable AV canal has developed. As discussed above, the AV canal is comprised of an outer myocardial and inner endocardial cell layer separated by a thin layer of extracellular matrix protein called the cardiac jelly. Commencing at E9.0, localized

swellings of the cardiac jelly in the AV canal form the superior and inferior cardiac cushions, comprised of extracellular matrix protein and glycosaminoglycans secreted by the myocardium (Eisenberg and Markwald 1995).

One of the important processes during AV canal development is the specification of the boundary between the functionally and molecularly distinct AV canal myocardium and the chamber myocardium. The AV canal myocardium does not acquire a high gap-junction density and conductivity as does the atrial and ventricular myocardium, or trabeculation as does the ventricular myocardium. In both the chick and the mouse, the AV canal uniquely expresses both *bone morphogenetic protein (BMP) 2* and the *T-box (Tbx) 2* transcription factor (Zhang and Bradley 1996; Harrelson et al. 2004). Cardiac-specific deficiency of *BMP2* results in AV canal defects, while *Tbx2*-deficiency results in expression of chamber specific myocardial genes in the AV canal (Harrelson et al. 2004; Ma et al. 2005). A series of experiments have further demonstrated that *Tbx2* is a downstream target of the BMP2 signaling pathway (Yamada et al. 2000; Ma et al. 2005). Although *BMP2* and *Tbx2* have been shown to be required for AV canal development, until recently what restricts *BMP2* to the AV canal was unknown.

Previous studies have revealed that both loss- and gain-of-function of the Notch pathway results in defects in AV canal development. The *Notch2*-hypomorphic allele, *Jagged1*-deficient, *Hey2*-deficient, *Hey1/2*-deficient, *Hey1/L*-deficient, *CSL*-deficient, and *Notch1*-overexpressing mice all display defects in some aspect of AV canal development (Oka et al. 1995; Xue et al. 1999; McCright et al. 2001; Gessler et al. 2002; Sakata et al.

2002; Fischer et al. 2004; Souilhol et al. 2006; Watanabe et al. 2006; Fischer et al. 2007a). However, due to the severity of defects in these mutants and the fact that heart defects can be secondary to defects in other embryonic tissues, it has been difficult to ascertain the role of the Notch pathway in AV canal myocardial development. Recently, two reports investigated the downstream molecular mechanisms responsible for the defects observed in the Notch pathway mutants. Both reports demonstrate that the Notch target genes *Hey1* and *Hey2* are critically involved in restricting *BMP2* and *Tbx2* expression to the AV canal (Rutenberg et al. 2006; Kokubo et al. 2007). However, several important differences were reported between the two reports, which will be discussed below.

The first study was mainly conducted in the developing chick heart; which only has two of the four mammalian Notch receptor homologues (*Notch1* and *Notch2*). *Notch2* was found to be the only Notch receptor expressed in the myocardium during chick cardiac development (Rutenberg et al. 2006). The Notch ligand *Jagged1* was found to be initially expressed throughout the heart tube myocardium but as the AV canal developed *Jagged1* expression was lost from the AV canal myocardium (Rutenberg et al. 2006). In contrast, *Jagged2* was found to be solely expressed in the atrial myocardium in an overlapping pattern with *Jagged1* (Rutenberg et al. 2006). The Notch target gene *Hey1* was found to be expressed in both the ventricle and atrial myocardium while *Hey2* was expressed exclusively in the ventricular myocardium (Rutenberg et al. 2006). Based on the expression patterns of Notch pathway components it suggests that a signaling axis comprising Jagged1/2, Notch2, and Hey1/2 may be involved in regulating AV canal boundary formation. To test this hypothesis the Notch pathway was activated by electroporation of a constitutively active

*Notch2* (*Notch2ICD*) or *CSL* (*CSL-vp16*) construct directly into the linear heart tube, at a stage prior to AV canal development. Following AV canal development, by *ex vivo* culture, misexpression of the constitutively active Notch components in the AV canal myocardium resulted in reduced *BMP2* expression (Rutenberg et al. 2006). Furthermore. overexpression of Hey1 or Hey2, by the same method, reduced *BMP2* expression in the AV canal myocardium, suggesting Notch through induction of the Hey genes represses *BMP2* expression (Rutenberg et al. 2006). When the Notch activated (*Notch2IC*) hearts were further analyzed for *Hey1* and *Hey2* expression, it was found that only *Hey1* expression was induced, suggesting Notch2 regulates *Hey1* but not *Hey2* expression during heart development (Rutenberg et al. 2006). Interestingly, neither Notch2IC nor Hey1/2 misexpression induced the expression of atrial or ventricular chamber specific genes in the AV canal, suggesting the specification of the chamber myocardium phenotype is not regulated by Notch but rather that Notch signaling maintains chamber myocardial cell phenotype and represses AV canal myocardial phenotype. These results explain how the chamber myocardium represses *BMP2* or *Tbx2* expression; however, it does not explain why expression of *Jagged1/2* and the *Hey* gene are excluded from the chick AV canal. One hypothesis tested is that BMP2 signaling or Tbx2 directly negatively regulates expression of Notch pathway genes in the AV canal. To investigate this possibility *Tbx2* was missexpressed in the ventricular myocardium, using the same electroporation method. *Tbx2* misexpression resulted in reduced expression of both *Hey1* and *Hey2*, suggesting that a negative regulatory loop exists between Tbx2 and *Hey1/2* expression (Rutenberg et al. 2006). Further analysis of *Tbx2* misexpressing hearts failed to reveal an effect on *Jagged1* expression, suggesting Tbx2 regulates the Notch pathway downstream of receptor-ligand activation (Rutenberg et al. 2006). However, *Notch2*

expression or activation level was not assessed in the *Tbx2* missexpressing heart, thus a direct effect of Notch2 activation cannot be ruled out. This report further demonstrated that *Hey2*-deficient mice have an increased expression zone of *BMP2* in the developing heart (Rutenberg et al. 2006), supporting the findings in the chick that Notch via the Hey genes regulates AV boundary formation by regulating the BMP2/Tbx2 pathway.

The second study was conducted in the developing mouse heart. It had previously been demonstrated that *Hey1* is predominantly expressed in the atrial myocardium while *Hey2* is predominantly expressed in the subcompact layer of the ventricular myocardium (Leimeister et al. 1999). In the mouse, *Notch2* and *Jagged1* are not expressed in the ventricular myocardium as they are in the chick (Hamada et al. 1999; Loomes et al. 1999; McCright et al. 2001; Loomes et al. 2002). Gene targeting studies have revealed that *Hey1* or *HeyL* alone are not required for heart development (Fischer et al. 2004; Fischer et al. 2007a). While the phenotype of *Hey2*-deficient mice is variable, these mice have high mortality in the first weeks after birth due to cardiovascular defects including ventricular septal defects, pulmonic stenosis, AV canal valve irregularities and cardiac hypertrophy (Donovan et al. 2002; Fischer et al. 2004; Kokubo et al. 2004). Further, *Hey1* and *Hey2* double-deficient embryos die at E9.5 due to severe heart defects including a thin ventricular myocardium and lack of arterial differentiation (Fischer et al. 2004), suggesting compensation between Hey family members. When *Hey1*-deficient mouse embryos were analyzed for *BMP2* expression it was found that BMP2 expression extended from the AV canal into the atrial myocardium, while in wild-type embryos BMP2 expression was only detected in the AV canal myocardium (Kokubo et al. 2007). When *BMP2* expression was analyzed in *Hey2*-deficient

or *Hey1/2* double-deficient embryos it also revealed an increase in *BMP2* expression was observed, albeit not in a chamber specific manner (Kokubo et al. 2007). Similar to the results obtain in the *Hey1/2* misexpressing chick hearts, when *Hey1* or *Hey2* was overexpressed in all cells of the cardiac lineage in the mouse there was a reduction in *BMP2* and *Tbx2* expression in the AV canal myocardium (Kokubo et al. 2007). Furthermore, in *Hey1* misexpressing embryos the AV canal is reduced in size; however, a cardiac cushion still forms and EndMT occurs (Kokubo et al. 2007). In *Hey2* misexpressing embryos no AV canal forms and the ventricle is directly fused to the atria (Kokubo et al. 2007). Enforced expression of the Hey genes was accomplished through a *Mesp1*-cre X CAG-lox-CAT-lox Hey1/2 method, where the Hey proteins are overexpressed in all *Mesp1* derived cells. *Mesp1* (aka Mesoderm Posterior 1) is a bHLH-type transcription factor transcription factor expressed in the cardiac mesoderm starting at E7.0, and marks both the myocardial and endocardial lineages of the heart (Saga et al. 1999; Saga et al. 2000). In comparison to the first study, when the regulation of Hey genes was investigated two important differences were reported. Using the same overexpression system described above, when *Tbx2* was misexpressed throughout the mouse heart, expression of *Hey1* or *Hey2* was unaffected (Kokubo et al. 2007), suggesting no negative feedback loop between Tbx2 and the Hey genes exists in the mouse. One possible explanation for this discrepancy is the misexpression of Tbx2 was not accompanied by a necessary co-factor required for repression of the Hey genes in the mouse. A further difference between these two reports involves the regulation of the Hey genes themselves. When *Notch2*-deficient or constitutively-active Notch2 (Notch2ICD) overexpressing embryos were analyzed for the expression of the Hey genes no obvious alteration in Hey gene expression was evident (Kokubo et al. 2007), suggesting Hey gene

expression in the heart is independent of Notch2 signaling in the mouse. However, similar experiments done with overexpression of constitutively active Notch1 (Notch1ICD) in the mouse did result in the induction of *Hey1* and *Hey2* expression and the repression *BMP2* expression in the AV canal myocardium (Watanabe et al. 2006). However, in the Notch1ICD overexpressing embryos, the AV myocardium had undergone trabeculation, raising the possibility that the AV canal myocardium had differentiated into ventricular myocardium (which expresses *Hey2* but not *BMP2*). Taken together these reports suggest that the expression of the Hey genes in the atrial and ventricular myocardium creates a boundary between the AV canal and chamber myocardium. However, whether or not the Notch pathway regulates the Hey genes or whether a negative regulatory loop exists between Tbx2 and the Hey genes remains to be resolved, and may represent species-specific mechanisms.

Following proper AV canal boundary formation, endocardial cells lining the AV canal are activated by signals emanating from the myocardium and by inter-endocardial signaling pathways to undergo EndMT (Armstrong and Bischoff 2004). *Notch1*, *Notch2*, *Notch4*, *Jagged1*, and *Dll4* are all expressed in the AV canal endocardium (Loomes et al. 2002; Benedito and Duarte 2005; Fischer et al. 2007a). In addition, the Notch downstream target genes *Hey1*, *Hey2*, and *HeyL* are all expressed in the AV canal endocardium from the onset of EndMT (Fischer et al. 2007a). Analysis of the active Notch1 (Notch1ICD) revealed high levels of Notch1 activation in the cardiac cushion endocardium while Notch1 activity was not found in the mesenchyme or myocardium (Del Monte et al. 2007). In addition zebrafish injected with constitutively-active Notch1ICD or mice overexpressing Notch1ICD resulted in hypercellular AV canal and enlarged AV valves, suggesting an increase in

endocardial cushion EndMT with ectopic Notch activation (Timmerman et al. 2004; Watanabe et al. 2006). Of the Notch receptors and ligands expressed in the AV canal both *Notch1*-deficient and *CSL*-deficient embryos have previously been demonstrated to have a significant reduction in AV canal EndMT, as determined using an *ex vivo* AV canal explant assay which provides a measure of the degree of EndMT taking place (Timmerman et al. 2004). Analysis of the *Hey2*-deficient and *Hey1/L* double-deficient embryos also revealed a defect in AV canal EndMT using the *ex vivo* AV canal explant assay (Fischer et al. 2007a). Furthermore, when *Hey1/L* double-deficient hearts were analyzed *in vivo* fewer cells were observed in the cardiac cushions (Fischer et al. 2007a). Further analysis of the EndMT defect observed in *Hey2*- or *Hey1/L*-deficient AV canal explants revealed similar numbers of migrating cells that did not maintain a endocardial morphology, however, the migrating cells did not adopt a mesenchymal morphology (Fischer et al. 2007a). This data suggest the initial events of EndMT occurred normally but the migrating cells failed to successfully transdifferentiate into mesenchymal cells. In comparison *Notch1*-deficiency results in defects in the induction of EndMT with fewer cells migrating and the acquisition of mesenchymal morphology (Timmerman et al. 2004; Fischer et al. 2007a). Thus, Notch may regulate the initial downregulation of endocardial morphology and the acquisition of a mesenchymal morphology through different downstream target genes. Further analysis of Notch mutant embryos revealed two possible mechanisms for the defects described. In the *Notch1*-, *Hey2*-, and *Hey1/L*-deficient embryos the EndMT defect was accompanied by decreased *matrix metalloproteinase (MMP) 2* expression (Fischer et al. 2007a). *MMP2*, in addition to other MMPs, is an important regulator of EndMT and is required for the migration and invasion of EndMT generated cells into the cardiac cushion. Furthermore, Notch has been shown to

directly regulate expression of *smooth muscle α-actin*, which is required for cardiac cushion EndMT (Noseda et al. 2006). The second mechanism by which Notch mediates EndMT involves the negative regulation of vascular endothelial (VE) cadherin expression in the AV canal endocardium. VE-cadherin is an endothelial specific adherens junction protein that is necessary for maintaining endothelial integrity (Crosby et al. 2005). The ability of Notch to regulate *VE-cadherin* expression was suggested to involved induction of the *Snail* transcription factor, which is a well known regulator of adherens junction proteins during development and disease (Timmerman et al. 2004). However, in this manuscript the authors may have not accurately identified *Snail* as a Notch target gene due to technical errors, which will be discussed later in this thesis. In this thesis, I will demonstrate that the Snail family member *Slug* is the true Notch target gene. Importantly, there are no reports that have demonstrated that either *Slug* or *Snail* is required for cardiac cushion EndMT in a mammalian system. Signaling cascades involved in AV canal EndMT are summarized in Figure 1.6.

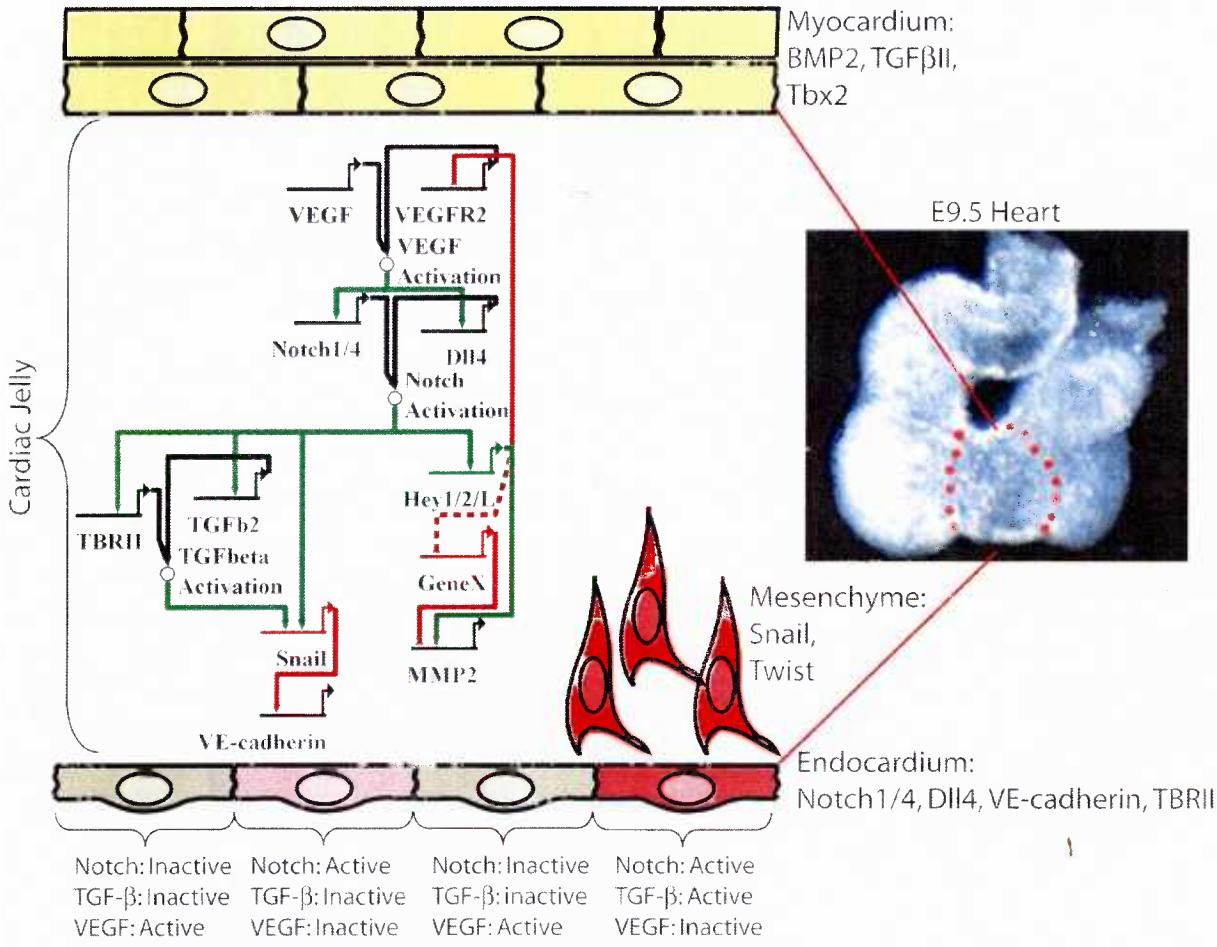


**Figure 1.6 EndMT signaling cascade in the AV canal.**
Initiation of EndMT in the AV canal at E9.5 involves the upregulation of Notch pathway components by activation of VEGF signaling. Upregulation of Notch components in turn activates the Notch pathway resulting in the upregulation of the Notch target genes Hey1/2/L, Snail family member, and components of the TGFβ pathway. Upregulation of Hey1/2/L in turn repress VEGFR2 expression and Hey1/2/L activate MMP2 expression and promote a mesenchymal phenotype. Induction of a Snail family member and activation of the TGFβ pathway then repress VE-cadherin expression and repress endothelial phenotype. This leads to a model where combined activation of the Notch and TGFβ pathways and the inhibition of the VEGF pathway are necessary for AV canal EndMT to occur.

### 1.6.2.2 The TGFβ superfamily

*BMP2*- or *BMP4*-deficiency is lethal prior to cardiac cushion development (Winnier et al. 1995; Zhang and Bradley 1996), while heart development appears normal in *BMP5*-deficient (Kingsley et al. 1992), *BMP6*-deficient (Solloway et al. 1998), and *BMP7*-deficient embryos (Dudley et al. 1995). As discussed above, BMP ligands have overlapping expression patterns during cardiac development and can activate the same receptors, suggesting a potential for compensation between BMP family members during cardiac development. To address the compensation of BMP family members, two different double-targeted mice have been made. *BMP5* and *BMP7* double-deficient mice die at approximately E10.5, unlike the single knockouts which are viable (Solloway and Robertson 1999). Interestingly, the *BMP5/7*-deficient embryos display defects in cardiac cushion development, although it is unclear whether the problem is due to defects in initiation of EndMT, or to the severe developmental delay seen in the mutant embryos (Solloway and Robertson 1999). Similar to the *BMP5/7*-deficient embryos *BMP6* and *BMP7* double-knockout mice die between E10.5 and E15.5, unlike the single knockouts which are viable. (Kim et al. 2001). The *BMP6/7*-deficient embryos die due to cardiac insufficiency with perturbations in heart valve morphogenesis and chamber septation in structures derived from the OFT (Kim et al. 2001). Interestingly, in *BMP6/7* double-deficient embryos structures of the AV canal appears normal, unlike the OFT where there is a decrease in mesenchymal cell numbers (Kim et al. 2001). However, it is unclear whether the cardiac defects in the *BMP6/7*-deficient embryos are due to decreased proliferation of endocardial-derived mesenchymal cells or a decrease in

neural crest derived mesenchymal cells which migrate into the OFT cardiac cushion around E10.5 to E11.0 (Chan et al. 2004).

To further investigate the importance of the BMP ligands during heart development the BMP receptor *Alk2* was selectively deleted in neural crest or endothelial cells. When *Alk2* was deleted from the neural crest cells the resulting mutant embryos resembled the *BMP5/7*- or *BMP6/7*-deficient embryos (Kaartinen et al. 2004), suggesting that the defects in the *BMP5/7*- and *BMP6/7*-deficient embryos are due to defects in the development of neural crest cells that contribute to the OFT. As discussed above, the *Alk2* receptor is expressed in the myocardium, endocardium, and mesenchymal cells of the developing heart (Roelen et al. 1997a). To investigate the role of *Alk2* during AV canal EndMT Wang and colleagues generated an endothelial-specific knockout (Wang et al. 2005). Embryos with endothelial *Alk2*-deficiency display defects of EndMT in the AV canal, which ultimately result in defects in the atrioventricular septa and valves (Wang et al. 2005). Interestingly, unlike the *BMP5/7* or *BMP6/7* double-deficient embryos, structures of the OFT were not affected in the endocardial-specific *Alk2*-deficient embryos, further confirming the additional role of *Alk2*, *BMP6*, and *BMP7* in the neural crest-derived cells in the OFT (Wang et al. 2005). Deletion of the *Alk3* receptor results in embryonic death prior to cardiac development (Gu et al. 1999). However, targeted deletion of *Alk3* in the myocardium of the developing heart results in death at E15.5 due to apoptosis of the myocardium of the ventricular septum and subsequent cardiac failure (Gaussin et al. 2002). Since *Alk3* was deleted in the myocardium in this study the importance of *Alk3* in cardiac cushion EndMT were not observed (Gaussin et al. 2002).

Of the three TGFβ ligands, *TGFβ1*- and *TGFβ3*-deficient mice do not develop cardiac defects, while *TGFβ2*-deficient embryos have hyperplastic AV canal and OFT cushions and heart valves, with no obvious defect in EndMT (Dickson et al. 1993; Sanford et al. 1997; Bartram et al. 2001; Molin et al. 2002; Molin et al. 2003). The phenotype observed in the *TGFβ2*-deficient embryos was further shown to be due to decreased apoptosis during the remodeling of the cardiac cushions, suggesting that an important role of TGFβ2 is in inducing apoptosis during cardiac cushion remodeling (Bartram et al. 2001). In comparison to the *TGFβ2*-deficient embryos, when TGFβ2 activity was blocked using neutralizing antibodies in an *ex vivo* EndMT assay a clear defect in EndMT was evident (Camenisch et al. 2002a). In addition, when activation through the TGFβ2 ligand receptor β-glycan was blocked, using neutralizing antibodies, a similar defect in EndMT was observed (Brown et al. 1999). These findings suggest that the absence of EndMT defects in *TGFβ2*-deficient embryos is the result of other TGFβs or BMPs rescuing EndMT, but that these factors are unable to rescue the critical role TGFβ2 during remodeling of the cardiac cushion. Additionally, embryos deficient for the TGFβ inhibitor *Smad6* have hypercellular cushions due to increased EndMT, as a result of hyperactive TGFβ signaling (Galvin et al. 2000). These data and others have established a clear role for the TGFβ pathway during mammalian heart development.

## 1.7 **Mutations of the Notch Pathway in Human Disease**

### 1.7.1 Aortic valve disease

In humans, mutations in the *Notch1* locus results in a spectrum of heart defects (Garg et al. 2005). The most prevalent malformations are bicuspid aortic valve disease and calcification of the aortic valve (Garg et al. 2005). Calcification of the aortic valve is the third leading cause of heart disease in adults while the presence of bicuspid aortic valve is present in 1-2% of the population (Hoffman and Kaplan 2002). Mutations in the *Notch1* locus result in a premature stop codon in the extracellular domain of Notch1 and is suggested to result in rapid degradation of the mRNA by the nonsense-mediated mRNA decay pathway (Garg et al. 2005). The mechanism by which human Notch1 mutations affect aortic valve calcification is poorly understood. The resulting cardiovascular defects may be due to haploinsufficiency, or alternatively, the premature stop codon could result in the expression of a truncated Notch1 protein that could function as a dominant-negative mutant. These hypotheses have yet to be tested experimentally. However, calcification of the aortic valve is thought to be the result of endothelial dysfunction and Notch pathway components are highly expressed in arterial endothelial cells, which correlate with the importance of the Notch pathway in regulating endothelial function in the aortic valve. Using an *in vitro* system it was demonstrated that Notch1, Hey1 and Hey2 repress the function of the transcription factor Runx2 (Garg et al. 2005). *Runx2* has been linked to valvular calcification in both rabbit and mouse where it regulates expression of several osteogenic genes, such as *osteopontin* and *osteocalcin* (Ducy et al. 1997). It was further suggested that Notch signaling via upregulation of *Hey1* and *Hey2*

result in Hey1 or Hey2 physically interacting with Runx2, thereby inhibiting Runx2 function (Garg et al. 2005). However, it is not known whether *Notch1* mutations found in humans results in lower *Hey1* and *Hey2* expression in the aortic valve, thereby allowing higher Runx2 activity, subsequent expression of osteogenic genes and calcification of the aortic valve.

### 1.7.2 Alagille syndrome (AGS)

Mutations in the *Jagged1* locus are associated with 94% of patients with Alagille syndrome (AGS) (Warthen et al. 2006). In addition, mutations in the *Notch2* locus have been identified in patients with Jagged1-independent AGS (McDaniell et al. 2006). AGS is an autosomal dominant disorder most commonly associated with neonatal jaundice and impaired development of intrahepatic bile ducts, with additional abnormalities of the eye, heart, kidney, and skeleton with variable penetrance. The most common cardiovascular defect in AGS patients is peripheral pulmonic stenosis. In addition, 13% of AGS patients have Tetralogy of Fallot, a condition characterized by ventricular septal defect, overriding aorta, infundibular pulmonary stenosis, and often right ventricular hypertrophy (Krantz et al. 1999; McElhinney et al. 2002; Kamath et al. 2004). In less frequent cases AGS has been associated with other defects of the cardiac cushion (Eldadah et al. 2001; McElhinney et al. 2002). The cardiac AGS phenotype is consistent with the expression pattern of *Jagged1* and Notch receptors in the cardiovascular system. Analysis of mutations in the *Jagged1* locus have revealed, in some cases, complete loss of the *Jagged1* locus, and in other cases inactivating mutations that lead to a misexpressed or truncated Jagged1 protein (Spinner et al.

2001). However, heterozygous mutations in *Jagged1* or *Notch2* do not reproduce the AGS phenotype in mice (Hamada et al. 1999; Xue et al. 1999). *Jagged1*-heterozygote mice display eye defects while *Jagged1*-null mice die at E10 due to vascular defects (Xue et al. 1999). *Notch2*-haploinsufficiency in mice results in kidney defects and myocardial hypoplasia, but the phenotype does not resemble findings of cardiovascular and kidney defects in patients with AGS (Hamada et al. 1999; McCright et al. 2001). However, mice doubly heterozygous for a *Jagged1*-null and a *Notch2*-hypomorphic allele develop jaundice and impaired development of intrahepatic bile ducts with associated abnormalities of the eye, heart, and kidney reproducing an AGS phenotype (McCright et al. 2002). The reason that human *Jagged1* haploinsufficiency results in AGS while in mice there is an additional requirement for *Notch2* insufficiency is unknown. Possible explanations include a higher basal expression of Jagged1 in mice, compensating expression of a Notch ligand or increased avidity of Notch receptor-ligand interaction in the mouse cardiovascular system.

### 1.7.3 Cerebral autosomal dominant arteriopathy with subcortical infarcts and leukoencephalopathy (CADASIL)

CADASIL is an autosomal dominant disorder associated with defects in arterial vascular homeostasis, resulting in increased incidence of stroke, migraine headaches, and mood disturbances (Chabriat et al. 1995; Joutel and Tournier-Lasserve 1998). CADASIL results from a progressive loss of the arterial vascular smooth muscle cells and increased vascular fibrosis leading to narrowing of the lumen of small and medium arteries (Chabriat et al. 1995). CADASIL is histologically characterized by accumulation of granular osmophilic

deposits (GOMs) in the vessel media (Ruchoux et al. 1994; Mayer et al. 1999). Arterial vascular defects seen in CADASIL patients can be systemically found, however, for unknown reasons vascular complications are only found in the brain (Ruchoux et al. 1995).

Missense point mutations in the first 5 EGF repeats in the *Notch3* locus resulting in an odd number of cysteine residues in the EGF repeat regions are found in 95% of CADASIL cases (Joutel et al. 1996; Joutel et al. 1997; Dichgans et al. 2000). The change in the number of cysteine residues from 6 to 5 or 7 in the EGF repeats are thought to result in a conformational change of the EGF repeats leading to accumulation of the ectodomain of the Notch3 receptor. As discussed above, Notch receptors are expressed as a heterodimer on the plasma membrane. In patients with CADASIL there is a specific accumulation of the 210-kDa ectodomain of Notch3 in the vascular smooth muscle plasma membrane in close association but not within the GOMs (Joutel et al. 2000).

The expression of Notch3 is restricted to the vascular smooth muscle cells which correlates with the smooth muscle defects seen in CADASIL. Mutant mice selectively expressing a similar mutation in the EGF repeats of Notch3 (Arg90Cys) in smooth muscle cells, using the SM22α promoter, recapitulate the CADASIL phenotype (Ruchoux et al. 2003). In Notch3-Arg90Cys transgenic mice the CADASIL phenotype requires 10-12 months to develop (Ruchoux et al. 2003). Mutated Notch3 receptors associated with CADASIL are capable of being expressed on the cell surface and binding Notch ligands, suggesting that the phenotype of CADASIL patients are downstream of Notch3 ligand binding (Haritunians et al. 2002). One possible reason for the defect seen in CADASIL is

that the impaired clearance of the Notch3 ectodomain results in a dominant-negative effect by sequestering ligands from the functional Notch3 receptors. In smooth muscle cells Notch3 has been shown to activate survival pathways which if blocked by accumulation of the Notch3 ectodomain could result in the loss of smooth muscle cells observed in CADASIL patients (Wang et al. 2002). However, as discussed above Notch3-deficient mice are viable and fertile with no observed defects in cardiovascular development (Krebs et al. 2003b). A recent manuscript by Monet et al. demonstrated that the Notch3 (Arg90Cys) mutation found in CADASIL patient is still capable of activating the Notch pathway (Monet et al. 2007). In addition, this manuscript demonstrates that even when the Notch3-extracullular domain accumulates on the SMC plasma membrane activation of the Notch pathway is unaffected (Monet et al. 2007). These results suggest that accumulation of the Notch3-extracellular domain and the pathogenesis of CADASIL are not a result of the Notch3-extracellular domain acting in a dominant-negative manner. This suggests that accumulation of the Notch3-extracellular domain may block another pathway or may have a general toxic effect, or result in activation of an alternate signaling pathway, perhaps by preferentially binding a different subset of Notch ligands.

### 1.7.4 Waardenburg syndrome

In humans, mutations in the *Slug* locus result in Waardenburg syndrome (Sanchez-Martin et al. 2002), an autosomal dominant congenital disorder usually involving sensorineural hearing loss and pigmentary abnormalities caused by defects in neural crest development (Read and Newton 1997). Waardenburg syndrome is classified into four types

(WS1-4) depending upon the presence or absence of additional symptoms. WS1 and WS3 are due to mutations in the *Pax3* locus (Tassabehji et al. 1992). While WS2 is heterogeneous and has been shown to be due to mutations in the *Slug* locus (Sanchez-Martin et al. 2002) or *MITF* locus (Tassabehji et al. 1994). WS4 is due to mutations in the *Sox10* (Pingault et al. 1998), *Endothelin3* (Edery et al. 1996) or its receptor *EDNRD* (Puffenberger et al. 1994) locus. Interestingly, Slug expression has been shown to induce *Pax3* expression in neural crest cells in the hindbrain of the chick (del Barrio and Nieto 2002). Hence, reduction of levels of Slug or a Slug-dependent factor (Pax3) is a key component of Waardenburg syndrome. There is also evidence that patients with Waardenburg disease have congenital heart defects, including atrial septal defects, at a rate higher than that of the general population (Banerjee 1986). While this may in part be due to defects of neural crest cells it suggests that Slug may play an additional role in cardiac development.

### 1.8 Aim of the Study

It has been clearly established that the Notch and TGFβ pathways are critically required for EndMT during heart development. However, the downstream target genes responsible for regulating EndMT remain largely unknown. At the start of this thesis, several studies had demonstrated that the TGFβ pathway regulates *Slug* expression in the chick heart (Romano and Runyan 2000), while the Notch pathway regulates *Hey1* and *Hey2* in the mouse heart (Fischer et al. 2004). During the time of this thesis, a manuscript was published demonstrating the Notch pathway regulates expression of *Snail* (Timmerman et al. 2004), which conflicted with preliminary data that I had generated demonstrating Notch signaling

regulated *Slug* but not *Snail* expression. *Snail* and *Slug* belong to the Snail family of transcriptional repressors and have been shown to be involved in regulating epithelial-to-mesenchymal transformation during development and disease (Nieto 2002). Because of the importance of the Notch and TGFβ pathways we wanted to investigate and clarify which Snail family member(s) are regulated by the Notch and TGFβ pathways. The results described in this thesis confirm that the Notch pathway regulates *Slug* expression while TGFβ regulates *Snail* expression in endothelial cells. Interestingly, activation of both the Notch and TGFβ pathways results in synergistic activation of *Snail* expression.

The role of *Snail* or *Slug* during cardiac development has not been established due to the severe phenotype of *Snail*-deficient mice, and apparently normal cardiac phenotype of *Slug*-deficient mice (Jiang et al. 1998; Carver et al. 2001). We were particularly interested in the role of *Slug* due to its connection with Notch signaling. We first investigated the expression pattern of *Slug* during heart development. We next investigated the importance of *Slug* during heart development using the atrioventricular canal explant assay. Finally, we investigated the role of *Slug* in modulating endothelial cell phenotype. These results revealed a critical role for *Slug* in the regulation of EndMT during mouse cardiac cushion development.

Our results demonstrated a critical defect in embryonic heart development in *Slug*-deficient mice, yet no obvious heart defects are observed in *Slug*-deficient adult mice. Given that *Snail* has a similar expression pattern as *Slug* in the heart and very similar function *in vitro* we next investigated whether *Snail* was able to compensate for *Slug*-deficiency. These

studies suggest that *Snail* compensates for *Slug*-deficiency during heart development. The experiments undertaken in this thesis better our understanding of the regulation of the Snail family of transcription factors by the Notch and TGFβ pathways and the mechanisms by which these pathways regulate EndMT during heart development.

# *Chapter 2*

# METHODS AND MATERIALS

## 2.1 Reagents

The mouse monoclonal antibody against the FLAG-(M2) epitope, mouse anti-h1-calponin, and mouse anti-tubulin were purchased from Sigma-Aldrich, St. Louis, MO. Goat anti-VE-cadherin (C-19), rabbit anti-Tie2 (Clone C-20) and goat anti-Slug (Clone G-18) were from Santa Cruz Biotechnology Inc., Santa Cruz, CA. Rabbit anti-Snail and mouse anti-GFP antibodies were from Abcam, Cambridge, UK. Mouse anti VE-cadherin (TEA1/31) was from Beckman Coulter Inc, Fullerton, CA. Rabbit anti-alpha-Smooth Muscle Actin (SMA) was obtained from Lab Vision Corporation, Fremont, CA. Rabbit anti-total Smad1, total-Smad2, and total Smad3 were purchased from Zymed-Invitrogen, Carlsbad, CA. Rabbit anti-phospho-Smad1, phospho-Smad2, and phosphor-Smad3 were purchased from Cell Signaling Danvers, MA. Rabbit anti-goat horseradish peroxidase (HRP), goat anti-mouse HRP, and goat anti-rabbit HRP were from Bio-Rad Laboratories, Hercules, CA. Images were acquired using the MulitiImage$^{TM}$ Light Cabinet with FluorChem$^{TM}$ FC Software (Alpha Innotech Corporation, San Leandro, CA). Human TGFβ1, TGFβ2 and BMP2 were purchased from R&D Systems, Minneapolis, MN.

## 2.2 Cell culture

The HMEC-1 microvascular endothelial cell line, hereafter referred to as HMEC, was provided by the Centers for Disease Control and Prevention (Atlanta, GA) (Ades et al, J

Investig Dermatol 1992). HMEC lines were cultured in MCDB 131 medium (Sigma-Aldrich, St. Louis, MO) supplemented with 10% heat-inactivated calf serum (CS) (HyClone, Logan, Utah), 10 ng/ml of epidermal growth factor (Sigma-Aldrich, St. Louis, MO), and 100 U each of penicillin and streptomycin (Sigma-Aldrich, St. Louis, MO). Human umbilical vein endothelial cells (HUVEC) were isolated as previously described (Karsan et al. 1997), and maintained in MCDB 131 medium supplemented with 10% heat-inactivated fetal calf serum (HyClone, Logan, Utah), 10% heat-inactivated CS, 20 ng/ml endothelial cell growth supplement (BD Bioscience, Bedford, MA), 16 U/ml heparin (Sigma-Aldrich, St. Louis, MO) and 100 U each of penicillin and streptomycin. Human aortic endothelial cells (HAEC) were purchased from Clonetics (BioWhittaker, Inc., Walkersville, MD) and were cultured in EBM media (BioWhittaker, Inc., Walkersville, MD) according to manufacturer's specifications. The retroviral producer cell line AmphoPhoenix was obtained from Dr. Gary Nolan (Stanford University, Pal Alto, CA) and cultured in DMEM (Sigma-Aldrich, St. Louis, MO) supplemented with 10% heat-inactivated CS and 100 U each of penicillin and streptomycin. All cells were maintained at 37°C in 5% $CO_2$.

2.3 Gene transfer

Endothelial cells (HMEC/HAEC/HUVEC) were transduced using the retroviral vectors pLNCX, pLNC-Slug-Flag, pLNC-FLAG-CSL, MIY, MIY-Slug-FLAG, MIY-Notch4IC-HA, MIY-Notch1IC, and MIY-CSL-VP16 as previously described (Karsan et al. 1996; Noseda et al. 2004). Briefly, the retroviral producer cells AmphoPhoenix were seeded to a density of 3 x $10^6$ in a 100 mm plate 24 hour prior to transfection with 6 μg of plasmid

DNA using the Fugene 6 transfection reagent (F. Hoffman-La Roche, Basal, Switzerland). 24 hours after transfection medium was replaced with 7 ml fresh medium and target cells were seeded in 100 mm dishes at the following densities: HMEC 2 x $10^6$, HUVEC 9 x $10^5$, HAEC 1 x $10^6$. 48 hours after transfection the viral supernatant was collected, filtered through a 0.45 μm filter, 8 μg/ml Polybrene (Sigma-Aldrich, St. Louis, MO) was added, and fresh medium was added back to the virus producing cells. Medium on the target cells was then aspirated and replaced with the viral supernatant + polybrene. This procedure was repeated 3 additional times, every 12 hours. Following the last round of infection the medium on the target cells was replaced and cells were allowed to recover for 24 hours. The pLNCX transduced cells were then selected for Neomycin (pLNCX) resistance using 300 μg/ml G418 (Invitrogen, Carlsbad, CA), or the MIY cells were flow sorted for YFP using a FACS-440 flow-sorter (Becton Dickinson Inc, Franklin Lakes, NJ). pcDNA3-Slug-FLAG cDNA was a generous gift from Dr. Eric R. Fearon, The University of Michigan Heath Systems.

## 2.4 Immunoblotting

For immunoblotting, cells were lysed in RIPA buffer (PBS, 1.0% NP-40 (Sigma-Aldrich, St. Louis, MO), 0.5% sodium deoxycholate (Sigma-Aldrich, St. Louis, MO), 0.1% SDS (Sigma-Aldrich, St. Louis, MO)) with addition of fresh protease inhibitor cocktail (F. Hoffman-La Roche, Basal, Switzerland). 50 μg of total protein, as measured using Bio-Rad DC Protein Assay System (Bio-Rad Laboratories, Hercules, CA), were analyzed by sodium dodecyl sulfate-polyacrylamide gel electrophoresis, transferred to nitrocellulose membranes (Bio-Rad Laboratories, Hercules, CA), and developed by enhanced chemiluminescence

(PerkinElmer Life Sciences, Boston, MA). Membranes were probed using the following dilutions of antibodies: 1:10000 mouse anti-FLAG-M2, 1:5000 mouse anti-h1-calponin, 1:10000 mouse anti-tubulin, 1:2000 goat anti-VE-cadherin, 1:1000 rabbit anti-Tie2, 1:1000 goat anti-Slug, 1:1000 rabbit anti-Snail, 1:10000 rabbit anti-goat HRP, 1:10000 goat anti-rabbit HRP, and 1:10000 goat anti-mouse HRP.

2.5 RNA Collection and RT-PCR

RNA was isolated using TRIzol Reagent (Invitrogen, Carlsbad, CA) coupled with Phase-Lock gels (Qiagen Inc., Mississauga, ON) and quantitated by spectrophotometry. 2.5 μg of total RNA was DNAse treated (Invitrogen, Carlsbad, CA) and converted to 1$^{st}$ strand cDNA using SuperScript®II in a 50 μl reaction volume (Invitrogen, Carlsbad, CA). PCR was performed using 2 μl of cDNA on a PTC-200 PCR cycler (Bio-Rad Laboratories, Hercules, CA) or Applied Biosystems 7900HT (Applied Biosystems, Foster City, CA) with the following primers: Table 2.1.

**Table 2.1 – List of Primers**
**Human RT-PCR and qRT-PCR**

| | |
|---|---|
| Human GAPDH Forward | GCA AAT TCC ATG GCA CCG T |
| Human GAPDH Reverse | TCG CCC CAC TTG ATT TTG G |
| Human Snail Forward | CCT CAA GAT GCA CAT CCG AAG CCA |
| human Snail Reverse | AGG AGA AGG GCT TCT CGC CAG TGT |
| Human Slug Forward | AGA TGC ATA TTC GGA CCC AC |
| Human Slug Reverse | CCT CAT GTT TGT GCA GGA GA |
| Human Tie2 Forward | CCA TGA AGA TGC GTC AAC AAG |
| Human Tie2 Reverse | GTC TGG GAG ACA GAA CAC ATA AGA C |
| Human CD31 Forward | CCC AGC CCA GGA TTT CTT AT |
| Human CD31 Reverse | ACC GCA GGA TCA TTT GAG TT |
| Human VE-cadherin Forward | CAG CCC AAA GTG TGT GAG AA |
| Human VE-cadherin Reverse | TGT GAT GTT GGC CGT GTT AT |

**Table 2.1 – List of Primers**

| | |
|---|---|
| Human CBF1 Forward | CTC AGG AAC AAA GGT GGC TCT G |
| Human CBF1 Reverse | GGA GTG CCA TGC CAG TAA CTG |
| Human Hey1 Forward | AGA GTG CGG ACG AGA ATG GAA ACT |
| Human Hey1 Reverse | CGT CGG CGC TTC TCA ATT ATT CCT |
| Human Hey2 Forward | TTG AAG ATG CTT CAG GCA ACA GGG |
| Human Hey2 Reverse | TCA GGT ACC GCG CAA CTT CTG TTA |
| Human HeyL Forward | ATG CAA GCC AGG AAG AAA CGC AGA |
| Human HeyL Reverse | AGC TTG GAA GAG CCC TGT TTC TCA |
| Human Smad7 Forward | GCC CTC TCT GGA TAT CTT CT |
| Human Smad7 Reverse | GCT GCA TAA ACT CGT GGT CA |
| Human Smad6 Forward | GTG AAT TCT CAG ACG CCA GCA TGT |
| Human Smad6 Reverse | TGC CCT GAG GTA GGT CGT AGA AGA T |
| **Mouse qRT-PCR** | |
| Mouse Snail Forward | TCT GAA GAT GCA CAT CCG AAG CCA |
| Mouse Snail Reverse | AGG AGA ATG GCT TCT CAC CAG TGT |
| Mouse Slug Forward | AGA TGC ACA TTC GAA CCC AC |
| Mouse Slug Reverse | GTC TGC AGA TGA GCC CTC AG |
| Mouse Hey1 Forward | CAC GCC ACT ATG CTC AAT GT |
| Mouse Hey1 Reverse | TCT CCC TTC ACC TCA CTG CT |
| Mouse Hey2 Forward | TTC TGT CTC TTT CGG CCA CT |
| Mouse Hey2 Reverse | TTT GTC CCA GTG CTT GTC TG |
| Mouse GAPDH Forward | TGC AGT GGC AAA GTG GAG AT |
| Mouse GAPDH Reverse | TTT GCC GTG AGT GGA GTC ATA |
| **ChIP Primers** | |
| ZNF3 Forward | AAT CAG CCT GGG TGA CAA GAG TGA |
| ZNF3 Reverse | TCT CTA GAG CCA GCC TTT GCT GTT |
| Slug (-846) Forward | CAG GAA ACT GGT AGA TAC TGA GAT GG |
| Slug (-846) Reverse | TTG GAA CCA CCG GAC ATT CTC TCA |
| Slug (-1679) Forward | AGA CTG TGT AGA GTG AAA CAA GG |
| Slug (-1679) Reverse | TCT CCA CAC ACA AAC TGG AAC CTG |
| **EMSA Primers** | |
| Slug-EMSA-1700 Forward | TGT GTG TTT TGT GGG AAA TGG AG |
| Slug-EMSA-1700 Reverse | CTC CAT TTC CCA CAA AA |
| Slug-EMSA-1700 Forward Mutant | TGT GTG TTT TGT GCT GCA TGG AG |
| Slug-EMSA-1700 Reverse Mutant | CTC CAT GCA GCA CAA AA |
| Slug-EMSA-900 Forward | GGC CCT TTT TCC CAT AAA AAA A |
| Slug-EMSA-900 Reverse | GGT TTT TTT ATG GGA AAA AGG G |
| Slug-EMSA-900 Forward Mutant | GGC CCT TTG CAG CAT AAA AAA A |
| Slug-EMSA-900 Reverse Mutant | GGT TTT TTT ATG CTG CAA AGG G |
| VE-cadherin-EMSA-97 Forward | GGG CCA GGG CCA GCT GGA AAA CCT GA |
| VE-cadherin-EMSA-97 Reverse | TCA GGT TTT CCA GCT GGC CCT GG |
| VE-cadherin-EMSA-97 Forward Mutant | GGG CCA GGG CAA GCT AGA AAA CCT GA |
| VE-cadherin-EMSA-97 Reverse Mutant | TCA GGT TTT CTA GCT TGC CCT GG |

**Table 2.1 – List of Primers**

| | |
|---|---|
| VE-cadherin-EMSA-234 Forward | GGG GTG ATG ACA CCT GCC TGT AGC AT |
| VE-cadherin-EMSA-234 Reverse | GGA ATG CTA CAG GCA GGT GTC ATC AC |
| VE-cadherin-EMSA-234 Forward Mutant | GGG GTG ATG AAA CCT ACC TGT AGC AT |
| VE-cadherin-EMSA-234 Reverse Mutant | GGA ATG CTA CAG GTA GGT TTC ATC AC |
| VE-cadherin-EMSA-379 Forward | GGG GTG ATG ACA CCT GCC TGT AGC ATT |
| VE-cadherin-EMSA-379 Reverse | GGA ATG CTA CAG GCA GGT GTC ATC A |
| VE-cadherin-EMSA-379 Forward Mutant | GGG GTG ATG AAA CCT ACC TGT AGC ATT |
| VE-cadherin-EMSA-379 Reverse Mutant | GGA ATG CTA CAG GAA GGT TTC ATC A |
| **Site Directed Mutagenesis Primers** | |
| VE-cadherin-44 Forward Mutant | AGT GGG CCA GGG CAA GTT AGA AAA CCT GCC |
| VE-cadherin-44 Reverse Mutant | AGG CAG GTT TTC TAA CTT GCC CTG GCC CAC |
| VE-cadherin-341 Forward Mutant | AGT GGG GGA TAT GAA ACC TAC CTC CCA GGG |
| VE-cadherin-341 Reverse Mutant | ATC CCT GGG AGG TAG GTT TCA TAT CCC CCA C |

2.6 Phase Contrast and Immunofluorescent Imaging

Light micrographs were taken with a Nikon COOLPIX 990 on a Nikon Eclipse TS100 standard inverted microscope. (Nikon Corporation, Tokyo Japan). For immunofluorescence staining, cells plated at a density of 1.5 x $10^5$ cells on a 4-well chamber slide (BD Biosciences, San Jose, CA), cells were allowed to attach and grow until confluent, approximately 48 hours. The cells were fixed in 4% paraformaldehyde (Sigma-Aldrich, St. Louis, MO), and blocked/permeablized in 4% FBS + 0.2% TritonX-100 (Sigma-Aldrich, St. Louis, MO) in PBS. Rabbit anit-VE-cadherin and mouse anti-GFP were used at a dilution of 1:100 and the secondary antibodies were goat anti rabbit-Alexa-594 or goat anti-mouse-Alexa-488 conjugated antibodies used at a dilution of 1:300 (Molecular Probes, Eugene,

OR). Images were acquired using a 1350EX cooled CCD digital camera (QImaging, Burnaby, BC) on a Zeiss Axioplan II Imaging microscope (Carl Zeiss Canada Ltd, Toronto, ON) and analyzed using Northern Eclipse Image Analysis Software (Empix Imaging, Mississauga, ON).

## 2.7 Luciferase Reporter Assay

HMEC ($8 \times 10^4$) were plated 24 hours prior to transfection in 24 well plates, cells were transfected using SuperFect reagent (Qiagen Inc., Mississauga, ON), with 0.3125 μg of total plasmid DNA using manufacturer's recommendations. Each well was transfected with 0.3 μg of the pGL3-VE-cadherin promoter or mutant VE-cadherin promoter constructs 5 ng pcDNA3 or pcDNA3-Slug-Flag, and 7.5 ng pRL-CMV (Promega, Madison, WI). The transfected cells were analyzed 24 hours after transfection using the dual-luciferase reporter assays according to manufacturer's recommendations (Promega Corporation, Madison, WI) and luminescence was measured on a Lumat LB 9507 (EG&G Berthold, Bad Wildbad, Germany). Briefly, transfected cells were washed once with PBS then lysed in 40 μl 1X Passive Lysis Buffer (Promega Corporation, Madison, WI) for 20 min, followed by one freeze-thaw cycle to ensure compete lysis. Then in a 5 ml glass tube 50 μl of *firefly* luciferase substrate (LARII) and 10 μl of protein were mixed and luminescence activity was measured for 15 seconds. The firefly luciferase activity was then quenched and the *renilla* luciferase activity was measure using 50 μl *renilla* luciferase substrate (Stop-and-Glo) for 15 seconds. The *firefly* luciferase activity (VE-cadherin promoter) was then normalized to the *renilla* luciferase (transfection control) activity.

## 2.8 Electrophoretic Mobility Shift Assays (EMSA)

*In vitro* translated Slug-FLAG or luciferase protein (TNT® T7 Quick Coupled transcription and translation system, Promega, Madison, WI) was incubated with 150,000 cpm $^{32}$P-labeled double-stranded oligonucleotides for 30 minute at room temperature. For supershift controls the *in vitro* translated proteins were pre-incubated with 12 μg FLAG-M2 antibody overnight at 4°C in 12 mM HEPES-pH7.9, 4 mM Tris-pH7.9, 133 mM KCl, 10% Glycerol, 2 μg PolydI-dC (Sigma-Aldrich, St. Louis, MO) binding buffer and for competition assays 50-fold excess non-radioactive duplex oligos were pre-incubated for 15 min on ice, followed by $^{32}$P-labeled double-stranded oligonucleotides for 30 minute at room temperature. Binding reactions were run on 5% Tris-borate EDTA gels and exposed to a phosphor-imager plate for 12-16 hours. For CSL EMSA assays, nuclear lysates were collected from FLAG-CSL overexpressing HMEC cells. Binding reaction and detection were the same as used for Slug-FLAG EMSA assays (Oligonucleotide sequences are in Table 2.1).

## 2.9 Chromatin Immunoprecipitation

HMEC were transduced with pLNCX or pLNC-FLAG-CSL. Cells were fixed using 1% formaldehyde (Sigma-Aldrich, St. Louis, MO) for 10 minutes at room temperature and the fixation was terminated by adding glycine (Sigma-Aldrich, St. Louis, MO) to a 125 mM final concentration and incubated at room temperature for 5 minutes. Cells were then harvested using lysis buffer (50 mM Tris-HCl, pH 7.6, 150 mM NaCl, 1 mM EDTA, 1% Triton X-100, 1 X PIC) and the cell lysate was sonicated to shear the chromatin.

Immunoprecipitation was conducted using anti-FLAG M2 affinity agarose overnight at $4^0$ C and beads was washed three times sequentially using low salt wash buffer (20 mM Tris-HCl, pH 8.0, 150 mM NaCl, 2 mM EDTA, 1% Triton X-100, 1 X PIC), high salt wash buffer (20 mM Tris-HCl, pH 8.0, 500 mM NaCl, 2 mM EDTA, 1% Triton X-100, 1 X PIC) and LiCl wash buffer (10 mM Tris-HCl, 250 mM LiCl, 1 mM EDTA, 1% Triton X-100, 1 X PIC) buffer once and TE buffer (10 mM Tris-HCl, pH 8.0, 1 mM EDTA, 1 X PIC) twice. DNA-protein complex were eluted twice from the beads using 250 µl elution buffer (1% SDS and 0.1M $NaHCO_3$). The eluted DNA-protein complex was then RNAase treated and de-crosslinked at $65^0$C for 5 hours. DNA was then precipitated using 1 ml of 100% EtOH for overnight at $-20^0$ C. Precipitated DNA was resuspended in 100 µl TE (pH7.6), proteinase K (Invitrogen, Carlsbad, CA) treated and purified using QIAquick PCR purification kit (Qiagen Inc., Mississauga, ON) according to the instruction manual. 2 µl of the 50 µl total eluate was used for each PCR reaction using primers flanking the putative CSL binding sites in the *Slug* promoter. One per cent of total chromatin was treated and purified the same way as eluted DNA-protein complex and included as a positive control for PCR (labeled as input) (Primer sequences are in Table 2.1).

## 2.10 Migration Assays

The ability of Slug-expressing HMEC to migrate was measured by two methods, a scratch (wound) assay, and a modified Boyden Chamber assay. For the scratch assay $5 \times 10^5$ vector or Slug-overexpressing cells were plated in a 6 well plate and allowed to grow to confluence, approximately 48 hours. The confluent monolayers were then put into serum

reduced conditions (MCDB + 0.2% HICS) for 16 hours to reduce proliferation. A scratch was then made using a p1000 tip, the plate was washed 2X with PBS and serum reduced medium was then added. Migration was analyzed for up to 24 hours, and distance migrated as calculated from the images. For the Boyden Chamber migration assay a chemoattractant gradient was formed using MCDB + 0.1% BSA + 20 ng/ml PDGF-BB in the lower chamber of a 24 well plate separated from the upper chamber of MCDB + 0.1% BSA using a polycarbonate filters with 8 μm pores. HMEC vector control or Slug-overexpressing cells were cultured in serum reduced medium for 16 hours, cells were then trypsinized and 2 x $10^5$ cells were added to the upper chamber. Cell migration was assayed after 4 hours by counting the number of cell on the underside of the filter after fixing cells with 4% paraformaldehyde and visualizing cells with crystal violet staining (0.5% Crystal Violet (Sigma-Aldrich, St. Louis, MO) in 20% methanol).

## 2.11 Mice and Atrioventricular (AV) Canal Explant Assay

*Slug*-lacZ mice were generously provided by Dr. Thomas Gridley. *Slug*-lacZ$^{(+/-)}$ mice were crossed to C57Bl/6J mice for embryo collection. Embryos were dissected in ice-cold PBS, embryonic hearts were removed and assayed for β-galactosidase activity. Briefly, embryonic hearts were fixed in 0.2% glutaraldehyde for 30 minutes then stained for with 1 mg/ml X-gal for 4 hours at 37°C following published protocols in the Manipulating the Mouse Embryo: A Laboratory Manual, Cold Spring Harbor Laboratory Press.

AV canal explant assays were performed using the following protocol: rat tail collagen type I (BD Biosciences, San Jose, CA, Cat#354236) was prepared to a final

concentration of 1mg/ml and dispensed into a 24 well tissue culture plate, 300 μl per well, and allowed to solidify in a 37°C, 5% $CO_2$ incubator for 45 minutes. Collagen gels were then washed three times with DMEM + 5%HIFBS, ITS (insulin, transferring, and selenium) (Invitrogen, Carlsbad, CA), and penicillin/streptomycin. Collagen was then drained and AV canals dissected from E9.5 *Slug*-lacZ$^{(+/-)}$ X *Slug*-lacZ$^{(+/-)}$ matings were placed endocardial side down onto the drained collagen. Remaining tissues from each embryo were collected for genotyping. AV explants were allowed to attach overnight in a 37°C, 5%$CO_2$ incubator then 0.5 ml DMEM supplemented with 5% HIFBS, ITS, P/S was added. Explants were cultured for a further 48 hours then fixed with 4% paraformaldehyde and analyzed by visualizing cell nuclei with DAPI. AV-explants that did not attach or that were not actively beating after 48 hours were not included in the analysis.

## 2.12 Analysis of AV Canal Explants

DAPI images of AV canal explants were analyzed using the NIH-Image software and user defined algorithms. Briefly, pixels with a value of 0 (white) were set to 1 and pixels with values of 255 (Black) were set to 254. The boundaries of the AV canal tissue was then marked with 255 (Black) pixels, the threshold between the DAPI stained nucleus and background was then determined. The NIH-software then calculated the number of pixels and the distance of each pixel to the closest point of the AV canal tissue (255-Black pixel). See Figure 2.1.

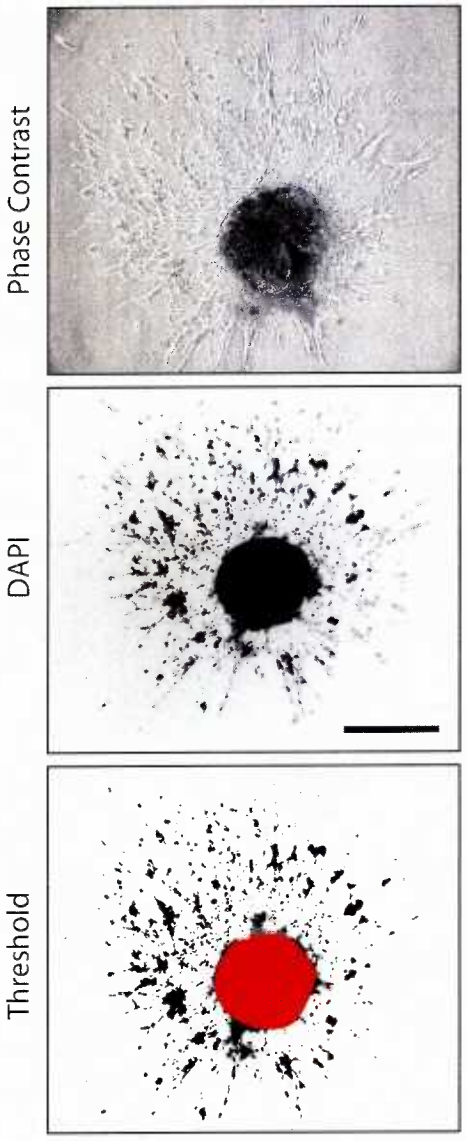


| Pixel distance from AV canal tissue | Distance from AV canal tissue (μm) | # of Pixels above threshold | normalized to the area | Sample Name |
|---|---|---|---|---|
| | | AV #1 d1th-80 64765 | AV #1 d1th-80 | Threshold Area |
| 1 | 2.66 | 338 | 0.005219 | |
| 2 | 5.32 | 232 | 0.003582 | |
| 3 | 7.98 | 197 | 0.003042 | |
| 4 | 10.64 | 223 | 0.003443 | |
| 5 | 13.30 | 166 | 0.002563 | |
| 6 | 15.96 | 184 | 0.002841 | |
| 7 | 18.62 | 168 | 0.002594 | |
| 8 | 21.28 | 190 | 0.002934 | |
| 9 | 23.94 | 185 | 0.002856 | |
| 10 | 26.60 | 207 | 0.003196 | |
| 11 | 29.26 | 216 | 0.003335 | |
| 12 | 31.91 | 224 | 0.003459 | |
| 13 | 34.57 | 231 | 0.003567 | |
| 14 | 37.23 | 214 | 0.003304 | |
| 15 | 39.89 | 213 | 0.003289 | |
| ..... | ..... | ..... | ..... | |
| 235 | 625.00 | 9 | 0.000139 | |
| 236 | 627.66 | 7 | 0.000108 | |
| 237 | 630.32 | 5 | 7.72E-05 | |
| 238 | 632.98 | 2 | 3.09E-05 | |
| 239 | 635.64 | 0 | 0 | |
| 240 | 638.30 | 0 | 0 | |
| 241 | 640.96 | 0 | 0 | |
| 242 | 643.62 | 0 | 0 | |
| 243 | 646.28 | 0 | 0 | |
| 244 | 648.94 | 3 | 4.63E-05 | |
| 245 | 651.60 | 8 | 0.000124 | |
| 246 | 654.26 | 14 | 0.000216 | |
| 247 | 656.91 | 17 | 0.000262 | |
| 248 | 659.57 | 17 | 0.000262 | |
| 249 | 662.23 | 16 | 0.000247 | |
| 250 | 664.89 | 15 | 0.000232 | |

**Figure 2.1 Analysis of AV canal explant assays.**
AV canal explants were fixed and nuclei were visualized with DAPI staining. Images were captured on an inverted fluorescent microscope. Using the NIH Image software the threshold for each image was determined and the margins of the AV canal tissue was identified (Red). The threshold images were analyzed for the number of pixels above threshold and the distance for each pixel to the closest point of the AV canal tissue. The NIH Image software analyzes for the number of pixels above threshold (Column 3) up to 250 pixels (Column 1) from the AV canal tissue, which corresponds to 665 μm (Column 2). To take into account the different sizes of starting tissue the data was then normalized to the area of the AV canal tissue (Column 4). Scale bar represents 500 μm.

## 2.13 Analysis of Cardiac Cushions

Analysis of E9.5 cardiac cushions was performed as follows: E9.5 pregnant mice were injected (intraperitoneal) with 1500mg/kg bromodeoxyuridine (BrdU) (Sigma-Aldrich, St. Louis, MO) at 5pm, embryos were collected at 7pm and fixed overnight in 4% paraformaldehyde (Sigma-Aldrich, St. Louis, MO). Embryos were washed in PBS then paraffin embedded and 6μm sections were cut on a microtome. Sections were then visualized for BrdU using anti-BrdU-Alexa-594 (Molecular Probes, Eugene, OR) according to manufactures protocols and the nuclei were then costained with DAPI. The total number cells and the number of BrdU positive cells in the cardiac cushions were visually counted in all sections which contained identifiable and complete AV canal cushions. Analysis of E10.5 cardiac cushions was performed using the same method as the E9.5 cushion analysis, except the BrdU and DAPI steps were omitted and cells were visualized using Nuclear Fast Red staining.

## 2.14 RNA Interference

siRNA's targeting human CSL mRNA (NM_005349); shCSL-A 367-GCATGGCACTCCCAAGATTGA-387 and shCSL-B 286-GAGTCTCAACCGTGTGCAT-304, human Slug mRNA (NM_003068) shSlug-A 661-GCATTTGCAGACAGGTCAAAT-681 and shSlug-B 604-GGACACATTAGAACTCACA-622, mouse Snail mRNA sequence (NM_011427) shSnail 573-GATGCACATCCGAAGCCAC-591 and shRandom GTTGCTTGCCACGTCCTAGAT were cloned into the HpaI and XhoI sites of the

pLentilox3.7 vector (Rubinson et al. 2003). Constructs were sequence verified and tested for efficient knockdown. Lentiviral particles were produced in 293T cells by transfection of 6 μg pLentilox shRNA vector, 3 μg pVSVG, 3 μg RSV-REV, and 3 μg pMDL g/p RRE for a 100mm dish using the Fugene 6 transfection reagent. Infection of target cells was performed in the same way as discussed above for the AmphoPhoenix retroviral infection.

## 2.15 Collection of Human Tissues

Human embryonic hearts were collected following institutionally-approved protocols at the University of British Columbia and Children's and Women's Health Sciences Centre (Vancouver, BC Canada). Tissue was fixed in 4% paraformaldehyde overnight, embedded in OCT, and 10 μm cryosections were cut onto Histobond slides (Paul Marienfeld GmbH & Co. KG, Baden-Württemberg, Germany).

## 2.16 *In situ* Hybridization

Whole mount and section *in situ* hybridization was performed as previously described (Wilkinson 1992). Briefly, E10.5 and E11.5 wild-type and *Slug*-deficeint hearts were dissected then fixed overnight in 4% paraformaldehyde (Sigma-Aldrich, St. Louis, MO). The tissue was then washed in PBS + 0.1% Tween-20 (Sigma-Aldrich, St. Louis, MO) and treated with 6% $H_2O_2$ (Sigma-Aldrich, St. Louis, MO) for 1 hour followed by proteinase K (Invitrogen, Carlsbad, CA) treatment for 10 minutes. Proteinase K treatment was terminated by addition of 2 mg/ml glycine (Sigma-Aldrich, St. Louis, MO), followed by re-fixation in

4% paraformaldehyde. The tissue was then put into hybridization mixture (50% Formamide (Invitrogen, Carlsbad, CA), 1.3X SSC (Sigma-Aldrich, St. Louis, MO), 5 mM EDTA (Sigma-Aldrich, St. Louis, MO), 50 μg/ml Yeast RNA (Sigma-Aldrich, St. Louis, MO), 0.5% CHAPS (EMD Chemicals Inc, Darmstadt, Germany), 100 μg/ml Heparin (Sigma-Aldrich, St. Louis, MO), 0.2% Tween-20) for 1 hour at 65°C. 1 ug/ml DIG-labeled RNA probe (F. Hoffman-La Roche, Basal, Switzerland) was then added and incubated overnight at 70°C. Tissue was then washed in fresh hybridization buffer, followed by several washes in MABT buffer (100 mM Maleic acid (Sigma-Aldrich, St. Louis, MO), 150 mM NaCl, 0.1% Tween-20, pH 7.5). Tissue was then blocked in 2% Boehringer Blocking Reagent (BBR) (Boehringer Ingelheim GmbH, Ingelheim, Germany) for 1 hour followed by BBR + 20% goat serum (Sigma-Aldrich, St. Louis, MO) for 2 hours followed by the addition of 1:2500 anti-DIG-alkaline phosphatase antibody (F. Hoffman-La Roche, Basal, Switzerland) overnight. Tissue was then washed several times in MABT followed by NTMT buffer (0.1 M Levamisole (Sigma-Aldrich, St. Louis, MO), 0.1 M NaCl, 50 mM TrisHCL pH 9.5, 25 mM $MgCl_2$, 1% Tween-20). Alkaline phosphatase activity was then detected using the BM-Purple substrate (F. Hoffman-La Roche, Basal, Switzerland) for up to 24 hours at 4°C. Whole mount *in situ* hybridized embryos were then photographed on a Leica MZ16FA stereomicroscope (Leica Microsystems, Richmond Hill, Ontario). Mouse *Snail* probe (-55 to +454) was cloned into pBluescript. Human *Snail* and human *Slug* probes were comprised of the entire open reading frame cloned into pCDNA3.

## 2.17 Neutral Red and Annexin-V Staining

For Neutral Red assays HMEC transduced with vector control, NotchICD, or Slug expression constructs were seeded to a density of 3.5 x $10^4$ in a 96 well plate. 24 hours later the cells were treated with 0 or 100 ng/ml Lipopolysaccharide from *Escherichia coli* (LPS) (Sigma-Aldrich, St. Louis, MO) and 25 μM ALLN (Sigma-Aldrich, St. Louis, MO) for 16 hours. The cells were then stained with 0.0025% Neutral for 4 hours, washed one times with PBS, lysed in 100 μl Lysis Buffer (1% Acetic acid, 50% Ethanol), and absorbance at 550 nm was determined using a Tecan GENios microplate reader (Tecan Systems Inc. San Jose, CA).

For Annexin-V staining HMEC transduced with vector control, NotchICD, or Slug expression constructs were seeded to a density of 4 x$10^5$ in 12 well plates. 16 hours later cells were treated with 0, 10, or 100 ng/ml LPS and 25 μM ALLN for 8 hours. Cells were then washed once with PBS, trypsinized, resuspended in 5 ml HMEC medium, collected into 5 ml round bottom tube, cell were spun at 15000 x g for 5 minutes, and resuspended in 100 μl Annexin-V Binding Buffer (10mM HEPES, 140mM NaCl, 2.5mM $CaCl_2$, pH7.0). 2.5 μl of Annexin-V reagent (Invitrogen, Carlsbad, CA) was then added and incubated at room-temperature for 15 minutes, followed by 400 μl of ice cold Annexin V Binding Buffer and samples were then kept on ice. Percent Annexin-V positive cells were analyzed on an EPICS ELITE-ESP flow cytometer (Beckman Coulter Inc, Fullerton, CA) and data was analyzed using FCS Express software (De Novo software, Thornhill, ON).

## 2.18 Statistical Analysis

To determine statistical significance for the qRT-PCR, Neutral Red assay, and Annexin V staining data was analyzed using a pairwise T-test. To determine statistical significance for the scratch assay and Boyden chamber migration assay data a two-tailed students T-test was used. Statistical significance was taken at a $P$ value of $\leq 0.05$.

*Chapter 3*

# SLUG IS A DIRECT TARGET OF NOTCH SIGNALING

## 3.1 Abstract

Endothelial-to-mesenchymal transformation (EndMT) is necessary for proper heart valve and atrioventricular septa formation during cardiac development. EndMT is characterized by the modulation of endothelial cell phenotype by inductive signals emanating from the overlying myocardium as well as inter-endothelial signals (Brand 2003; Armstrong and Bischoff 2004). EndMT occurs in two specific regions of the developing heart, the atrioventricular (AV) canal and outflow tract (OFT) (Armstrong and Bischoff 2004). Because a) the Notch pathway has been shown to regulate cell fate decisions, b) mutations in the Notch pathway result in cardiovascular defects, and c) Notch pathway components are highly expressed in the developing cardiovascular system, we sought to investigate the role of the Notch pathway during cardiovascular development. Our initial study demonstrated that activation of the Notch pathway induces EndMT *in vitro*; however, the mechanism by which Notch signaling regulates endothelial cell phenotype remained unknown.

In the first part of this thesis, I studied the effect of the Notch pathway on the expression of known regulators of EndMT in endothelial cells. Using endothelial cells from various vascular beds transduced with either constitutively-active Notch receptor constructs or a co-culture system with ligand overexpressing cells, the *Slug* transcriptional repressor was identified as a Notch regulated gene. Using both chromatin immunoprecipitation assays and

electrophoretic mobility shift assays, CSL was demonstrated to directly bind the *Slug* promoter, demonstrating *Slug* is a direct target of Notch signaling. We further studied the effect and importance of *Slug* during Notch-mediated EndMT. Using endothelial cells ectopically expressing *Slug,* it was demonstrated that *Slug* regulates endothelial cell phenotype. Using a lentiviral shRNA knockdown technique, it was demonstrated that *Slug* expression was required for the Notch pathway to regulate endothelial cell phenotype. Together these data show that *Slug* plays an important role in regulating Notch-mediated EndMT and suggest *Slug* has an important role during cardiac development.

### 3.1.1 Screen for factors involved in regulating cadherin gene expression

It has previously been shown, by our lab and others, that activation of the Notch pathway results in EndMT, characterized by loss of endothelial markers and acquisition of mesenchymal markers (Noseda et al. 2004; Timmerman et al. 2004). The cadherin family of proteins is an important class of junction proteins that are involved in maintaining adherens junctions that link the plasma membrane to the cytoskeleton. Vascular endothelial (VE) cadherin (also known as Cadherin-5) is an endothelial specific type-II cadherin protein that is known to regulate vessel permeability and maintain endothelial structure and survival (Vittet et al. 1997; Carmeliet et al. 1999; Crosby et al. 2005). VE-cadherin forms homophilic interactions between neighboring endothelial cells and links the plasma membrane to the cytoskeleton via interaction with the β-catenin/α-catenin/actin or plakaglobin/α-catenin/actin complexes (Wallez et al. 2006). In addition, VE-cadherin expression is required for maintaining endocardial morphology during heart development and is downregulated during

EndMT in the cardiac cushion (Crosby et al. 2005). The mechanism by which Notch activation results in the downregulation of VE-cadherin was unknown; to investigate a possible mechanism a screen for proteins known to effect cadherin gene expression in either endothelial or epithelial cells was performed. The screen included positive regulators of cadherin expression: v-ets erythroblastosis virus E26 oncogene homolog 1 (*Ets1*) (Lelievre et al. 2000) and *SMAD4* (Muller et al. 2002) and repressors of cadherin expression: smad interacting-protein 1 (*SIP1*) (Vandewalle et al. 2005), integrin linked kinase (*ILK*) (Novak et al. 1998), *E12/E47* (also known as E2A) (Perez-Moreno et al. 2001), *Snail* (Cano et al. 2000), and *Slug* (Hajra et al. 2002). RT-PCR analysis for these genes in HMEC transduced with vector control, constitutively active Notch4 (Notch4ICD), or constitutively active Notch1 (Notch1ICD) constructs demonstrated that *Ets1* was downregulated and *Slug* was upregulated by Notch activation (Figure 3.1). Around the same time as these data were generated, a manuscript was published demonstrating Notch activation results in the upregulation of *Snail* in porcine aortic endothelial cells (Timmerman et al. 2004). Additionally, it was demonstrated that there was an inverse correlation between *Snail* and *VE-cadherin* expression in Notch activated cells and that Snail can repress the *VE-cadherin* promoter in a promoter-reporter assay (Timmerman et al. 2004). These findings conflicted with the findings in Figure 3.1 that demonstrated that *Slug,* but not *Snail,* was regulated by Notch activation. However, in the above manuscript the authors used a set of degenerate primers to amplify Snail mRNA and these primers were originally designed to amplify all Snail family members and therefore their conclusions that Notch signaling regulates *Snail* expression may not have been accurate (Locascio et al. 2002; Timmerman et al. 2004). Therefore, further investigation to define which of the Snail family member(s) are regulated by Notch signaling was required.

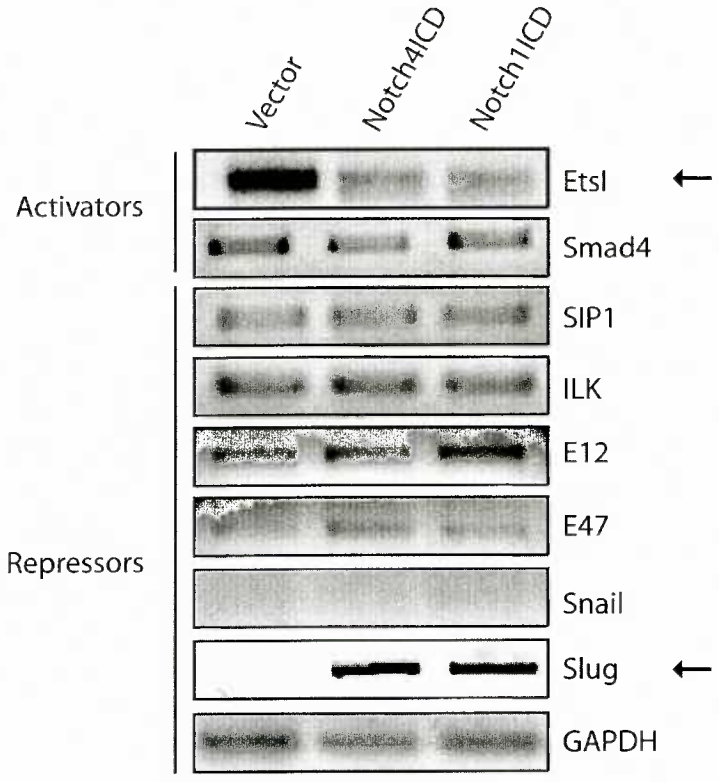


**Figure 3.1 Screen for regulators of cadherin gene expression.**
RT-PCR analysis for genes involved in regulating cadherin expression in HMEC overexpressing constitutively active Notch4 (Notch4ICD) or Notch1 (Notch1ICD). Ets1 was identified as being repressed by Notch signaling and Slug was identified as induced by Notch signaling (arrows).

### 3.1.2 Activation of the Notch pathway upregulates *Slug* but not *Snail* or *Snai3* in human endothelial cells

To clarify which Snail family member(s) are regulated by Notch signaling in endothelial cells, vector control, Notch1ICD, or Notch4ICD constructs were transduced into human and mouse endothelial cells from various vascular beds. The human endothelial cells used were human microvascular endothelial cells (HMEC, a transformed cell line), human umbilical vein endothelial cells (HUVEC, a primary large vein endothelial cell), and human aortic endothelial cells (HAEC, a primary arterial endothelial cell). The Notch1 and Notch4 receptors were chosen because both have been shown to be expressed in the cardiac cushion endocardial cells (Noseda et al. 2004). These results demonstrated that activation of the Notch pathway upregulates *Slug*, but not *Snail* or *Snai3* in all endothelial cells tested, as demonstrated by RT-PCR (Figure 3.2A), quantitative RT-PCR (qRT-PCR) (Figure 3.2B) and immunoblotting (Figure 3.2C and 3.2D), confirming our previous data (Figure 3.1). As a positive control, we confirmed that the known Notch targets *Hey1*, *Hey2*, and *HeyL* were induced by NotchICD (Figure 3.2A and 3.2B) (MacKenzie et al. 2004b). In addition, we have also observed that activation of the Notch pathway induces *Slug* expression in human foreskin fibroblasts (HFF) and umbilical artery smooth muscle cells (UASMC), suggesting the effect of Notch on *Slug* expression is not cell-type specific (data not shown).

In the previous experiments the overexpression of NotchICD was used to determine Snail family gene regulation. However, NotchICD constructs activate the Notch pathway to an extremely high level, which may not represent an endogenous response to Notch signaling.

To overcome this problem a co-culture system was used, where HMEC cells overexpressing the Notch ligands, Jagged1 or Dll4, were co-cultured with parental HMEC. In this system the availability of Notch receptors limit the activation of the Notch pathway. We have previously demonstrated that in the co-culture system, activation of the Notch pathway results in EndMT, although the upregulation of mesenchymal markers occurs at a much lower level in comparison to NotchICD overexpression (Noseda et al. 2004). Jagged1 and Dll4 ligands were chosen because both have been shown to be expressed in developing cardiac cushion endocardial cells (Loomes et al. 1999; Noseda et al. 2004). Similar to the NotchICD results, ligand-induced activation of endogenous Notch, following co-culture of parental HMEC with either Jagged1- or Dll4-expressing cells, also induced Slug, but not Snail protein expression (Figure 3.2D and 5.1C). Collectively, these findings indicate that Notch activation induces *Slug* but not *Snail* or *Snai3* expression in endothelial cells. As the Snail family of genes regulate EMT in epithelial cells we hypothesize that *Slug* may play a critical role in cardiac cushion EndMT by regulating VE-cadherin expression.

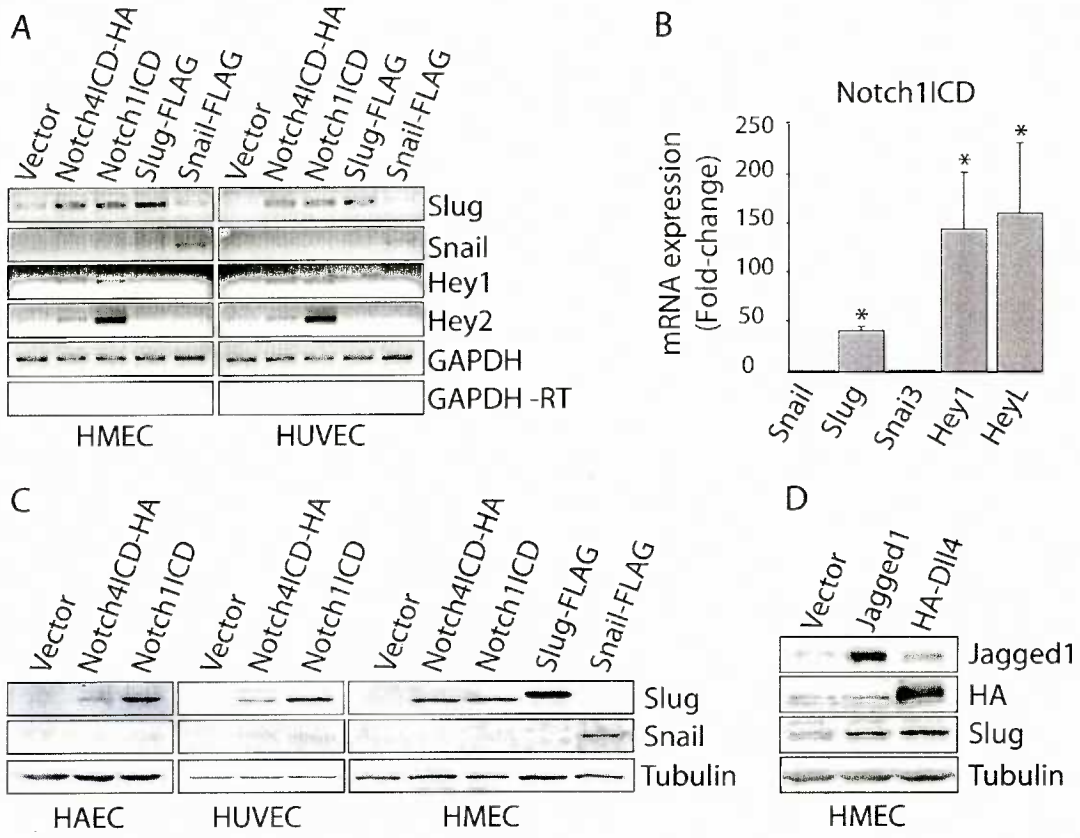


**Figure 3.2 Expression of *Slug* but not *Snail* or *Snai3* is induced by Notch signaling.**
(A) Analysis of mRNA expression by RT-PCR in HMEC and HUVEC overexpressing constitutively active Notch 1 (Notch1ICD) or Notch 4 (Notch4ICD). Hey1 and Hey2 are used as positive controls for active Notch signaling (B) Analysis of mRNA expression by qRT-PCR in HMEC overexpressing Notch1ICD, results are normalized to vector control sample ($n = 3$, $p < 0.05$). Hey1 and HeyL are used as positive controls for active Notch signaling (C) Analysis of protein expression in the human endothelial cells HMEC, HUVEC, and HAEC overexpressing Notch1ICD or Notch4ICD. (D) Analysis of protein expression in ligand induced activation of Notch signaling by coculture of parental HMEC with Jagged1 or Dll4 overexpressing HMEC.

### 3.1.3 Notch acts through CSL to induce *Slug* expression and repress endothelial phenotype

Notch signaling results in activation of downstream signaling by directly regulating gene transcription (Artavanis-Tsakonas et al. 1999). To determine the structural requirements of Notch-mediated *Slug* expression, a *Notch4ICD* deletion series was utilized (MacKenzie et al. 2004a). The *Notch4ICD* deletion constructs were overexpressed in HMEC cells to test which domain(s) of Notch4ICD were necessary or sufficient for the upregulation of *Slug* expression. It has previously been demonstrated that deletion of the RAM domain reduces nuclear translocation of the Notch4ICD, thus the ΔRAM deletion construct was fused to a nuclear localization sequence to force nuclear translocation (MacKenzie et al. 2004a). The *Notch4ICD* deletion constructs revealed that only the ankyrin repeats of the Notch4ICD protein were essential for the upregulation of *Slug* expression by Notch (Figure 3.3B). However, in contrast to our previous results showing that enforced expression of the ankyrin repeats alone was sufficient for induction of *Hey1* and *Hey2* (MacKenzie et al. 2004a), the ankyrin repeats alone were not sufficient for *Slug* induction (Figure 3.3B). The ankyrin repeats are involved in protein-protein interactions, suggesting the ankyrin repeats are necessary for recruiting co-factors necessary for *Slug* induction. In addition, the Notch4ICD domains that resulted in the upregulation of Slug correlated with the downregulation of VE-cadherin expression (Figure 3.3B), further suggesting Slug is the Notch downstream target gene responsible for the repression of VE-cadherin expression.

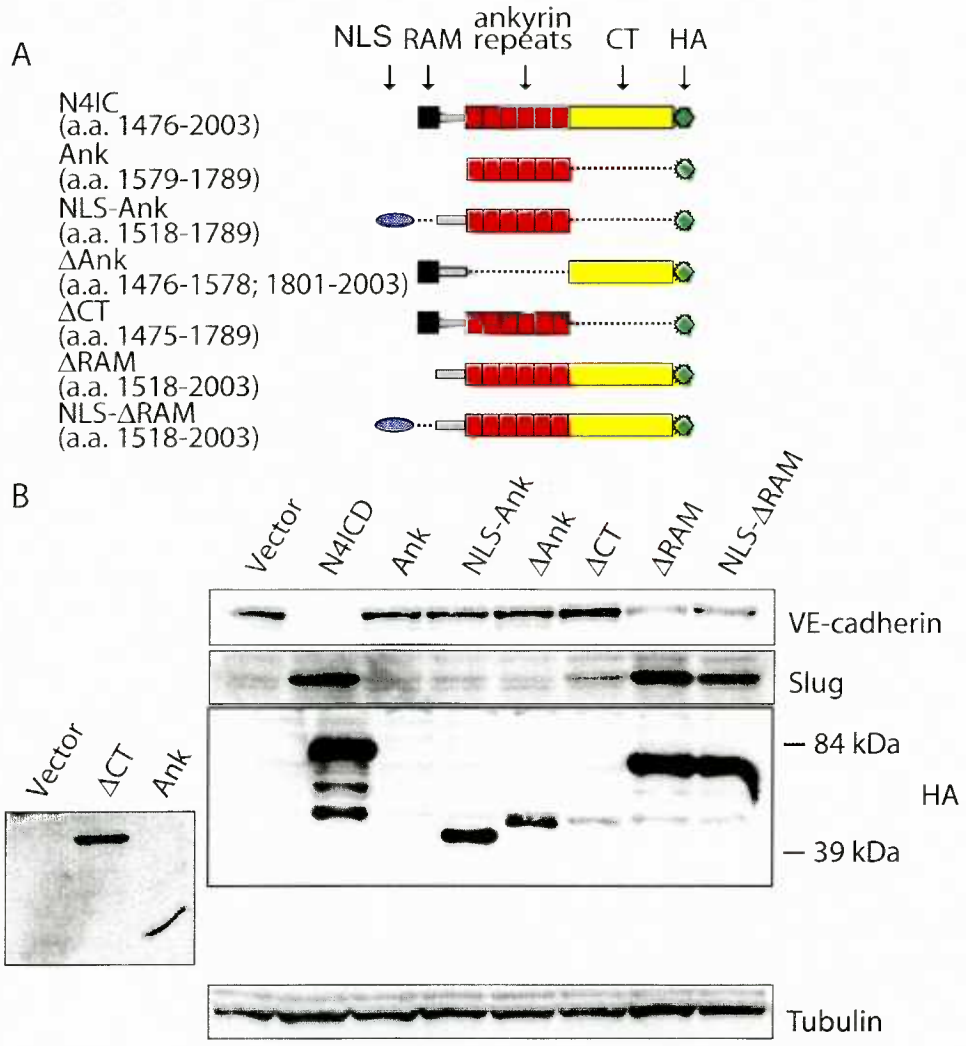


**Figure 3.3 Structural requirements for Slug upregulation by Notch signaling.**
(A) Schematic of the Notch4ICD deletion constructs used to test the domains necessary or sufficient for upregulation of Slug by Notch signaling. NLS - nuclear localization signal, RAM - RBP-jk associated module, CT - c-terminal of the NotchICD, HA - hemagglutinin tag. (B) Analysis of protein expression in HMEC transduced with the Notch4ICD deletion constructs. Due to differences in size, expression, and stability of the Notch4IC deletion construct the expression of the deletion constructs was confirmed using two different western blots.

The Notch pathway has been shown to regulate gene expression by at least two distinct pathways, the canonical CSL-dependent pathway and a less well-defined CSL-independent route (Ramain et al. 2001). To identify the pathway used by Notch to regulate *Slug* expression a lentiviral shRNA approach was used to knock down *CSL* expression in endothelial cells where Notch signaling was also activated by co-culture with Dll4-expressing cells. Two different shRNA constructs were designed to target unique sites within the CSL mRNA that are present in all four splice variants of *CSL*. Analysis of *CSL* mRNA and protein expression demonstrated an efficient (> 80%) CSL knockdown by both constructs (Figure 3.4A and 3.4B). As Figures 3.4C and 3.4E demonstrate, Dll4-mediated induction of *Slug* mRNA and protein was dramatically inhibited when *CSL* expression was knocked down using either of the two shRNA constructs. As expected, induction of the Notch target gene *HeyL* was also abolished by *CSL*-knockdown (Figure 3.4C). In addition, the ability of Notch activation to downregulate the endothelial markers *VE-cadherin* and *CD31* was abrogated when *CSL* was knocked down (Figure 3.4E and 4.4D), thus demonstrating the requirement of CSL-mediated induction of *Slug* expression during Notch-mediated EndMT.

In addition, two lentiviral-shRNA constructs targeting Slug were used to directly examine the requirement of Slug expression during Notch-mediated repression of VE-cadherin expression. As Figure 3.4E demonstrates both of the sh*Slug* constructs efficiently knocked down Slug protein expression (Figure 3.4E). When the upregulation of *Slug* expression by activation of the Notch pathway was blocked, the ability of Dll4-activated Notch signaling to downregulate *VE-cadherin* and *CD31* was also abrogated (Figure 3.4D and 3.4E). We were unable to test whether Slug expression was necessary for Notch-

mediated upregulation of mesenchymal markers due to the limitation of the Dll4 co-culture system. The Dll4 co-culture system results in rapid downregulation of endothelial phenotype but the upregulation of mesenchymal markers requires several weeks of co-culture. As will be discussed in more detail in later sections of this thesis, massive apoptosis results when *Slug* expression is knocked down in NotchICD activated cells. As with NotchICD expression, we found that recovery of *Slug*-knockdown cells in the Dll4 co-culture system was markedly diminished at later time-points, eliminating analysis of the upregulation of mesenchymal markers by activation of Notch pathway by *Dll4*. These data also suggest a survival function for *Slug* in Notch-activated cells, which will be discussed later.

To determine whether CSL activation was sufficient for induction of *Slug* expression, a constitutively-active *CSL* mutant (*CSL-VP16*) was ectopically expressed in endothelial cells. VP16 is a transcriptional activator from the Herpes Simplex Virus, and when expressed as a fusion protein with CSL, activates CSL target genes independently of active Notch signaling (MacKenzie et al. 2004b). It has previously been shown that VP16 fusion proteins undergo rapid turnover (Salghetti et al. 2000), and, as a result, the detection of CSL-VP16 protein was difficult. However, analysis of mRNA expression in HMEC transduced with vector control or CSL-VP16 constructs demonstrated *CSL* was successfully overexpressed and that CSL activation alone was sufficient to upregulate *Slug* expression, as well as the Notch target *HeyL* (Figure 3.4F). Thus the canonical *CSL*-dependent Notch pathway was necessary and sufficient for the upregulation of *Slug*.

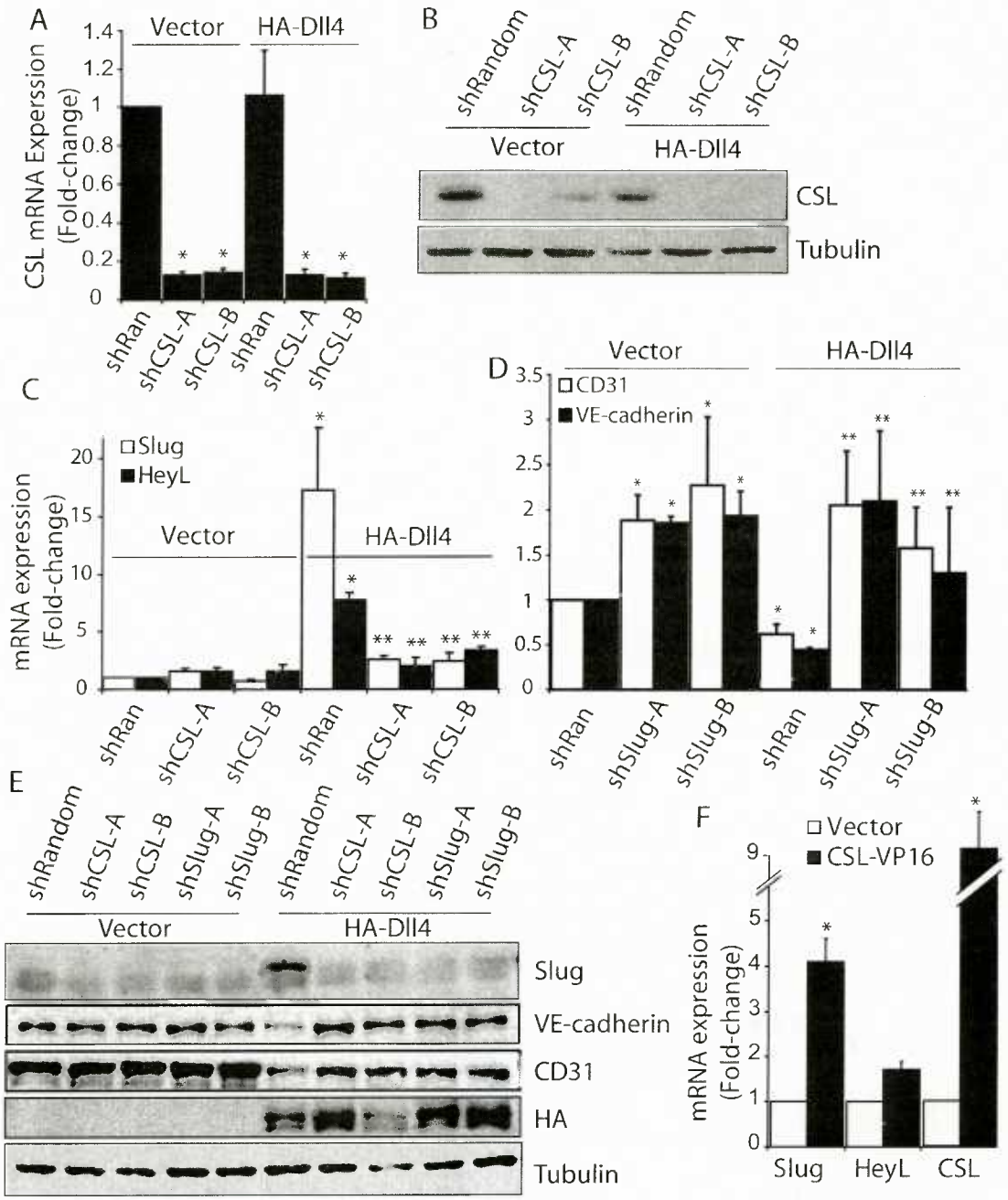


**Figure 3.4 Notch regulates *Slug* expression through a CSL dependent pathway.**
(A) Efficient knock down of CSL mRNA as measured by qRT-PCR in HMEC expression by a lentiviral shRNA technique by two different shRNAs. (B) Analysis of protein expression in HMEC transduced with shCSL constructs (C) Analysis of HeyL (Notch target gene) and Slug mRNA expression by qRT-PCR in vector or Notch activated HMEC transduced with shCSL constructs ($n = 3$, $p < 0.05$, * significant vs Vector shRandom, ** significant vs Dll4 shRandom). (D) Analysis of VE-cadherin and CD31 mRNA expression by qRT-PCR in vector or Notch activated HMEC transduced with shSlug constructs. ($n = 3$, $p < 0.05$, * significant vs Vector shRandom, ** significant vs Dll4 shRandom) (E) Analysis of protein expression in vector control or Notch activated HMEC transduced with shCSL or shSlug constructs. (F) Analysis of mRNA expression by qRT-PCR in vector or CSL-VP16 overexpressing HMEC ($n = 3$, $p < 0.05$).

### 3.1.4 CSL directly binds the human *Slug* promoter

Several signaling pathways have previously been implicated in regulating Snail family member expression, including the TGFβ, Wnt, and PI3-kinase pathways (Nieto 2002). To determine whether Notch signaling, via CSL, can directly regulate *Slug* expression, an analysis of the *Slug* promoter (-2000 to +100 relative to the transcriptional start site (TSS)) was performed in several species (Figure 3.5A). This analysis identified between one and six putative CSL binding sites ((C/T)(A/G)TG(A/G/T)GA(A/G/T)) in the *Slug* promoter, depending upon the species. In comparison, the Snail promoter contained no more than one CSL binding site (Figure 3.5B). Of the six putative binding sites in the human *Slug* promoter, two were further investigated based on conservation of the CSL binding sites in the mouse *Slug* promoter. The first binding site (TATGGGAA) is located at -846 to -853, while the second binding site (TGTGGGAA) is located at -1679 to -1686 base pairs upstream of the TSS. Using chromatin immunoprecipitation (ChIP) followed by PCR with primers that flank the CSL binding elements, CSL was observed to bind both the CSL consensus motifs in the *Slug* promoter (Figure 3.6A). In contrast, PCR of the same ChIP DNA did not enrich the *ZNF3* promoter, which lacks a putative CSL binding site (Figure 3.6A). To further confirm binding to the CSL binding sites, nuclear lysates harvested from FLAG-CSL-expressing endothelial cells were used to test CSL binding to the Slug promoter in an electrophoretic mobility shift assay (EMSA). The EMSA further confirmed that CSL was capable of binding both consensus elements present in the human *Slug* promoter (Figure 3.6B). In the Slug EMSA the FLAG-M2 super-shift control did not induce a dramatic super-shift band, although a faint band was visible, which may be explained by the fact that the CSL protein was pre-

incubated with the FLAG-M2 antibody which may block CSL binding of DNA. However, the competition assays with double-stranded oligos with a wild-type CSL binding site or double stranded oligos where the putative CSL binding site that was mutated (TG**GGAA** to TG**CTGC**) further demonstrated specific binding to the CSL consensus sequence. Taken together the above data demonstrate that *Slug* is a direct target of Notch signaling through a *CSL*-dependent pathway, and that *Slug* expression is required for Notch-mediated repression of endothelial phenotype.

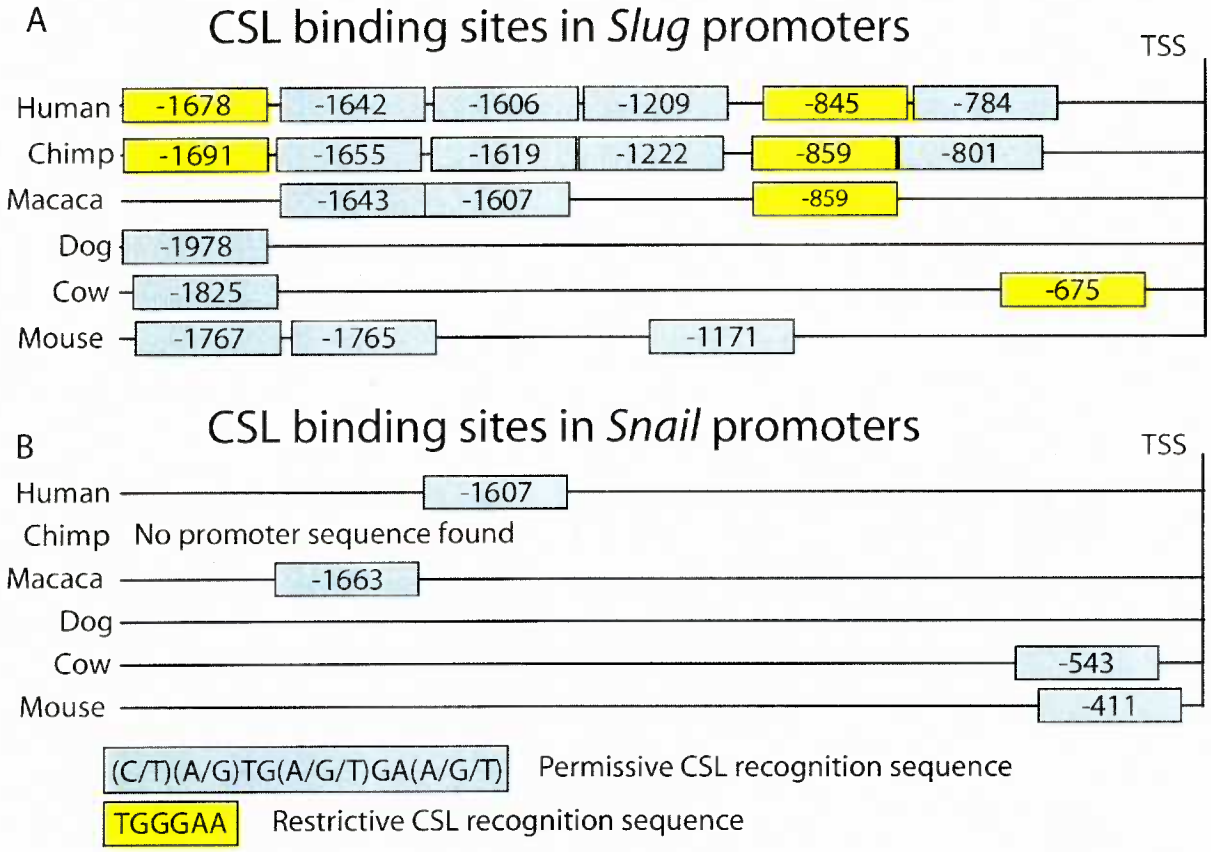


**Figure 3.5 *Slug* and *Snail* promoter analysis.**
Analysis of the Slug and Snail promoters (-2000 to transcriptional start site (TSS)) for putative CSL binding sites. CSL has been shown to preferentially bind the TGGGAA consensus sequence, however a more permissive consensus sequence is defined by (C/T)(A/G)TG(A/G/T)GA(A/G/T) and is commonly used to identify putative binding sites. Sequences used for the analysis were extracted using the Ensemble genome browser using the following Ensemble Gene ID's.
Slug: Human-(ENSG00000019549), Chimp-(ENSPTRG00000020235), Macaca-(ENSMMUG00000016195), Dog-(ENSCAFG00000006638), Cow-(ENSBTAG00000013227), Mouse-(ENSMUSG00000022676).
Snail: Human-(ENSG00000124216), Macaca-(ENSMMUG00000019719) Dog-(ENSCAFG00000011499), Cow-(ENSBTAG00000014554).

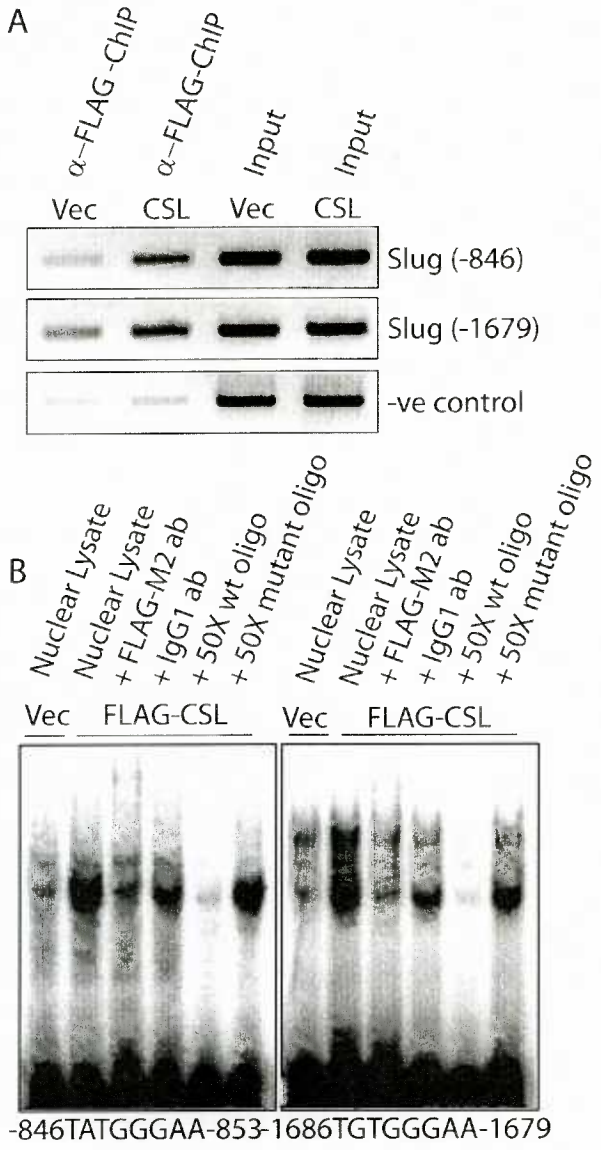


**Figure 3.6 CSL directly binds the human Slug promoter.**
(A) Chromatin immunoprecipitation (ChIP) was performed in HMEC transduced with vector control or FLAG-CSL using α-FLAG-M2 antibody. The starting genomic DNA was used as loading control (Input). Endpoint PCR using primers that flank the two Slug binding sites and a set of primers within the ZNF3 (-ve control) promoter were used to validate enrichment of the target sequences. (B) Analysis of CSL binding to the human Slug promoter using electrophoretic mobility shift assay (EMSA). EMSA using nuclear lysates collected from vector or FLAG-CSL overexpressing HMEC and $P^{32}$ labeled double-stranded oligonucleotides for the two CSL binding sites in the human Slug promoter. Supershift α-FLAG-M2 or IgG control and competition assays with 50X wt or CSL binding sequence mutant probes were also included.

# *Chapter 4*

# SLUG IS REQUIRED FOR CARDIAC CUSHION EndMT

## 4.1 Abstract

In humans, congenital heart defects occur in approximately 1% of newborn and 10% of spontaneously aborted fetuses (Hoffman and Kaplan 2002). One of the major causes of congenital heart defects are defects in the heart valves and membranous septa resulting from defects in EndMT (Hoffman and Kaplan 2002). *Slug*-deficiency in humans results in type-II Waardenburg's syndrome, an autosomal dominant congenital disorder usually involving sensorineural hearing loss and pigmentary abnormalities caused by defects in neural crest cell development (Read and Newton 1997). The phenotype of Waardenburg's syndrome is similar to *Slug*-deficiency in mice, however additional defects in hematopoiesis and palate formation have been identified in the *Slug*-deficient mice (Jiang et al. 1998; Inoue et al. 2002; Sanchez-Martin et al. 2002; Murray et al. 2007). In both human and mouse a detailed understanding of *Slug* expression during heart development and its role during cardiac cushion EndMT has not been established. Since, the data presented in Chapter 3 of this thesis demonstrated the importance of Slug during Notch-mediated EndMT, we investigated the role of *Slug* during cardiac development.

In the second part of the thesis, the expression of Slug during the period of time when the cardiac cushions were undergoing EndMT was investigated. Expression of *Slug* was measured both by immunofluorescence and using a *lacZ* knock-in mouse, in which β-

galactosidase is expressed from the endogenous *Slug* promoter (Jiang et al. 1998; Oram et al. 2003). Both techniques demonstrated that *Slug* was expressed in the mesenchymal cells and a subset of endothelial cells in the AV canal and OFT cardiac cushions. Furthermore, lacZ insertion into the Slug locus results in a null allele and using *Slug*-lacZ homozygous mice it was demonstrated that *Slug*-deficient mice display defects in the initiation of EndMT at E9.5 and have defects in the fusion of the cardiac cushions at E10.5. Three possible roles of Slug during EndMT were demonstrated. The first was to initiate EndMT by downregulating VE-cadherin expression; the second was for survival of the mesenchymal cells; and the third was for increased migration of the mesenchymal cells. These data demonstrate an important role for *Slug* during cardiac cushion development; however, it does not explain the apparent lack of heart defects in adult *Slug*-deficient mice.

### 4.1.1 Expression of *Slug* during murine heart development

The role of *Slug* during mammalian heart development is unclear. It has been reported that *Slug* mRNA is not expressed at E9.5 in the cardiac cushion (Timmerman et al. 2004) while other reports have demonstrated that *Slug* mRNA is expressed in the mesenchyme of cardiac cushions at E13.5 and later in the heart valves (Oram et al. 2003). Since Notch activation has been shown to be critical for EndMT during cardiac cushion development, defining the expression of *Slug* during the period of cellularization of the mammalian cardiac cushions, from E8.5 to E11.5, was investigated (Noseda et al. 2004; Timmerman et al. 2004). To accomplish this, mice which have the *lacZ* gene inserted into the *Slug* locus with concomitant deletion of the zinc-finger DNA binding motifs were analyzed for *lacZ*

expression. Expression of *lacZ* in this model has been shown to faithfully match expression of *Slug* mRNA in all tissues analyzed, as determined by *in situ* hybridization (Jiang et al. 1998). The E8.5 to E11.5 stages in heart development were chosen because it represents a stage prior to EndMT (E8.5), a stage during the initiation of EndMT (E9.5), and stages during the proliferation of the mesenchyme (E10.5, E11.5). Additionally, at E11.5 remodeling of the superior and inferior cushions is occurring, and EndMT in the two lateral cushions is initiated.

*Slug*-expressing ($LacZ^{+}$) cells were not observed in the endocardium in any of the heart chambers at E8.5, however, a rare positive cell was observed in the OFT myocardium (Figure 4.1A and 4.1B). To more closely determine the origin of Slug expressing cells at E8.5 the embryos were sectioned. *Slug*-expressing cells were observed in the 1$^{st}$ branchial arch (arrow) and a region that corresponds to the secondary heart field (arrowhead) (Figure 4.1B). Cardiac neural crest cells are known to migrate into the OFT myocardium and cardiac cushion, however, this occurs between E10.0-11.0 (Chan et al. 2004). Proepicardial cells are known to migrate into the heart at E9.5 from the septum transversum, however, this first occurs in the atria and only by E11.0 do epicardial cells reach the OFT (Viragh and Challice 1981; Komiyama et al. 1987; Reese et al. 2002). The only other cell type known to migrate into the developing heart are cells from the secondary heart field, which are known to contribute to the OFT myocardium at this stage (Waldo et al. 2001; Singh et al. 2005). Collectively this suggests that the *Slug*-expressing cells at E8.5 were from the secondary heart field and not cardiac neural crest cells or proepicardial cells. However, without a more rigorous investigation of the source of these cells a conclusive origin cannot be determined.

This could be accomplished by co-staining for *Slug* expression with known markers for the secondary heart field, such as *FGF-10* or *Nkx3.1* (Schneider et al. 2000; Kelly et al. 2001). A more conclusive method for examining the origin of the *Slug* positive cells at E8.5 would be to analyze for *Slug* expression in a mouse that is deficient for or ectopically forms the secondary heart field, such as the *FGF-10*-knockout and *Tbx1*-gain-of-function mutants, respectively (Hu et al. 2004; Marguerie et al. 2006).

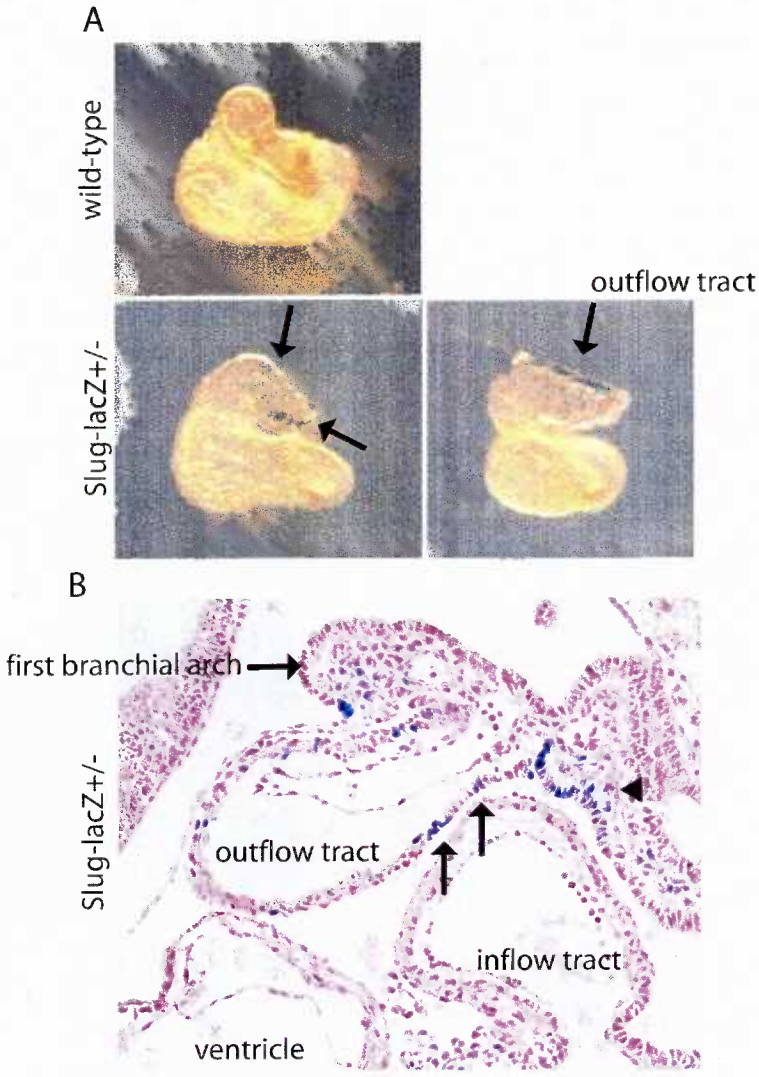


**Figure 4.1 *Slug* expression at E8.5 in the mouse.**
(A) Whole mount images of Slug (lacZ) expression at E8.5. Arrows indicate Slug positive cells (Blue) in the outflow tract. (B) Cross section of an E8.5 embryo stained for Slug expression (Blue) and counterstained with Nuclear Fast Red. Slug positive cells are observed in the outflow tract myocardium (arrows), the first branchial arch, and possibly the secondary heart field cells (arrowhead).

Whole mount images of E9.5 to E11.5 hearts revealed that *Slug*-expressing cells were abundant in the heart but were largely limited to the AV canal and outflow tract (Figure 4.2A, arrows). Additionally, in the E11.5 hearts a population of Slug-expressing cells were observed in the myocardium of the interventricular groove (Figure 4.2A, arrowhead). The interventricular groove is the site where proepicardial cells migrate and differentiate into the coronary vasculature (Viragh and Challice 1981; Komiyama et al. 1987). Detailed analysis of Slug expression between E9.0 and E10.0 revealed that Slug expressing cells were first observed in the OFT myocardium at the 18-21 somite stage (E9.0) (arrowhead) and by the 22-24 somite stage (early E9.5) Slug expressing cells were observed in the AV canal, although whether the cells were in the myocardium or endocardium was unclear (Figure 4.2B). At the 25-28 somite stage (late E9.5) and 29+ somite stage (E10.0) the number of cells expressing Slug in the AV canal increased and were observed in the atria (Figure 4.2B). It was unclear if Slug expressing cells were migrating from the OFT across the heart to the atria or whether cells within those heart structures induce Slug expression. As stated earlier the Slug expressing cells in the OFT may be migrating secondary heart field cells. However, cells of the secondary heart field are not known to contribute to the atria or AV canal myocardium, suggesting the cells in the atria were proepicardial cells that are known to migrate into the atrial and AV canal myocardium around E9.5. Serial sectioning of the hearts revealed *Slug* expression within the mesenchymal cells and a subset of endocardial cells of the AV canal and OFT at E9.5, with increasing expression from E10.5 and E11.5 (Figure 4.3A and 4.3B). Higher magnification images of the AV canal cardiac cushion revealed Slug-expressing cells at the endocardial surface with an elongated endocardial morphology. In some cases, the Slug-expressing cells appeared to be transforming endocardial cells. To further confirm Slug

expression, immunofluorescent staining of E11.5 mouse embryonic hearts for Slug and CD31 was performed. In the heart CD31 is an endothelial cell marker and is known to be downregulated during EndMT (Camenisch et al. 2002b). Immunofluorescence for CD31 and Slug revealed that Slug was expressed in the cardiac cushion mesenchyme and a subset of endothelial cells that co-stain for CD31 (Figure 4.3C, arrowheads). Slug-expressing cells can be observed in the superior and inferior cushions as well as the newly forming lateral cardiac cushions (Figure 4.3C, arrow). The CD31 and Slug co-staining in the endothelial layer suggests Slug is involved in the initial events of EndMT, and correlates with the known sites of active Notch signaling. However, unlike other Notch target genes, such as *Hey2*, *Slug* expression was maintained in the mesenchyme cells, suggesting that either Notch signaling was active in the mesenchymal cells, or *Slug* was regulated by another pathway. Detailed analysis of active Notch1 signaling (Notch1ICD) suggests that Notch1 is active in the endocardium but not active in the mesenchyme of the cardiac cushions (Del Monte et al. 2007). In addition the mRNA expression of Notch2, Notch3, and Notch4 suggest Notch signaling is not active in the cardiac cushion mesenchyme (Loomes et al. 2002; Noseda et al. 2004; Fischer et al. 2007a). One possibility for the maintained mesenchymal Slug expression is if Slug positively regulated its own expression, which has previously been demonstrated in *Slug* promoter-reporter assays (Sakai et al. 2006). However, Slug overexpression in HMEC did not alter endogenous *Slug* expression (Figure 4.4), suggesting Slug does not auto-regulate its promoter in this system. However, HMEC express *Slug* at a low level and the *in vitro* cell culture environment does not accurately represent what is occurring during heart development *in vivo* and activation of other pathways may be required for Slug to regulate its own promoter.

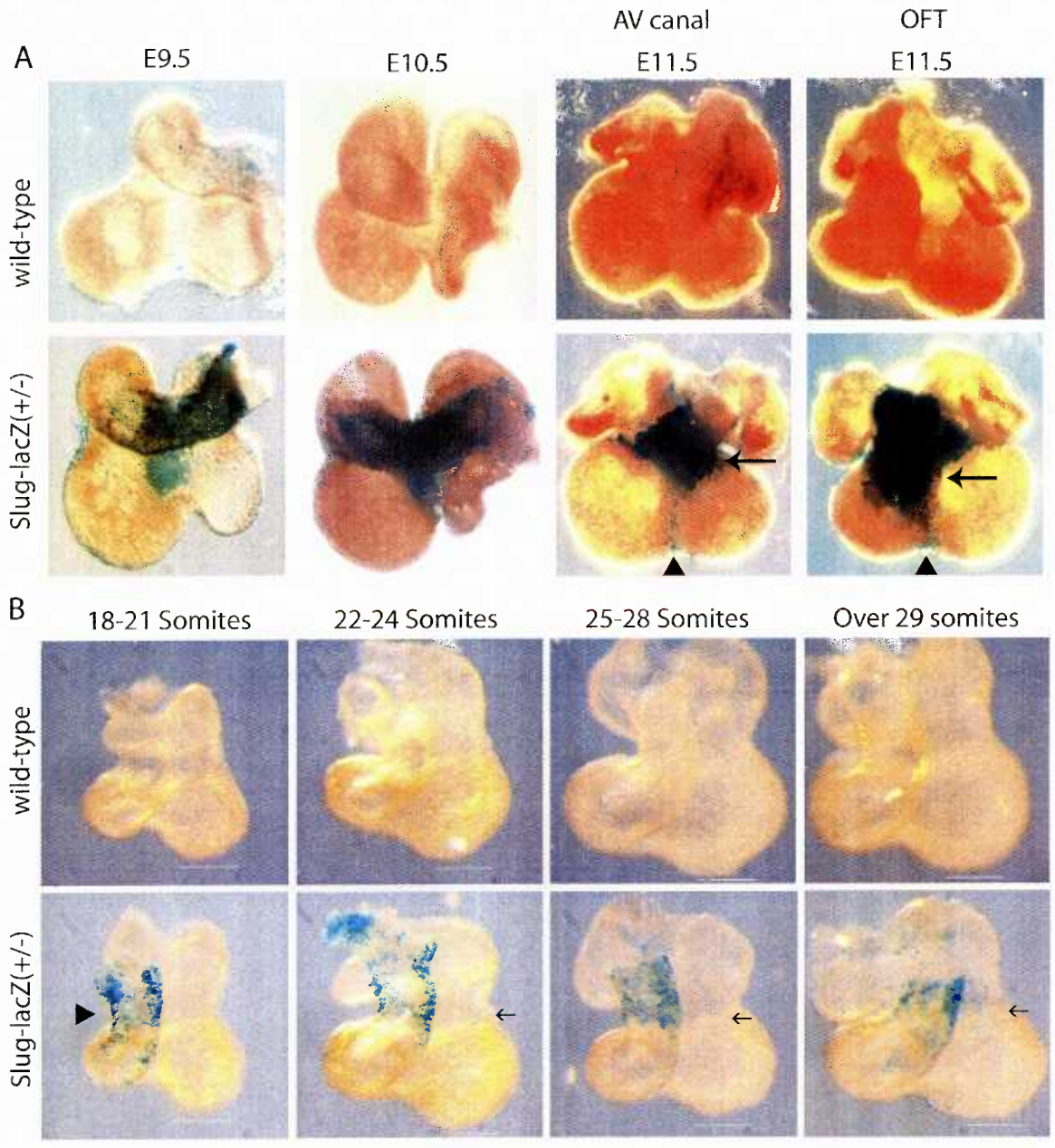


**Figure 4.2 *Slug* expression during mouse heart development.**
(A) Whole mount images of wild-type and Slug-lacZ$^{+/-}$ mice stained for lacZ expression (Blue) from E9.5 to E11.5. (Arrow marks the AV canal or OFT at E11.5). (B) Detailed analysis of Slug expression between E9.0 (18-21 somites) and E10.0 (over 30 somites). Arrowhead indicates the first Slug expressing cells observed in the outflow tract myocardium and the arrow indicates Slug expressing cells in the AV canal.

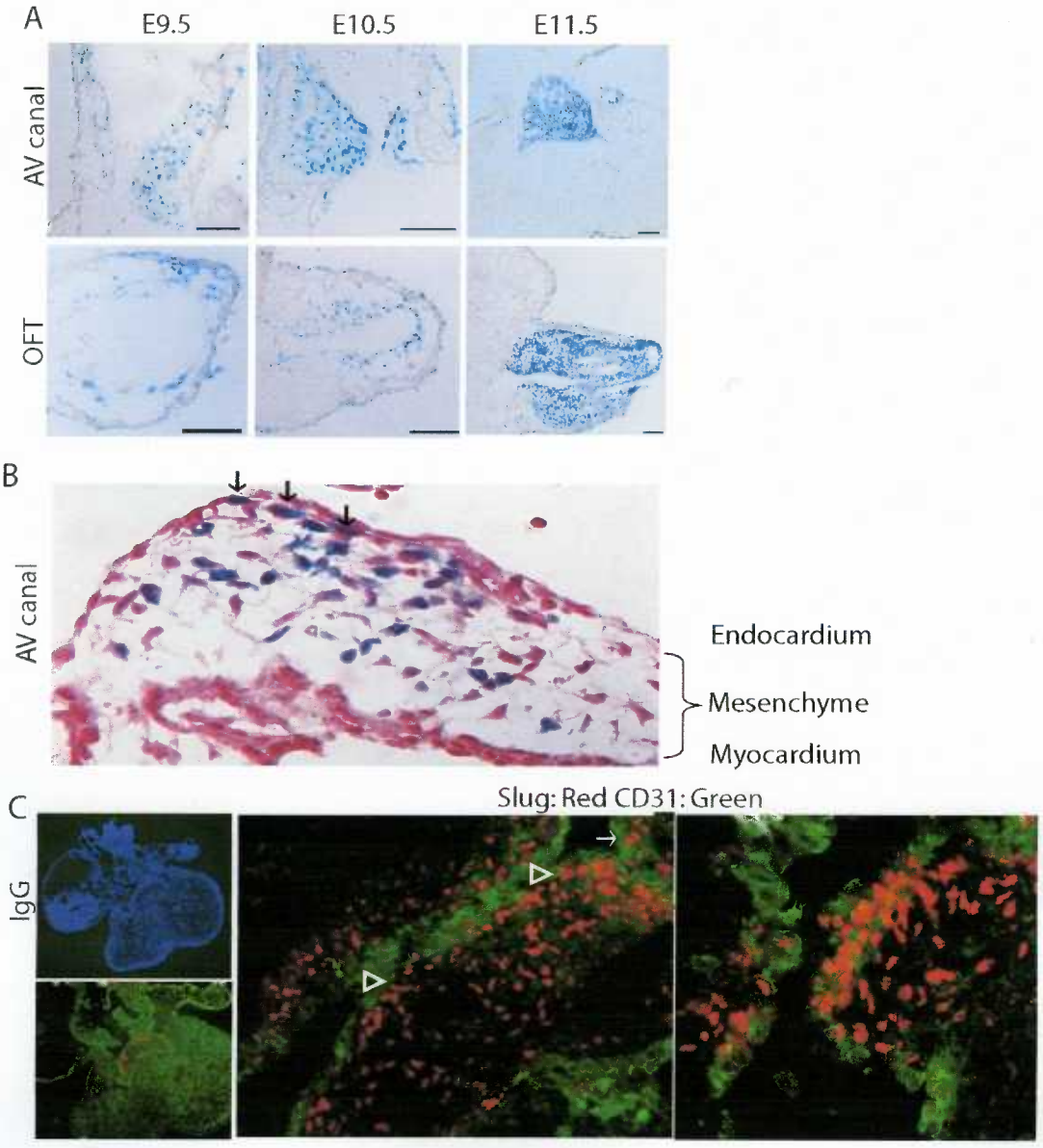


**Figure 4.3 *Slug* expression during mouse heart development.**
(A) Serial-sections through the AV canal and OFT of Slug-lacZ$^{+/-}$ hearts from E9.5 to E11.5. Scale bar represents 100 μm. (B) High magnification image of an AV canal cushion stained for Slug expression (Blue) and counterstained with Nuclear Fast Red. Arrows indicate Slug expressing cells with an elongated morphology at the endocardial surface. (C) Immunofluorescence staining for IgG (Small upper panel counterstained with DAPI) and Slug (Red) and CD31 (Green - endocardial marker) in E11.5 embryonic hearts, arrowheads indicate co-localization of Slug and CD31 in the cardiac cushion. Arrow indicates Slug expressing cells in the lateral cushion.

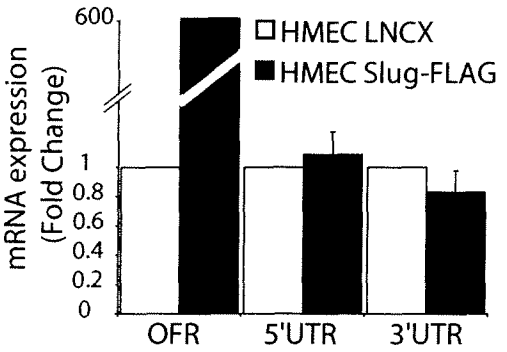


**Figure 4.4 Slug does not autoregulate its promoter.**
Analysis of mRNA expression by qRT-PCR for endogenous Slug expression by amplification of the 5' or 3' untranslated region (UTR) mRNA in HMEC ectopically expressing Slug (n = 3).

We next examined *Slug* expression during human heart development. However, due to the difficulties in collecting human embryonic tissue it was only possible to obtain tissue from approximately 9 weeks to 12 weeks of gestational age, which corresponds to E16.5 and later in the mouse. At these later stages the cardiac cushions have undergone remodeling and the heart valves are formed. However, it has been suggested that EndMT continues to take place to allow valvular remodeling later in development as well as in the adult (Armstrong and Bischoff 2004). To confirm a role for Snail family members in human, we examined the expression of *Snail* and *Slug* in embryonic human hearts at various developmental stages. As Figure 4.5 demonstrates, both *Snail* and *Slug* were expressed in the tricuspid and mitral valves, the atrioventricular septum, and the interatrial septum. This staining pattern was similar to *Slug* expression in later stages of mouse heart development (Oram et al. 2003). Higher-magnification images revealed that the mesenchymal cells of the valves, as well as endothelial cells at the root of the valves express *Snail* and *Slug* (Figure 4.5). As neural crest-derived cells have not been reported to populate the AV canal or the mitral and tricuspid valves, the expression of *Slug* during human heart development suggests that *Slug* has a conserved role in the initiation of cardiac EndMT during mammalian heart development.

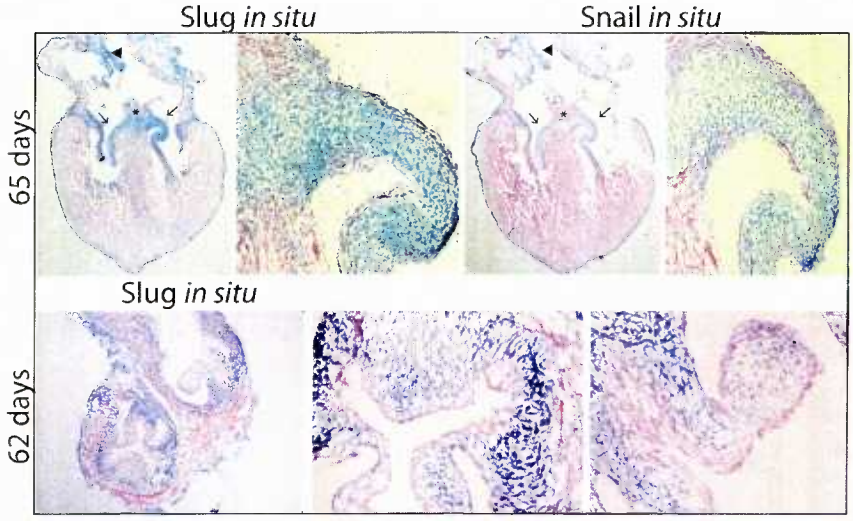


**Figure 4.5 *Snail* and *Slug* expression during human heart development.** *In situ* hybridization analysis of Snail and Slug mRNA expression (Blue) in a 65 day and Slug expression in a 62 day human embryonic heart that are counterstained with Nuclear Fast Red. (Arrow marks the mitral and tricuspid valves, the arrow head marks the interatrial septum, and the * marks the atrioventricular septum). High magnification images (panels on the right of low magnification images) demonstrate Slug expression in the mesenchyme of AV canal derived valves. Slug expression at 62 days also demonstrates Slug expression in the mesenchymal cells and a subset of endothelial cells on the OFT derived valves.

### 4.1.2 *Slug* is necessary for EndMT in the cardiac cushions

To determine whether targeted disruption of the *Slug* gene has a functional effect on endocardial cushion development, an AV canal explant assay was used (Runyan and Markwald 1983; Camenisch et al. 2002a). In this assay the AV canal of an E9.5 or E10.5 embryo is placed endocardial side down on a collagen gel and as EndMT is initiated the transformed mesenchymal cells invade and migrate into the collagen. Analysis of the number and the distance of the migrating cells give a direct measure of EndMT occurring in the AV canal. Insertion of *lacZ* into the *Slug* zinc finger domain inactivates the allele, and thus homozygous *Slug-LacZ* mutants behave as *Slug*-deficient ($Slug^{-/-}$) animals (Jiang et al. 1998; Inoue et al. 2002). Additionally, we have observed increased mortality in the first day after birth, a runt phenotype, pigmentation defects, and severe eye infections in the *Slug*-lacZ homozygous mice which are all published phenotypes of *Slug*-deficient mice. As shown in Figures 4.6A and 4.6B at E9.5 the *Slug*-deficient AV canal explants had significantly reduced migration and invasion compared to heterozygote or wild-type controls. Explants from *Slug*-deficient AV canals displayed either large endothelial outgrowths, not typically seen in the control AV canal explants, or significantly decreased numbers of migrating cells that had a rounded morphology (Figure 4.6A). The fact that a small population of rounded migrating cells can be observed in *Slug*-deficient AV explants suggests a primary defect in EndMT rather than a result of developmental delay in the *Slug*-deficient embryos. A similar reduction in the number of migrating cells and the appearance of a rounded cell morphology has been observed in the Notch1-deficient AV canal explants (Timmerman et al. 2004). In comparison, Hey2-deficient or Hey1/L-double deficient AV canal explants have a similar number of

migrating cells compared to wild-type controls, although the migrating cells fail to induce mesenchymal morphology (Fischer et al. 2007a). These data suggests that downstream targets of Notch signaling have two distinct roles, first to induce EndMT and second to induce mesenchymal morphology. Analysis of β-galactosidase activity in *Slug*-lacZ AV explants revealed *Slug* expression in the migrating mesenchymal cells and the proximal endocardial cells (Figure 4.6C). Interestingly, most of the migrating lacZ-positive cells showed rounded morphology consistent with a phenotype that is intermediate between endocardium and mesenchyme as previously described (Camenisch et al. 2002b). The intermediate phenotype is characterized by cells that still express endothelial markers, such as CD31 and VE-cadherin, but also express mesenchymal markers, such as smooth muscle actin.

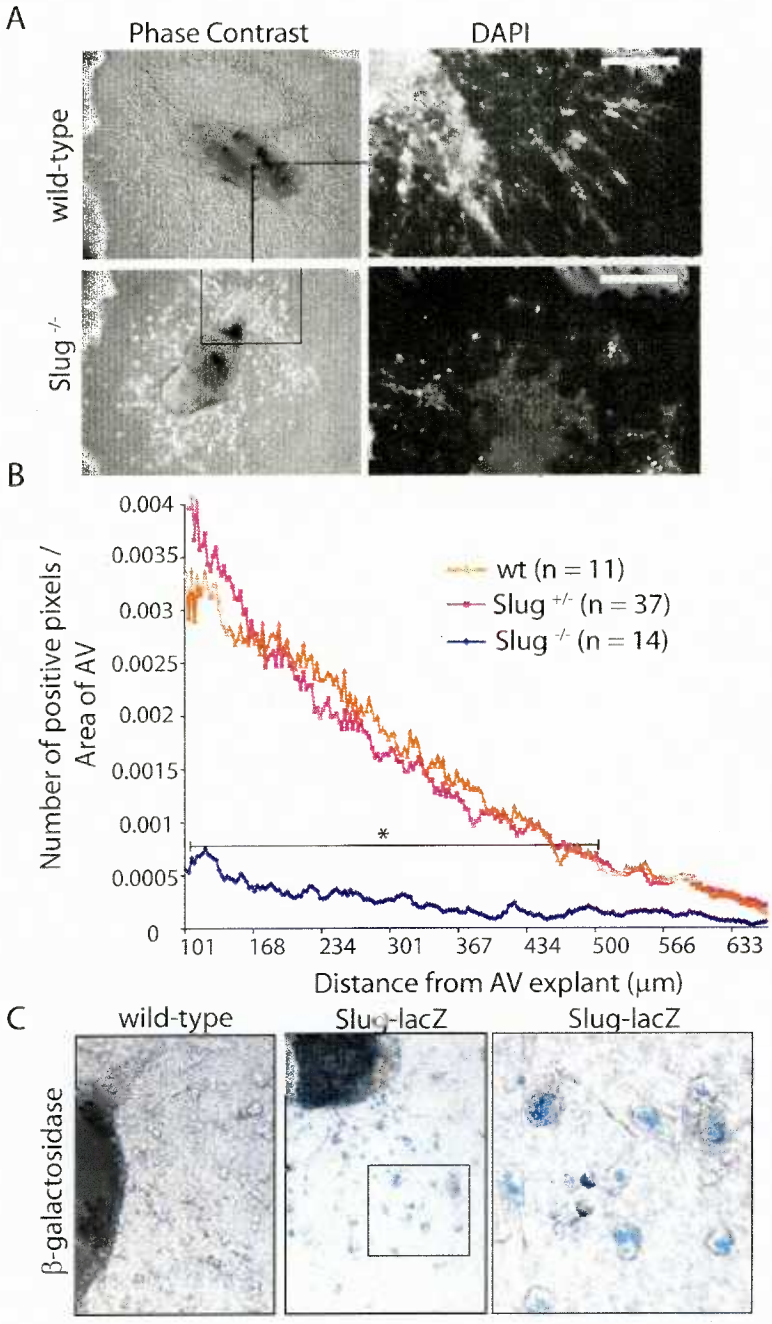


**Figure 4.6 Slug-deficiency results in AV canal EndMT defects at E9.5 *ex vivo*.**
(A) Representative images of a wild-type and Slug-deficient (Slug$^{-/-}$) AV canal explant after 48 hours in culture. Phase-contrast images show decease in cell number migrating after 48 hours. The cells that do migrate have a rounded non-mesenchymal morphology. The DAPI stained image reveals numerous migrating cells in the wild-type while the Slug-deficient has an endothelial outgrowth surrounded by single migrating cells. Scale bar represents 250 μm. (B) Analysis of EndMT of AV canal explants from E9.5 wild-type, Slug-heterozygous, and Slug-deficient embryos after 48 hours. Results are represented as distance of a pixel (nucleus) to the closest point of the AV canal and normalized to the size of the AV canal tissue. (C) Slug expression (lacZ-Blue) in AV canal explants, high magnification image (right panel) demonstrating Slug expression in migratory cells that have a rounded morphology.

To investigate whether Slug-deficient embryos have defects in cardiac cushion EndMT *in vivo*, E9.5 embryos were serially sectioned and the average total number of cells and the average number of proliferating cells in the AV canal cushions were counted. In this experiment pregnant mice were injected with 1500 mg/kg Bromodeoxyuridine (BrdU) at 5pm and embryos were collected at 7pm (late E9.5) to ensure EndMT had occurred in the AV canal. Both visual comparison and the analysis of the number of cells in the AV canal cushions demonstrated a clear reduction in cardiac cushion EndMT in *Slug*-deficient (n = 9) compared to wild-type (n = 9) embryos (Figure 4.7A and 4.7B). However, the percentage of AV canal endocardial cells and mesenchymal cells that were proliferating (BrdU positive) was not significantly different between wild-type (n = 3) and Slug-deficient (n = 3) embryos. During later stages of heart development the cardiac cushion undergoes extensive remodeling and fusion which is dependent upon EndMT derived cells. To determine whether *Slug*-deficient mice exhibited a defect in cardiac cushion maturation, embryonic hearts from wild-type (n = 8) and *Slug*-deficient (n = 6) mice were serially sectioned at E10.5 (between 8 and 20 sections for each heart). Sections were analyzed by quantifying the average minimum distance between the cushions, the length of fusion between the cushions, and the % cellularity of the cushions. Strikingly, none of the *Slug*-deficient hearts displayed fusion of the cushions at E10.5, while 6/8 wild-type hearts showed fusion of the cushions, resulting in an average maximum fusion length of ~90 μm in the wild-type hearts (Figure 4.8B). A delay in cardiac cushion fusion was also evident in the *Slug*-deficient embryos as demonstrated by a significant increase in the average distance separating the superior and inferior cushions (Figure 4.8C). However, the % cellularity of the cushions at E10.5 was similar between wild-type and *Slug*-deficient hearts (Figure 4.8D), suggesting the cellularity defect observed at

E9.5 was rescued. In the E10.5 heart the *Slug*-deficient cardiac cushions appear to be longer but thinner compared to the wild-type hearts, however, at E9.5 the AV canal cushions of wild-type and *Slug*-deficient embryos appear to be fused normally (Figure 4.7A and 4.8A). The reason for the fusion defect at E10.5 is unknown. The fusion process involves adhesion between the two endocardial layers in the lumen on the heart, followed by EndMT or apoptosis of the fused endocardial cells to form a single mesenchymal structure. Without a detailed analysis of the fusion process it is impossible to conclude the reasons for the fusion defect observed in E10.5 Slug-deficient embryos. These results demonstrated that there was a defect in the initiation of EndMT at E9.5, which cannot be explained by a delay in development. In addition, at E10.5 there was a defect in cardiac cushion fusion which indicates that the EndMT process and cardiac development is not occurring normally in *Slug*-deficient mice.

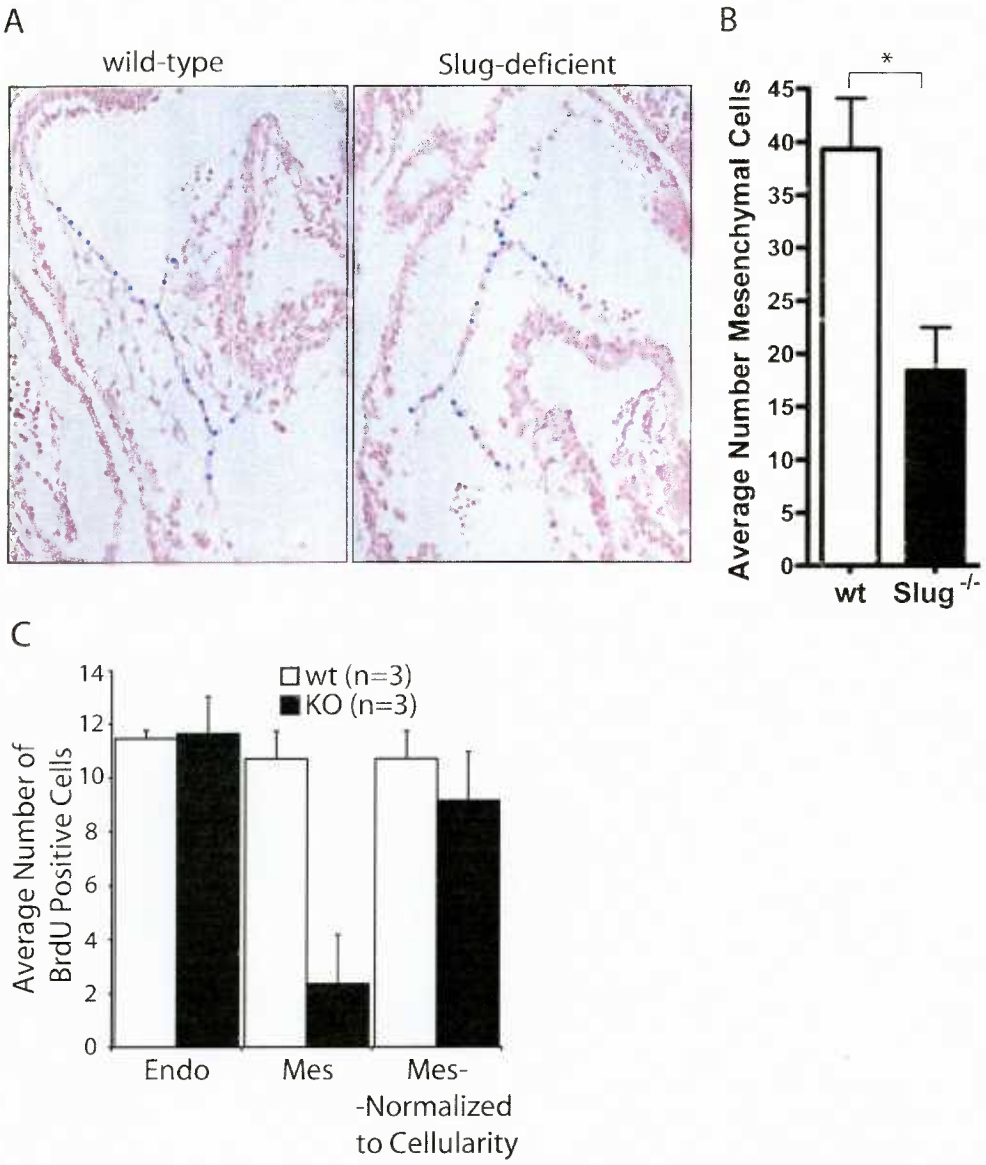


**Figure 4.7 Slug-deficiency results in AV canal EndMT defects at E9.5 *in vivo*.**
(A) Cross section of an E9.5 wild-type and Slug-deficient AV canal counterstained with Nuclear Fast Red. Blue dots outline the AV canal; notice the reduced number of mesenchymal cells in the Slug-deficient AV canal cushions. (B) Analysis of the average number of mesenchymal cells in the AV canal cushions in wild-type (n = 9) and Slug-deficient (n = 9) (Slug$^{-/-}$) embryos * $P < 0.05$. (C) Analysis of the average number of BrdU positive cells within the AV canal endocardium (Endo) and mesenchyme (Mes) in wild-type (n = 3) and Slug-deficient (n = 3) embryos, Slug-deficient mesenchyme data was also normalized to the average number of mesenchymal cells.

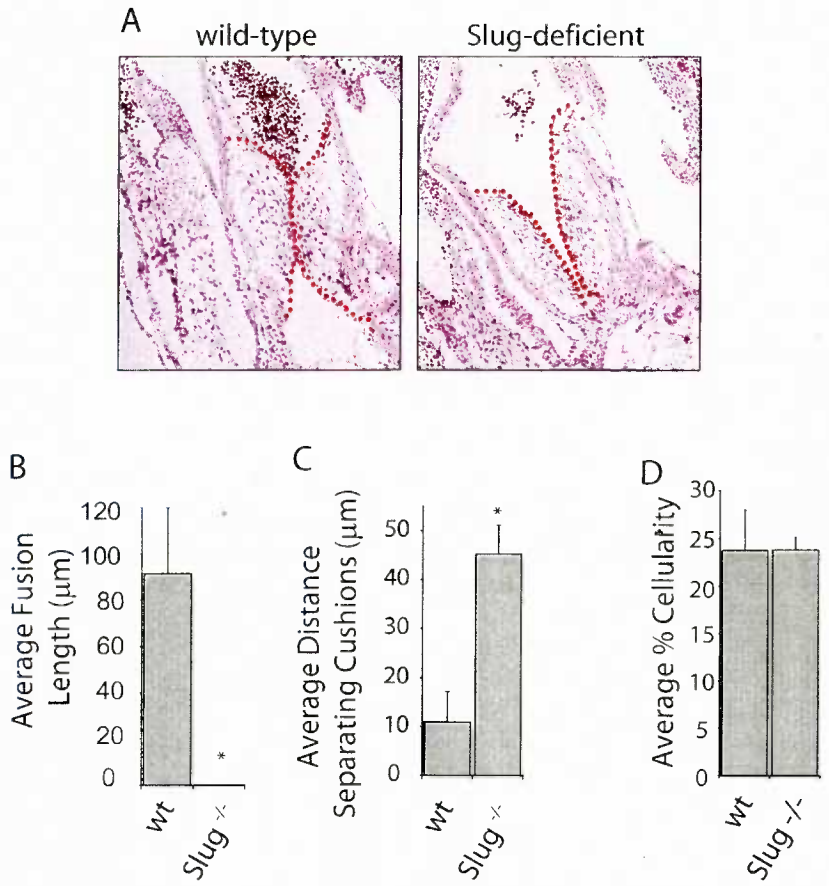


**Figure 4.8 Slug-deficiency results in AV canal fusion defects at E10.5 *in vivo*.**
(A) Cross section of an E10.5 wild-type and Slug-deficient AV canal counterstained with Nuclear Fast Red. Dotted red lines highlight the superior and inferior AV cushions. (*B*) Quantitation of the length of fusion of the superior and inferior cushions in wild-type (wt, n = 8) and *Slug*-deficient (n = 6) ($Slug^{-/-}$) embryos * $P < 0.05$. (8 to 20 serial sections for each heart) (C) Analysis of the average minimum distance separating the superior and inferior cushions in wild-type (wt, n = 8) and *Slug*-deficient (n = 6) ($Slug^{-/-}$) AV canals. * $P < 0.05$ (8 to 20 serial sections for each heart). (D) Analysis of the % cellularity in the superior and inferior cushions in wild-type (wt, n = 8) and *Slug*-deficient (n = 6) ($Slug^{-/-}$) AV canals (8 to 20 serial sections for each heart).

### 4.1.3 *Slug* represses endothelial cell phenotype

Given the findings demonstrating the requirement of *Slug* in cardiac EndMT, the role that *Slug* plays in modulating the endothelial phenotype was examined. HMEC and HUVEC transduced with vector control or Slug-expression constructs demonstrated that ectopic expression of Slug represses the expression of key endothelial genes such as *VE-cadherin*, *CD31*, and *Tie2* as determined by qRT-PCR, immunoblotting, and immunofluorescence (Figure 4.9A, 4.9B, 4.9C, and 4.9D). In contrast to activated Notch, Slug did not induce the mesenchymal markers *s*mooth muscle α-actin (SMA) and h1-calponin (Figure 4.9C). Similar results were also observed when Snail was ectopically expressed in endothelial cells (data not shown). These findings suggest that *Slug* promotes the initial phases of EndMT associated with the loss of endothelial phenotype but is not sufficient for the complete transition into a mesenchymal cell that is mediated by Notch activation. These findings were also compatible with the morphology of the *Slug*-expressing cells seen during EndMT in the AV canal, suggesting Slug is required for the downregulation of the endothelial phenotype.

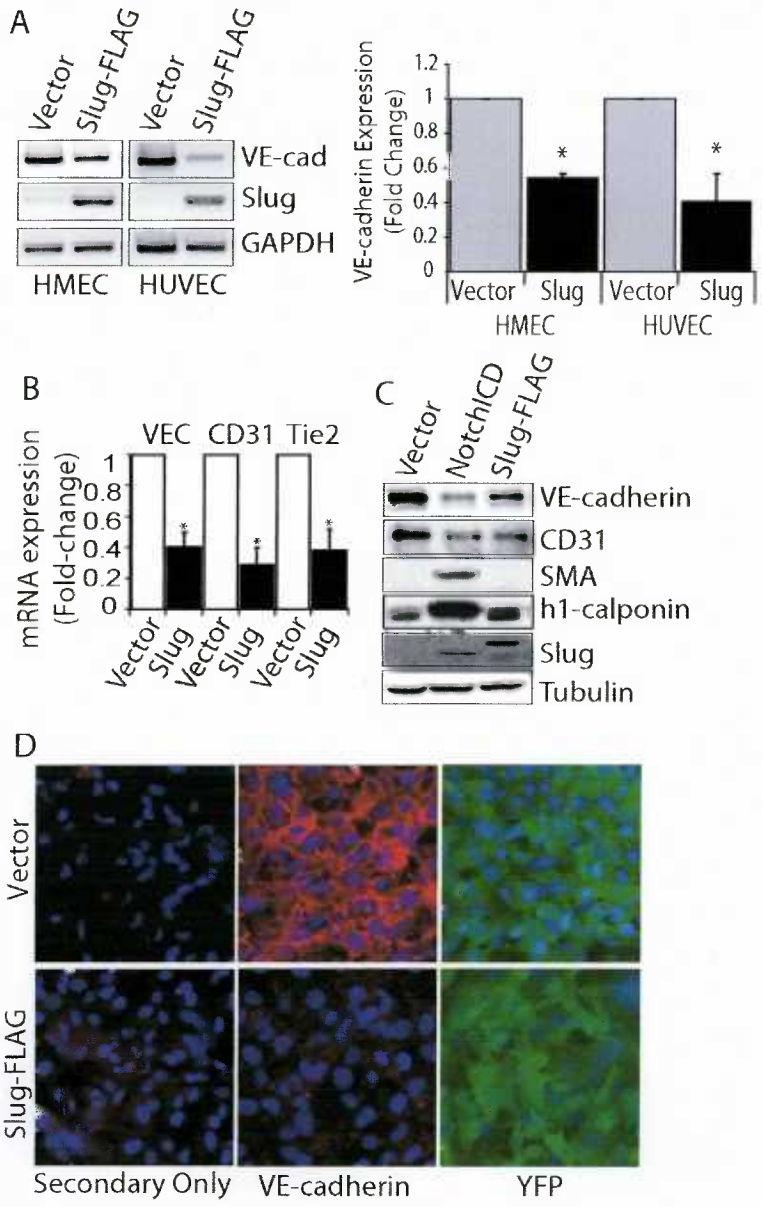


**Figure 4.9 Slug represses endothelial phenotype.**

(A) RT-PCR analysis of VE-cadherin expression in HMEC and HUVEC ectopically expressing Slug, graph represent densitometry from 3 independent batches cells, $P < 0.05$. (B) qRT-PCR analysis of VE-cadherin (VEC), CD31, and Tie2 expression in HMEC ectopically expressing Slug (n = 3), $P < 0.05$. (C) Analysis of protein expression in HMEC ectopically expressing Slug or Notch4ICD. Notice that overexpression of Notch4ICD or Slug in HMEC results in downregulation of VE-cadherin and CD31, however, in comparison to Notch4ICD Slug did not upregulate the mesenchymal markers smooth muscle actin (SMA) or h1-calponin. (D) Immunofluorescence staining for VE-cadherin in HMEC ectopically expressing Slug using a bicistronic vector where Slug is linked to yellow fluorescence protein (YFP) by an internal ribosomal entry sequence (IRES). Using this system Slug expression is indicated by YFP staining; cells were sorted for YFP expression and allowed to grow to confluence for 48 hours prior to immunofluorescence staining.

Targeted deletion of *Hey2* and double mutants of *Hey2* and *Hey1* or *Hey1* and *HeyL* has been shown to result in cardiac developmental defects (Fischer et al. 2004; Kokubo et al. 2004; Fischer et al. 2007a). It was therefore tested whether enforced expression of these key Notch targets, which act as transcriptional repressors, were capable of indirectly inducing *Slug* expression or repressing *VE-cadherin* expression. In contrast to *NotchICD*, enforced expression of *Hey1* and *Hey2* was not sufficient to upregulate *Slug* expression or repress *VE-cadherin* expression (Figure 4.10) or induce mesenchymal morphology (data not shown). This is in agreement with our previous data demonstrating Notch directly regulates Slug expression. Thus Notch acts through *Slug*, but not the *Hey* genes, to repress endothelial phenotype.

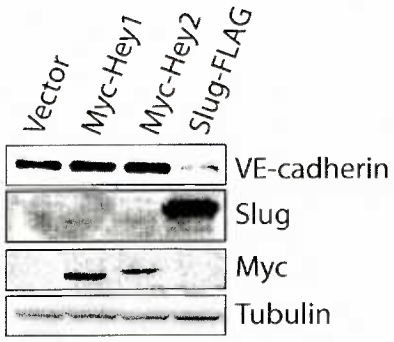


**Figure 4.10 Hey1 and Hey2 do not regulate *Slug* or *VE-cadherin* expression.**
Analysis of protein expression in HMEC ectopically expressing Hey1, Hey2, or Slug. Notice that Hey1 and Hey2 do not induce Slug expression or repress VE-cadherin expression.

VE-cadherin is a key endothelial adherens junction protein that is required for maintenance of endothelial homeostasis and must be downregulated prior to endothelial remodeling (Crosby et al. 2005). The Snail family of proteins selectively bind to E-box motifs (CANNTG) with high specificity for the E2-box element (CACCTG or CAGGTG) (Mauhin et al. 1993). Promoter analysis of *VE-cadherin* (-2000 to +100 of the TSS) identified three putative E2-box motifs 5' to the transcriptional start site (TSS) in the human VE-cadherin promoter (Figure 4.11) (Prandini et al. 2005). To examine whether *Slug* was capable of binding these sites, EMSA was performed using double-stranded oligonucleotides containing two of the three putative binding sites, located at -306 to -311 and -379 to -384. As Figure 4.12A demonstrates, *Slug* was capable of binding both of the E2-box motifs, but was unable to bind a CAGCTG E-box element located at -97 to -102 in the human *VE-cadherin* promoter. Similar to the CSL-FLAG EMSA, in the FLAG-M2 super-shift control lane, no super-shift band was visible; however, the disappearance of the shifted band (arrow) indicates a specific binding of Slug to the target sequence. In addition, the lack of a super-shift band may be due to the fact that the Slug-FLAG protein was preincubated with the antibody and the presence of the antibody can block DNA binding. In addition, the -379 to -384 mutant oligo competition assay partially blocked Slug binding, this was likely due to the base pairs mutated. In the -379 to -384 oligo only one base pair of the putative Slug binding site was mutated (***C***ACCTG to ***A***CCTG) however in the -306 to -311 oligo two base pairs of the putative Slug binding site were mutated (***C***ACCT***G*** to ***A***CCT***A***). Of the three E-box elements tested in the human *VE-cadherin* promoter, only the -379 to -384 E2-box and the -97 to -102 E-box motifs are conserved in the murine *VE-cadherin* promoter (Figure 4.11). However, there are additional E2 box motifs located more distally to the TSS in the mouse *VE-cadherin*

promoter. To demonstrate that the conserved *Slug* binding site was required for the ability of *Slug* to repress the *VE-cadherin* promoter the two conserved sites in the murine promoter were mutated in a luciferase reporter construct (**C**ANCT**G** mutated to **AA**NCT**A**). As Figure 4.12B demonstrated, when the *Slug* binding site was mutated the ability of Slug to repress *VE-cadherin* was significantly reduced. However, Slug still was capable of repressing the E2-box mutant compared to vector control, suggesting the E2-box motifs located more distally to the TSS may be functional Slug binding sites or the base pairs mutated did not fully block Slug binding. Consistent with the EMSA results, when the CAGCTG *cis* element, which does not bind *Slug*, was mutated there was no change in the ability of *Slug* to repress *VE-cadherin* (Figure 4.12B). These results demonstrate *VE-cadherin* is a direct transcriptional target of *Slug* in human and mouse endothelial cells.

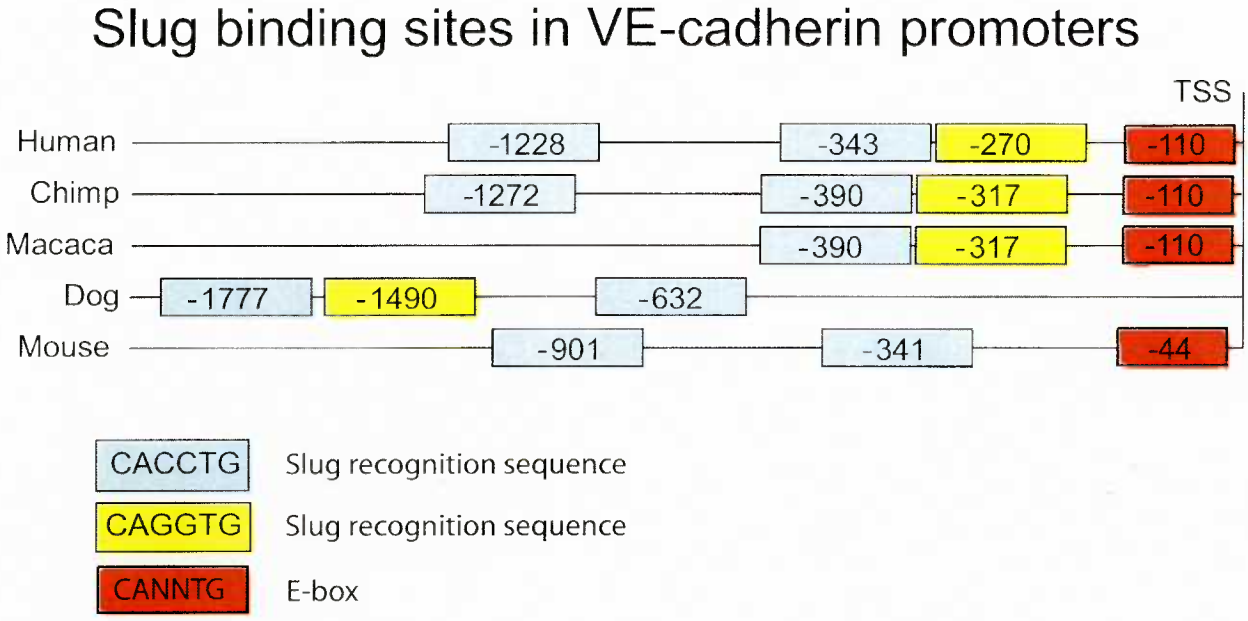


**Figure 4.11 *VE-cadherin* promoter analysis.**
Analysis of the VE-cadherin promoter (-2000 to transcriptional start site (TSS)) for putative Slug binding sites. Slug has been shown to preferentially bind the CACCTG or CAGGTG E2-box consensus sequence. The TSS of the human VE-cadherin promoter sequence is slightly different in the Ensemble genome browser compared to published results; in the following figures the published TSS will be used. Sequences used for the analysis were extracted using the Ensemble genome browser using the following Ensemble Gene ID's.
Human-(ENSG00000179776), Chimp-(ENSPTRG00000008190),
Macaca-(ENSMMUG00000023525), Dog-(ENSCAFG00000020413),
Mouse-(ENSMUSG00000031871).

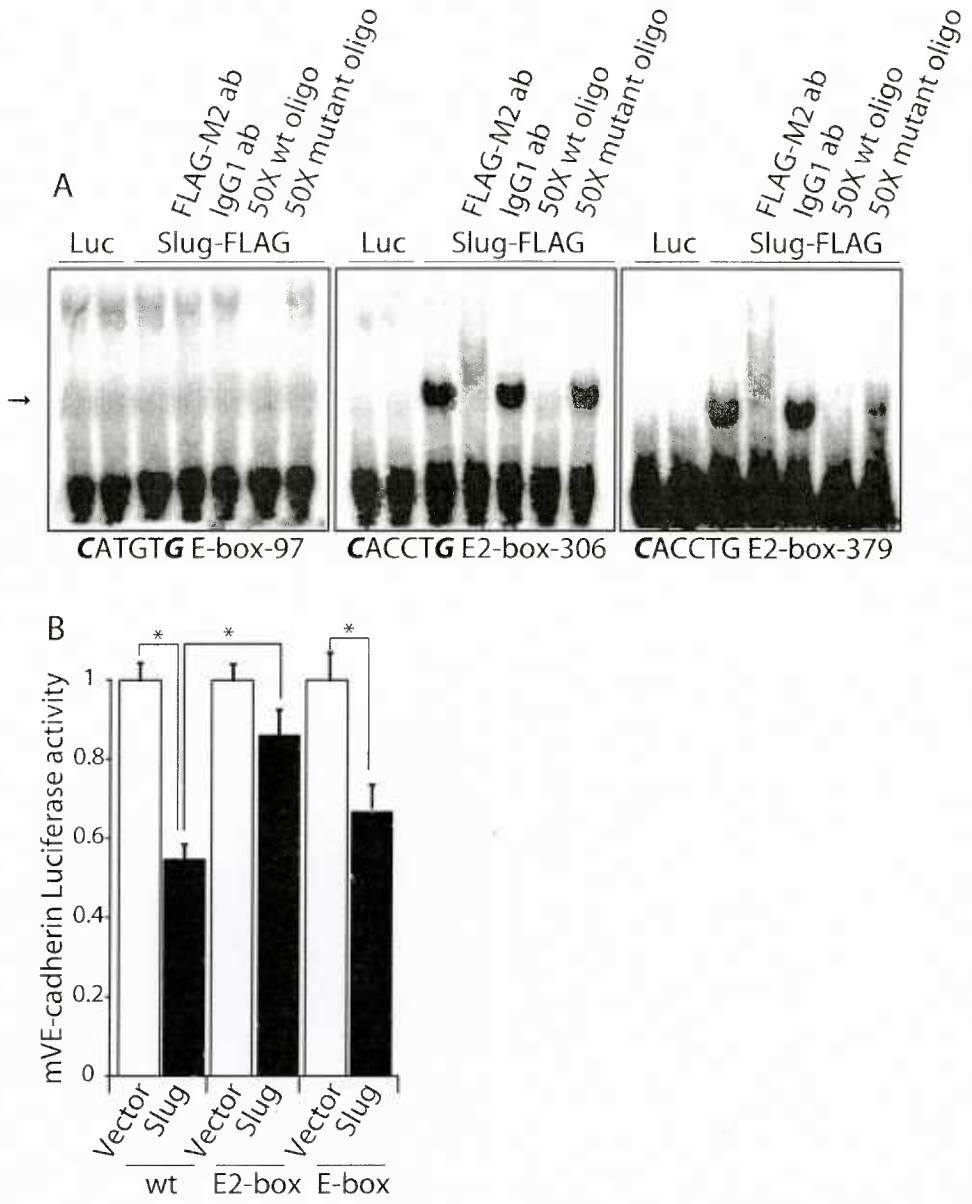


**Figure 4.12 Slug binds and regulates the *VE-cadherin* promoter.**
(A) Electrophoretic mobility shift assay (EMSA) for the Slug binding sites in the human VE-cadherin promoter. *In vitro* translated luciferase (Luc) or Slug-FLAG protein and $P^{32}$ labelled oligonucleotides for the E-box cys-element and the first two Slug E2-boxes binding sites in the human VE-cadherin promoter. Supershift α-FLAG-M2 or IgG control and competition assays with 50X wild-type or mutant probes are also included. Arrow indicates the bound oligonucleotides probe, confirming the Slug but not luciferase protein can bind the two E2-box elements but not the E-box element within the human VE-cadherin promoter. Nucleotides in **bold** were mutated to A in the competition assay. (B) VE-cadherin promoter activity in HMEC transfected with empty vector or Slug expression constructs. The conserved E2-box and E-box elements in the mouse VE-cadherin promoter were mutated from **C**ANNT**G** to **A**ANNT**A**. (n = 4 (12 total wells)), * $P < 0.05$. Notice the ability of Slug to repress the VE-cadherin promoter is reduced in the E2-box mutant.

### 4.1.4 Slug increases endothelial migration

The above findings imply a requirement for *Slug* in the downregulation of endothelial phenotype during cardiac cushion EndMT. Another hallmark of EndMT is the acquisition of a migratory phenotype which is required for the mesenchyme to invade the cardiac jelly (Hay 2005; Person et al. 2005). To determine whether *Slug* expression was sufficient to promote a motile phenotype in endothelial cells, an *in vitro* wound healing (scratch) assay was performed. In the wound healing (scratch) assay a confluent monolayer of HMEC cells transduced with vector control or *Slug* expression constructs was serum starved overnight to reduce proliferation and then a "scratch" is made in the monolayer. The cells at the scratch boundary were then allowed to migrate into the empty space for the next 24 hours while under serum free conditions to prevent proliferation. The scratch assay revealed increased migration of *Slug*-expressing endothelial cells as early as 4 hours and up to 24 hours following wounding of the endothelial monolayer, resulting in *Slug*-expressing cells migrating 1.96-fold ± 0.55 ($n = 4$, $P < 0.05$) further than the vector-transduced cells after 24 hours (Figure 4.13A and 4.13B). Platelet-derived growth factors (PDGF) have been shown to be expressed in the endocardial cushions during EndMT (Van Den Akker et al. 2005). In addition we have previously demonstrated that Notch activated cells have increased directed migration towards the chemokine PDGF-BB (Noseda et al. 2004). Using a modified Boyden chamber assay with PDGF-BB (20 ng/ml) present in the lower chamber *Slug*-expressing endothelial cells showed significantly increased directed migration towards PDGF-BB (Figure 4.13C). Thus, *Slug* expression increases motility and directed migration of endothelial cells.

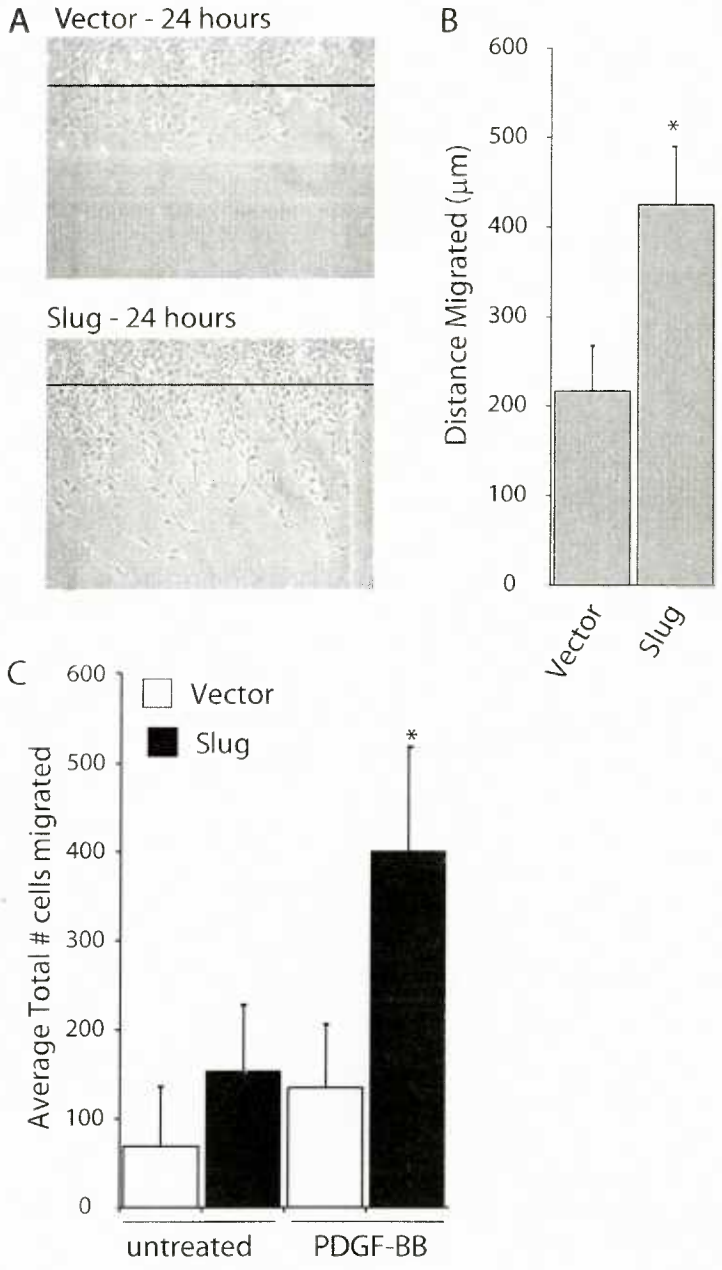


**Figure 4.13 Slug expression increases endothelial migration.**
(A) Phase contrast images of vector control or Slug ectopically expressing HMEC 24 hours after the endothelial monolayer was scratched. Black line represents the edge of scratch boundary at time 0. (B) Quantitation of the average distance of cell migration after 24 hours of migration. (n = 4) * $P < 0.05$. (C) Quantitation of the directed migration after 4 hours towards PDGF-BB (20 ng/ml) of vector control or Slug ectopically expressing HMEC in a modified Boyden chamber assay. Bars represent the total average number of cells migrated after 4 hours (n = 6). * $P < 0.05$.

Another critical step during EndMT requires that the transforming/transformed endothelial cells acquire the ability to survive without cell-cell contacts. *Slug* has been shown to have an anti-apoptotic function in both hematopoietic and epithelial cells (Inukai et al. 1999; Inoue et al. 2002; Kajita et al. 2004). The first clue that Slug has a survival function in endothelial cells was the observation that shRNA-mediated knockdown of *Slug,* but not *CSL*, in NotchICD-transduced HMEC resulted in massive cell death (Figure 4.14A). Due to the high cell death in the NotchICD cells transduced with the sh*Slug* construct it was impossible to detect *Slug* knockdown, however, in the vector control cells, which have low basal expression of *Slug*, *Slug* was successfully knocked down by 70% (Figure 4.14B). To determine whether Slug could protect endothelial cells against apoptosis, as has previously shown with Notch activation (MacKenzie et al. 2004b), apoptosis was induced in endothelial cells transduced with vector control or Slug-expression constructs. A neutral red assay was used to measure the number of viable cells after a prolonged treatment with an apoptotic agent, while Annexin-V staining was used to test for the initial phase of membrane instability after short apoptotic stimulation. In both methods apoptosis was induced by treating cells with lipopolysaccharide (LPS) as the apoptotic stimulus and the calpain inhibitor ALLN to block survival pathways and promote apoptosis (MacKenzie et al. 2004b). These methods demonstrated that enforced expression of NotchICD and Slug protects endothelial cells against lipopolysaccharide-induced apoptosis, as measured by neutral red incorporation (Figure 4.15A) or Annexin-V labeling (Figure 4.15B). Collectively, these data suggest that *Slug* has three roles during cardiac cushion EndMT; first to initiate transdifferentiation of endothelial cells in response to Notch activation, second to ensure the survival of trans-differentiated endothelial cells, and third to promote migration of the transdifferentiated cells.

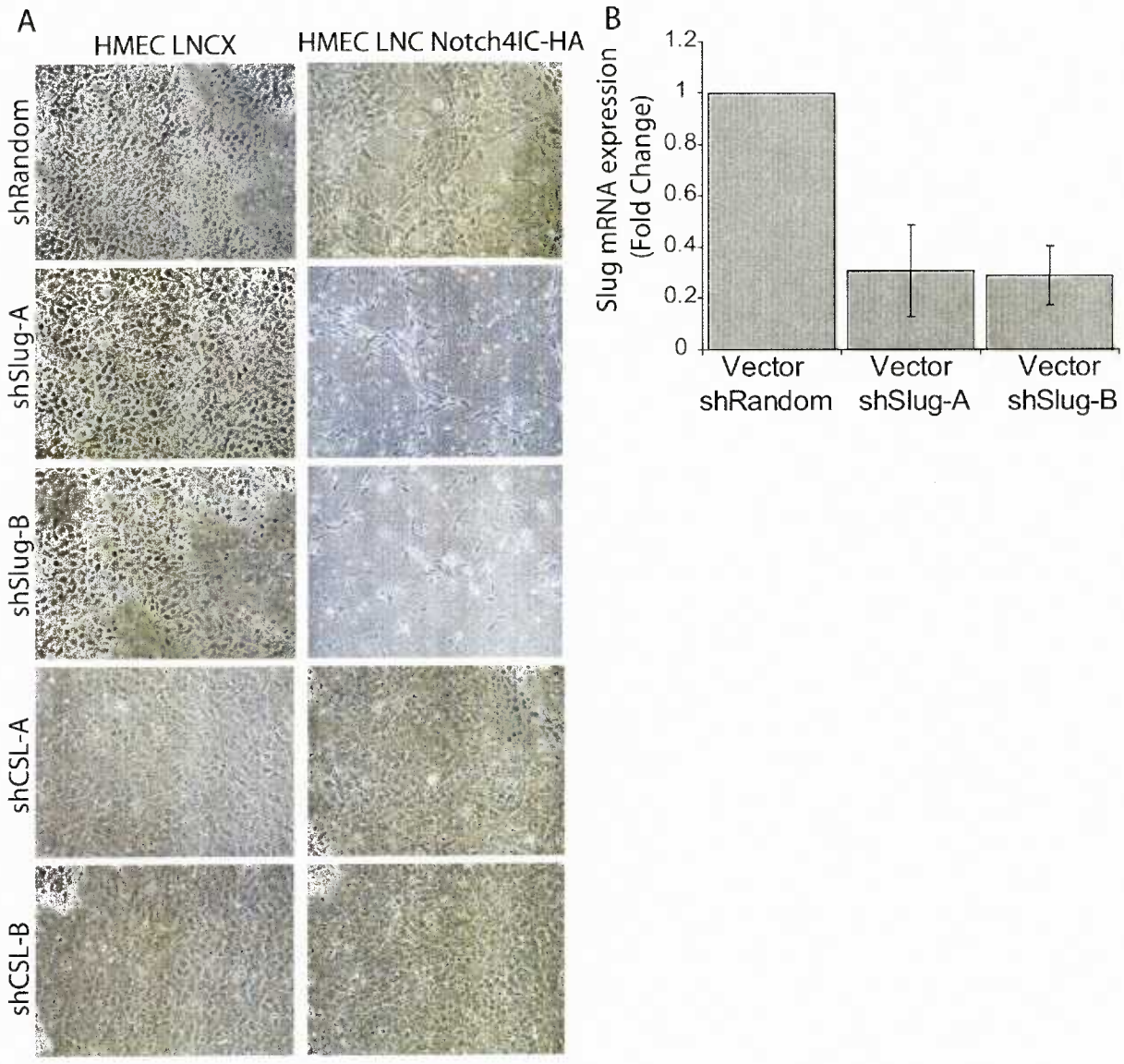


**Figure 4.14 Slug protects Notch activated endothelial cells from apoptosis.**
(A) Phase contrast images of vector control or Notch1ICD ectopically expressing HMEC transduced with lentiviral shRNA constructs against Slug or CSL. Notice the cell death and reduced cell numbers in cells that have combined Notch1ICD and shSlug-A or shSlug-B transduction. (B) qRT-PCR analysis of Slug mRNA expression in HMEC vector control cells transduced with shRandom, shSlug-A, or shSlug-C constructs.

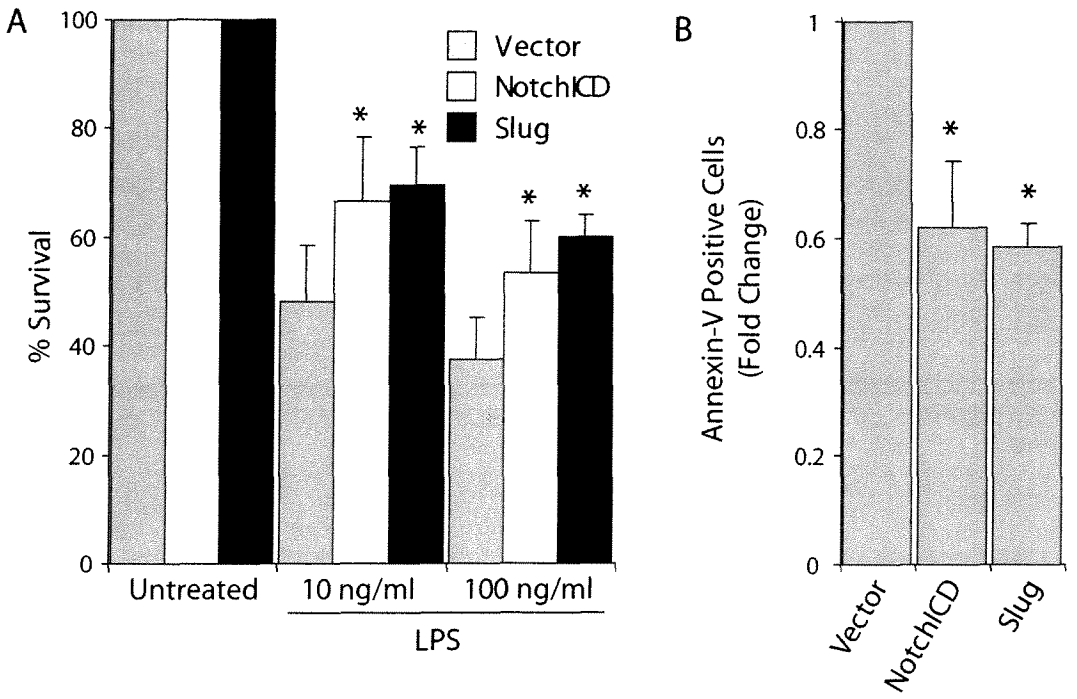


**Figure 4.15 Slug protects endothelial cells from cell death.**
(A) Neutral red analysis of cell survival in vector control, NotchICD, or Slug ectopically expressing HMEC treated with various concentrations of LPS (n = 3, each experiment performed in triplicate). * $P < 0.05$ for NotchICD- or Slug-expressing cells compared to vector-transduced cells. (B) Annexin-V-staining for apoptotic cells in vector control, NotchICD, or Slug ectopically expressing HMEC treated with LPS (100 ng/ml) (n = 3). * $P < 0.05$ for NotchICD- or Slug-expressing cells compared to vector-transduced cells.

# *Chapter 5*

# SNAIL COMPENSATES FOR SLUG-DEFICIENCY

## 5.1 Abstract

*Slug*-deficiency in both mice and humans is typically associated with defects in neural crest derived structures. Our analysis of *Slug* expression and its role during EndMT demonstrates a critical role of *Slug* during heart development. However, no obvious heart defects are observed in *Slug*-deficient mice. The Snail family members have long been speculated to function in a similar manner and compensate for each other in tissues where they are co-expressed (Nieto 2002; Murray et al. 2007). Analysis of *Snail* and *Slug* downstream targets has revealed that Snail and Slug regulate the expression of many of the same target genes (Sefton et al. 1998; Seki et al. 2003; Kajita et al. 2004). In addition, ectopic expression of either Snail or Slug in epithelial cells results in the same outcome, EMT (Castro Alves et al. 2007). As our data demonstrate a clear defect in EndMT in both the AV canal explant assay and in the cardiac cushion *in vivo*, we sought to investigate whether *Snail* was compensating for *Slug*-deficiency.

A recently published manuscript demonstrated that 50% of *Slug*-deficient mice die at birth due to defects in palate formation that results in a cleft palate and the inability to eat (Murray et al. 2007). The cleft palate phenotype was further increased to 100% in a *Slug*-deficient plus *Snail*-heterozygous background (Murray et al. 2007) Furthermore, it was demonstrated that in *Snail*-heterozygous mice *Slug* expression was increased in the

developing palate (Murray et al. 2007). These results demonstrate that *Snail* functionally compensates for *Slug*-deficiency and there was an increase in *Slug* expression in *Snail*-heterozygous mice during palate development. In contrast, we demonstrate that *Snail* expression is increased in the heart of *Slug*-deficient embryos and that *Snail* functionally compensates for *Slug*-deficiency during cardiac development.

### 5.1.1Notch and TGFβ act synergistically to induce *Snail* expression

As discussed in the Introduction, the TGFβ pathway is required for EndMT and regulation of Snail family genes during heart development (Romano and Runyan 2000; Camenisch et al. 2002a; Wang et al. 2005). Additionally, the Notch and TGFβ pathways have been shown to co-regulate target gene expression in some cell types, including endothelial cells (Blokzijl et al. 2003; Zavadil et al. 2004). To investigate the relationship between the Notch and TGFβ pathways and Snail family member expression, endothelial cells co-cultured with vector- or Dll4-expressing cells were treated with TGFβ2 (2.5 ng/ml). Maximal activation of the TGFβ pathway was observed at this concentration (Figure 5.1A). A time-course of TGFβ2 treatment in control and Dll4-activated HMEC cells revealed that TGFβ2 stimulation induced maximal induction of *Snail* mRNA and protein expression after 2 hours of treatment in control cells followed by a rapid downregulation (Figure 5.1B and 5.1C). Although, Dll4 stimulation alone did not induce *Snail*, combined activation of the Notch and TGFβ pathways resulted in a synergistic increase of *Snail* mRNA levels and maintenance of expression for at least 8 hours after stimulation with TGFβ2 (Figure 5.1B). Protein expression of Snail peaked slightly later (4 hours) and at a much higher level in the

context of Dll4 and TGFβ2 co-stimulation compared to TGFβ2 stimulation alone (Figure 5.1C). Furthermore, Snail protein expression in response to Dll4 and TGFβ2 co-stimulation was maintained for at least 10 hours at a level that was similar to the 2 hour peak level when cells were stimulated with TGFβ2 alone (Figure 5.1C). In contrast, there was minimal induction of Slug by TGFβ2, while Notch activation alone dramatically upregulated Slug (Figure 5.1B). Co-stimulation by Dll4 and TGFβ2 did not increase the level of Slug induction over that seen with Dll4 alone (Figure 5.1B, 5.2A, 5.2B).

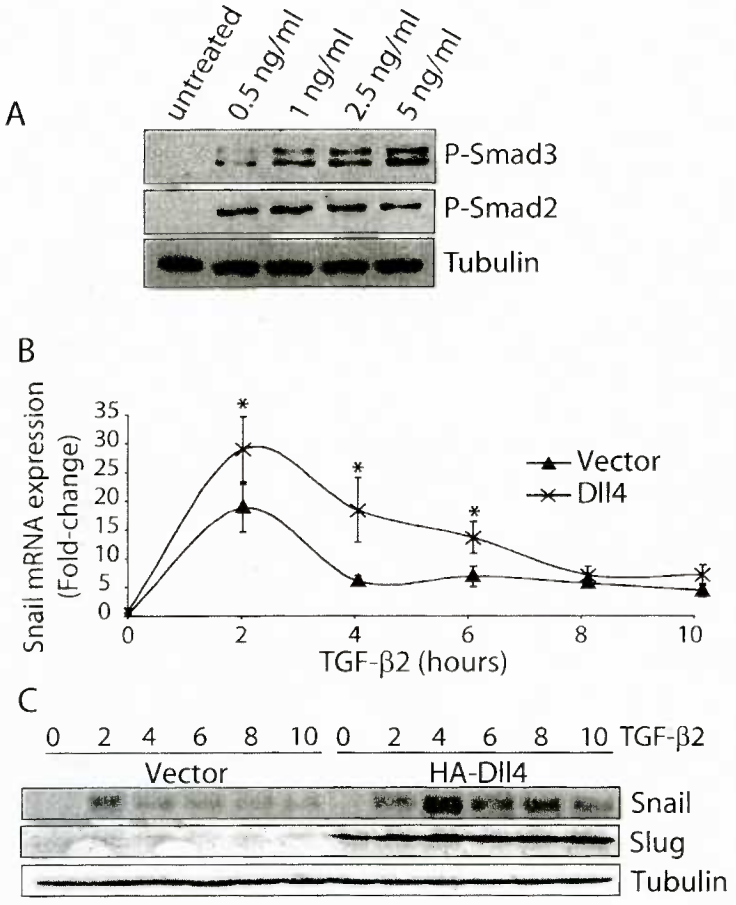


**Figure 5.1 Notch and TGFβ synergistically induce *Snail* expression.**
(A) Analysis of phosphorylated Smad2 and Smad3 protein levels in HMEC treated with various doses of TGFβ2 for 1 hours. (B) qRT-PCR analysis for Snail expression in control or Notch activated (Dll4) HMEC treated with TGFβ2 (2.5 ng/ml) at various time points (n = 3) * $P$ <0.05. (C) Analysis of Snail and Slug protein expression in control or Notch activated HMEC treated with TGFβ2 (2.5 ng/ml) at various time points. Note the synergistic induction and prolonged expression of Snail mRNA and protein expression in Notch activated TGFβ2 treated HMEC.

To further investigate the role of Notch activation in TGFβ-mediated induction of Snail expression, the γ-secretase inhibitor DAPT was used to block ligand-activated Notch signaling. Because DAPT blocks γ-secretase activity it potentially influences many other proteins and pathways. In addition to Notch receptors, γ-secretase is known to be involved in cleaving E-cadherin (Marambaud et al. 2002), Ephrin-B1 (Tomita et al. 2006), ErbB-4 (Ni et al. 2001), CD44 (Murakami et al. 2003), and the amyloid precursor protein (Evin et al. 1995). However, DAPT is commonly used to study the effects of the Notch pathway and the TGF-β time course clearly demonstrate that *Slug* and *Snail* were regulated by the Notch and TGFβ pathways, respectively.

TGFβ2 or TGFβ1 treatment dramatically upregulated the expression of *Snail* in control HMEC and the addition of DAPT did not affect the ability of TGFβ2 or TGFβ1 to induce *Snail* expression, consistent with Notch-independent induction (Figure 5.2A ad 5.2B). In the context of combined Notch and TGFβ2 or TGFβ1 activation, the synergistic upregulation of *Snail* expression was reduced by DAPT to the level seen by TGFβ2 or TGFβ1 stimulation alone (Figure 5.2A and 5.2B). TGFβ2 or TGFβ1 had minimal effects on *Slug* levels, and the addition of DAPT abrogated *Slug* induction by *Dll4*, suggesting a complete dependence on Notch activation for *Slug* upregulation (Figure 5.2A and 5.2B). As expected, stimulation of endothelial cells with TGFβ2 or TGFβ1 induced expression of the TGFβ target gene, *Smad7* to similar levels in control and Notch activated cells (Figure 5.2A and 5.2B). Addition of DAPT appeared to block the ability of TGFβ2 or TGFβ1 to induce *Smad7*, but the results were variable and did not reach statistical significance for TGFβ2 or TGFβ1 (Figure 5.2A and 5.2B), suggesting a minimal role for Notch activation in TGFβ-

induced *Smad7* induction. *Hey1* expression was induced by Notch, TGFβ2, or TGFβ1 and was dependent upon active Notch signaling, as demonstrated by reduced expression in presence of DAPT (Figure 5.2A and 5.2B). *Hey1* was also synergistically induced to very high levels by TGFβ2 or TGFβ1 and *Dll4* (Figure 5.2A and 5.2B). *Hey1* has previously been shown to be synergistically induced by Notch and *BMP4* or *BMP6* (Dahlqvist et al. 2003; Itoh et al. 2004). To test if the synergistic induction of *Snail* by Notch and TGFβ was specific to the TGFβ family of ligands, Notch-activated cells were treated with BMP2. BMP2 was used as it has been demonstrated to be highly expressed in the AV canal myocardium during cardiac cushion EndMT, and BMP2 signaling deficient embryos have AV canal EndMT defects (Ma et al. 2005; Rutenberg et al. 2006). As Figure 5.3 demonstrates, when control HMEC were treated with two different concentrations of BMP2 (20 ng/ml or 50 ng/ml) there was a strong induction of *Snail* expression and only a minimal induction of *Slug* expression. However, in comparison to TGFβ1/2, activation of the BMP2 pathway did not synergistically activate *Snail* expression in Notch activated cells. In comparison to *Snail* expression, there was clear synergistic activation of *Hey1* expression by Notch and BMP2 activation (Figure 5.3). In addition, BMP2 treatment robustly induced *SMAD6* expression, a known BMP2 target gene (Figure 5.3). The above findings clearly confirm that *Slug* is a direct target of Notch while *Snail* is not; however, *Snail* is synergistically induced when Notch activation is superimposed on TGFβ, but not BMP2, stimulation.

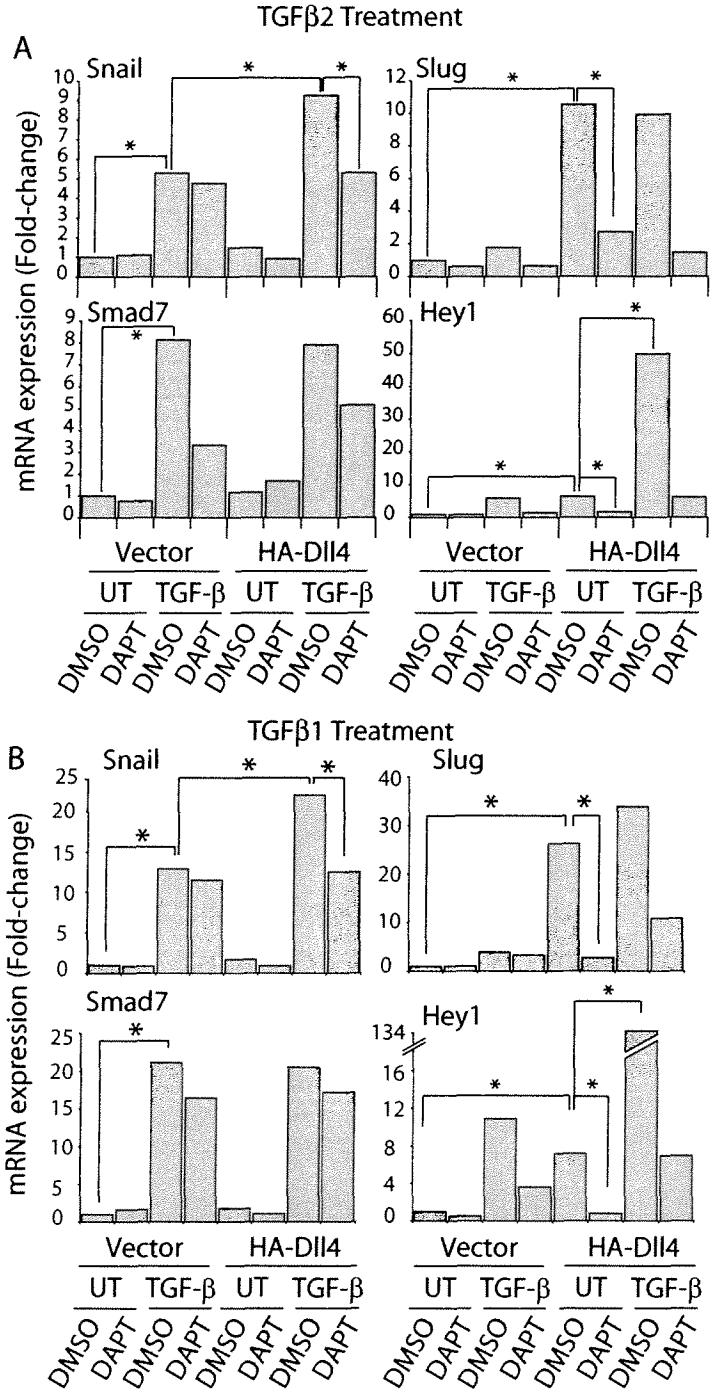


**Figure 5.2 Notch and TGFβ Synergistically Induce Snail and Hey1 Expression.**
qRT-PCR analysis for mRNA expression in HMEC vector control (Vector) or Notch activated cells (HA-Dll4) pre-treated with DMSO or the Notch inhibitor DAPT for 16 hours, followed by a 2 hour treatment vehicle control (UT), TGFβ2 (2.5 ng/ml) (A), or TGFβ1 (2.5 ng/ml) (B). (n = 3) $P < 0.05$. Note that the synergistic induction of Snail by the Notch and TGFβ pathways is blocked by the addition of DAPT.

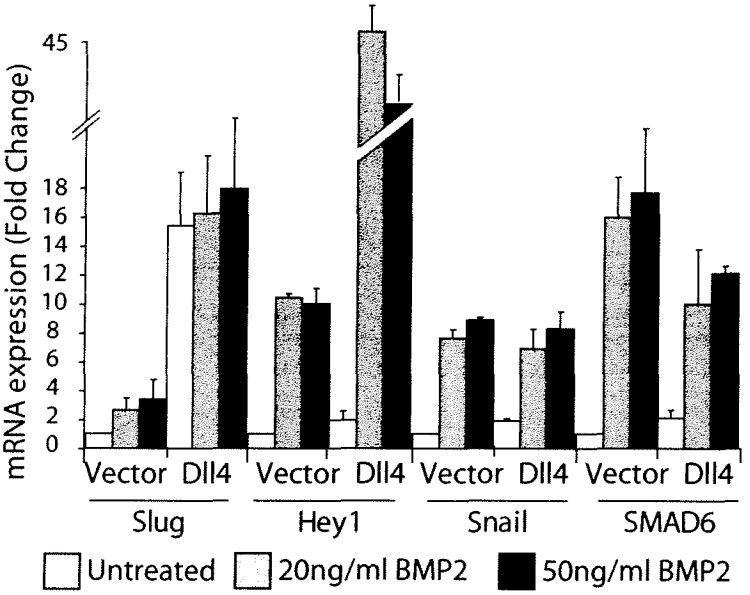


**Figure 5.3 Notch and BMP2 do not Synergistically Induce Snail Expression.**
qRT-PCR analysis of vector control or Notch activated (Dll4) HMEC treated with 20 ng/ml or 50 ng/ml BMP2 for 3 hours. Note that there is a synergistic induction of Hey1 but not Snail in Notch activated BMP2 treated HMEC (n = 3).

### 5.1.2 Activation of the Notch pathway results in increased Smad3 expression

Crosstalk between the Notch and TGFβ pathways involves the interaction of the NotchICD/CSL complex and the Smad proteins for the regulation of Notch target gene expression (Blokzijl et al. 2003; Dahlqvist et al. 2003; Itoh et al. 2004; Zavadil et al. 2004). However, the results just described demonstrate a synergistic induction of *Snail*, a TGFβ target gene, by combined activation of the Notch and TGFβ pathways. Furthermore, analysis of the *Snail* promoter revealed no stringent CSL binding sites (TGGGAA), although in two of the *Snail* promoters there was a single more permissive CSL binding site (Figure 3.5B). To further investigate the mechanism for the synergistic regulation of *Snail,* the hypothesis that the Notch pathway regulates expression of TGFβ pathway components that result in the hyperactivation of the TGFβ pathway was examined. To investigate the activity of the TGFβ pathway, immunofluorescence for Smad3 in vector control or Notch activated cells treated with TGFβ1 was performed. Smad3 was chosen because it is the main downstream target of TGFβ signaling (Massague et al. 2005). Immunofluorescence for Smad3 demonstrated an increase in nuclear Smad3 levels in vector control cells treated with TGFβ1 (Figure 5.4A). In Notch-activated cells, increased nuclear Smad3 was observed in the absence of TGFβ1 treatment and with TGFβ1, nuclear Smad3 increased to an even higher level than in vector control cells (Figure 5.4A). Further analysis of Smad1, Smad2, and Smad3 protein expression confirmed that both the total and the phosphorylated level of Smad3 were dramatically increased in Notch-activated cells (Figure 5.4B and 5.5). However, the mRNA induction of *Smad3* was much less dramatic in Dll4 co-cultured HMEC (Figure 5.4C). In addition, qRT-PCR and immunoblotting demonstrated that *Smad1* and *Smad2* expression

decreased in Notch-activated cells (Figure 5.4B, 5.4C, and 5.5). Smad1 and Smad5 are the main downstream targets of BMP signaling in endothelial cells while Smad2 and Smad3 are the main downstream targets of TGFβ signaling (Massague et al. 2005). The finding of increased Smad3 levels and decreased Smad1 and Smad2 levels is consistent with the synergistic activation of *Snail* expression by Notch and TGFβ1/2 but not BMP2 treatment. This area of research is currently being investigated by another Karsan lab member.

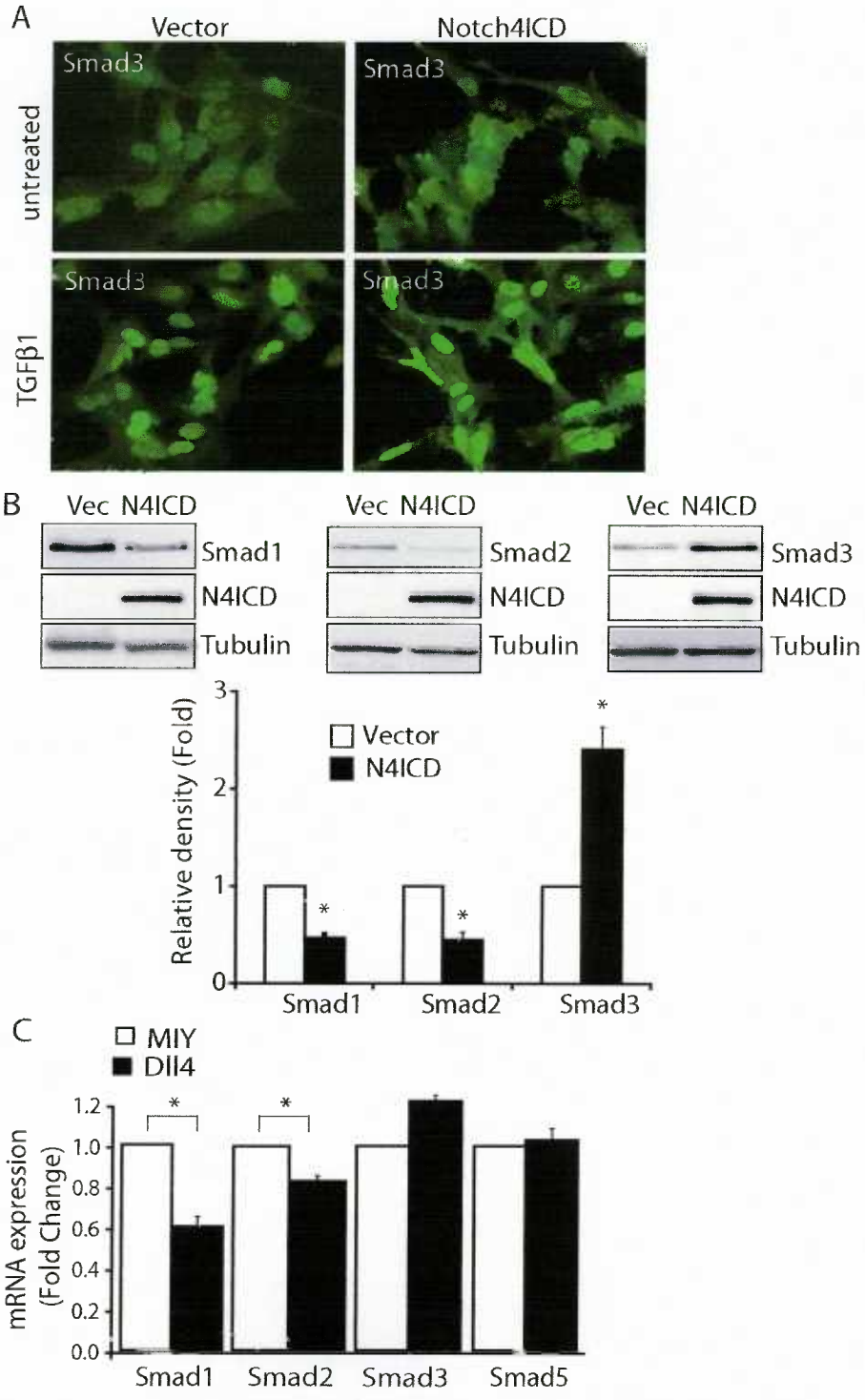


**Figure 5.4 Activation of the Notch pathway modulates the TGFβ pathway.**
(A) Smad3 immunofluorescence in vector control or Notch4ICD ectopically expressing HMEC treated with TGFβ1 (1 ng/ml) for 1 hours. Note that there is increased nuclear Smad3 after TGFβ1 treatment and increased Smad3 in Notch4ICD-expressing cells with and without TGFβ1 treatment. (B) Analysis of Smad1/2/3 protein expression in vector control or Notch4ICD ectopically expressing HMEC. Graph represents densitometry from 3 independent batches of HMEC * $P < 0.05$. (C) qRT-PCR analysis of Smad1/2/3/5 expression in vector control or Notch activated (Dll4) HMEC. (n = 3) * $P < 0.05$.

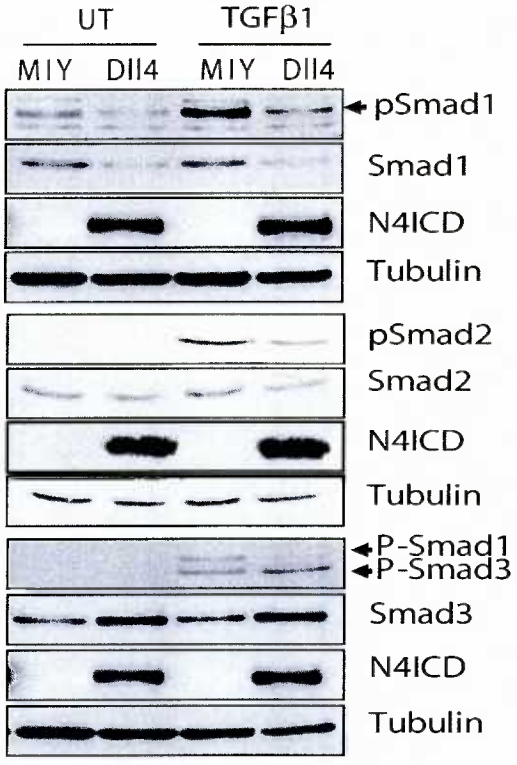


**Figure 5.5 Activation of the Notch pathway activates Smad3- and represses Smad1- and Smad2-dependent signaling.**

Analysis of protein expression of vector control of Notch activated (Dll4) HMEC untreated (UT) or treated with TGFβ1 (1 ng/ml) for 1 hours. Note that the total and phosphorylated (p) levels of Smad1 and Smad2 decrease in Notch activated cells with or without TGFβ1 treatment. In comparison total and phosphorylated levels of Smad3 increase in Notch activated cells with or without treatment of TGFβ1.

### 5.1.3 *Snail* and *Slug* cooperatively induce cardiac EndMT

The results described above demonstrate that *Slug* expression is solely regulated by Notch signaling, while Notch and TGFβ but not BMP2 signaling cooperatively induce *Snail* expression. Given that the *in vivo* phenotype observed in the *Slug*-deficient mice is less dramatic than the effect seen in the AV canal explant studies (Figure 4.6A and 4.6B), we sought to determine whether *Snail* was compensating for the absence of *Slug in vivo*. To test this hypothesis RNA was extracted from E9.5, E10.5, and E11.5 wild-type and *Slug*-deficient hearts followed by qRT-PCR analysis for *Snail*, *Slug*, *Hey1*, and *Hey2* mRNA expression. Interestingly over the three days of development analyzed, *Slug* expression increased steadily, while *Snail* expression remained constant or even decreased (Figure 5.6A). One possibility for this result was that induction of Snail expression occurs prior to E9.5 and therefore was missed in this analysis. This analysis further revealed a relative increase in *Snail* and *Hey2* expression in *Slug*-deficient hearts at E10.5 and E11.5 (Figure 5.6B), while there was no consistent change in *Hey1* (Figure 5.6B). Analysis of *Snail* expression by *in situ* hybridization at E10.5 and E11.5 revealed *Snail* expression in the AV canal and OFT in both wild-type and $Slug^{-/-}$ hearts (Figure 5.6C). Taken together the qRT-PCR and *in situ* hybridization data suggest that the domain of *Snail* expression was not expanded in *Slug*-deficient hearts, but rather that the cells normally expressing *Snail* do so at a higher level.

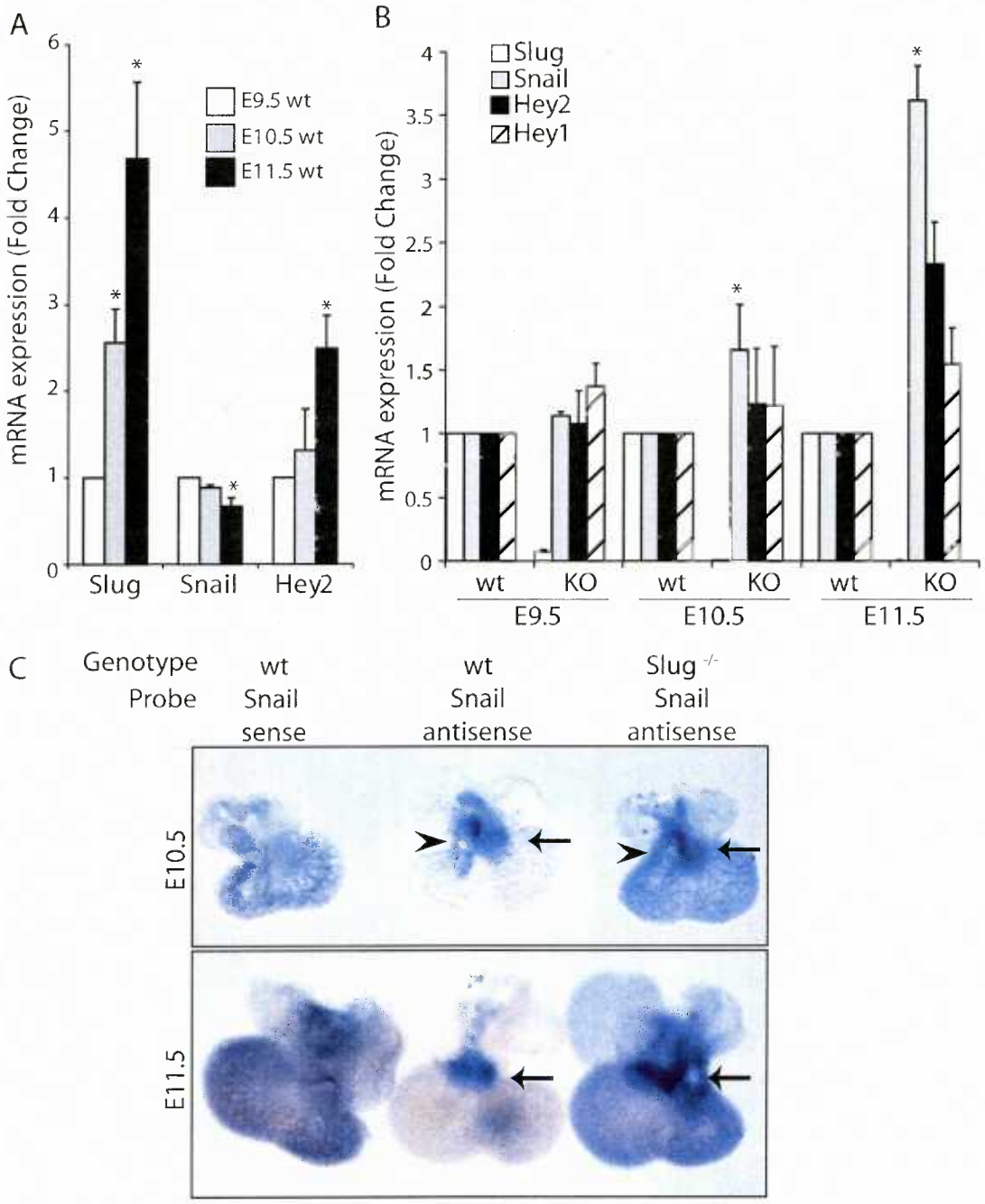


**Figure 5.6. Increased *Snail* expression in *Slug*-deficient hearts.**
(A) qRT-PCR analysis for Snail, Slug, and Hey2 mRNA expression in whole hearts isolated from E9.5, E10.5, and E11.5 wild-type embryos. Expression is normalized to E9.5 hearts sample (n = 3) * $P < 0.05$. (B) qRT-PCR analysis for Snail, Slug, Hey2, and Hey1 in whole hearts isolated from E9.5, E10.5, and E11.5 wild-type embryos. Expression is normalized wt hearts for developmental stage (n = 3) * $P < 0.05$. (C) *In situ* hybridization for Snail expression in E10.5 and E11.5 wild-type (wt) and Slug-deficient ($Slug^{-/-}$) hearts. The far left heart at E10.5 and E11.5 were probed with Snail sense probes. Arrows indicate the AV canal and arrowheads indicate the outflow tract.

The data presented in Chapter 4 demonstrate a dramatic EndMT defect in *Slug*-deficient AV explants at E9.5 (Figure 4.6A and 4.6B) and Figure 5.6 demonstrates there was an increase in *Snail* expression at E10.5 at E11.5 in *Slug*-deficient hearts (Figure 5.6B). To determine whether the enhanced *Snail* expression could compensate for *Slug*-deficiency, AV canal explants were performed at E10.5 when no difference in cushion cellularity was observed *in vivo* (Figure 4.8A and 4.8B). As Figure 5.7A demonstrates, there was no significant defect in EndMT between wild-type and *Slug*-deficient embryos at E10.5 in the AV canal explant assay. In contrast to the E9.5 AV explants where most of the wild-type migrating cells had typical fibroblastoid mesenchymal morphology, only a small percentage of migrating cells in the E10.5 AV explants had typical mesenchymal morphology and a large percentage had a rounded morphology. This could suggest that there was a reduced level of EndMT at E10.5 or that the transition from the rounded intermediate morphology to mesenchyme requires additional factors that are expressed at lower levels at E10.5. For example, *VEGF* is involved in negatively regulating EndMT and its expression becomes restricted to the AV canal myocardium at E10.5. Given the increased Snail expression in *Slug*-deficient embryos and the increased TGFβ activity in Notch-activated cells we next determined whether the TGFβ pathway, potentially through *Snail*, could compensate for *Slug*-deficiency at E9.5. Treatment of E9.5 AV canal explants with TGFβ2 (5 ng/ml) completely rescued the EndMT defect previously seen in E9.5 *Slug*-deficient embryos (Figure 5.7C). These data support the hypothesis that the TGFβ pathway through induction of *Snail* expression compensates for the absence of *Slug* expression and also implies that TGFβ does not require *Slug* to propagate cardiac EndMT.

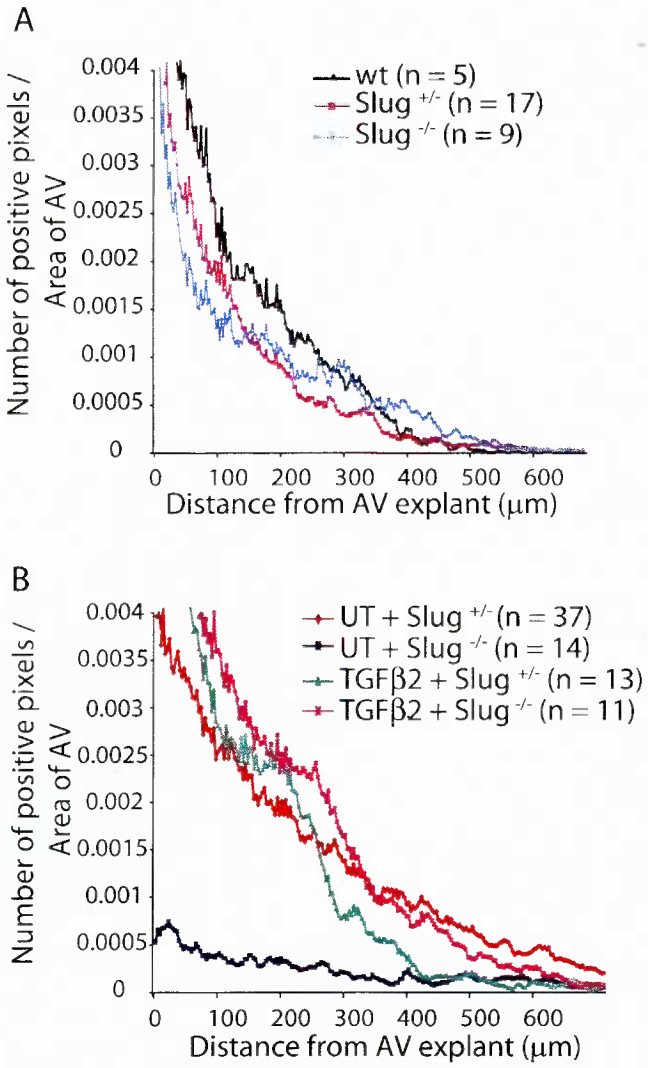


**Figure 5.7 TGFβ2 rescues the Slug-deficient AV canal EndMT defect.**
(A) Quantitation of EndMT in AV canal explants from wild-type (wt), Slug-heterozygous ($Slug^{+/-}$) and Slug-deficient ($Slug^{-/-}$) embryos at E10.5. Notice there is no obvious EndMT defect at E10.5 in comparison to the previous data at E9.5. (B) Quantitation of EndMT in AV canal explants from E9.5 wild-type (wt), Slug-heterozygous ($Slug^{+/-}$), and Slug-deficient ($Slug^{-/-}$) embryos treated with TGF-β2 (5 ng/ml) or vehicle (UT). Note that the TGFβ2 treatment rescues the EndMT defect at E9.5.

To further investigate the possibility that *Snail* compensates for the absence of *Slug*-deficiency after E9.5 in the cardiac cushions, lentiviral-delivered shRNA was used to knock down *Snail* expression in *Slug*-deficient AV canal explants at E10.5. The effective knock down of *Snail* expression by the sh*Snail* was first tested in SVEC cells (Figure 5.8A) and transduction efficiency of the shSnail lentivirus was tested in the AV canal explant assay (Figure 5.8B). Knock down of *Snail* in wild-type or *Slug*-heterozygous AV canal explants did not result in a decrease in the number or distance of migrating cells at E10.5 (Figure 5.8C). In contrast, knockdown of *Snail* in *Slug*-deficient AV canal explants resulted in a significant reduction in the number of migrating/invading cells (Figure 5.8C). These data support the redundancy of *Slug* and *Snail* during the later stages of EndMT in the cardiac cushions, and suggest that parallel activation by the Notch and TGFβ pathways is required to maintain the appropriate level of expression of Snail family members in order for cushion development to proceed. It has previously been suggested that Snail family members bind and regulate their own promoters (Nieto 2002). To test whether Slug directly regulates *Snail* expression in endothelial cells, *Snail* expression in *Slug*-expressing or TGFβ2-treated HMEC was analyzed. These results demonstrated that ectopic *Slug* expression does not result in repression of *Snail* expression, nor does it affect the ability of TGFβ to induce *Snail* expression (Figure 5.9A). Additionally, it has recently been shown that Slug does not regulate the *Snail* promoter (Peiro et al. 2006). Analysis of *Slug*-deficient hearts revealed an increase in *Hey2* expression, in a similar pattern to *Snail*, which could suggest increased Notch signaling in the AV canal was responsible for the increased *Snail* expression. Interestingly expression of *Hey2* but not *Hey1* or *HeyL* was decreased in HMEC overexpressing Slug (Figure 5.9B) However, *Hey2* expression is not limited to the AV canal and the whole embryonic heart was used in this

analysis, therefore it is difficult to make the conclusion that the Notch pathway was hyperactive in *Slug*-deficient embryos. These results also demonstrate that Snai3 expression is not regulated by either the Notch or TGFβ pathways.

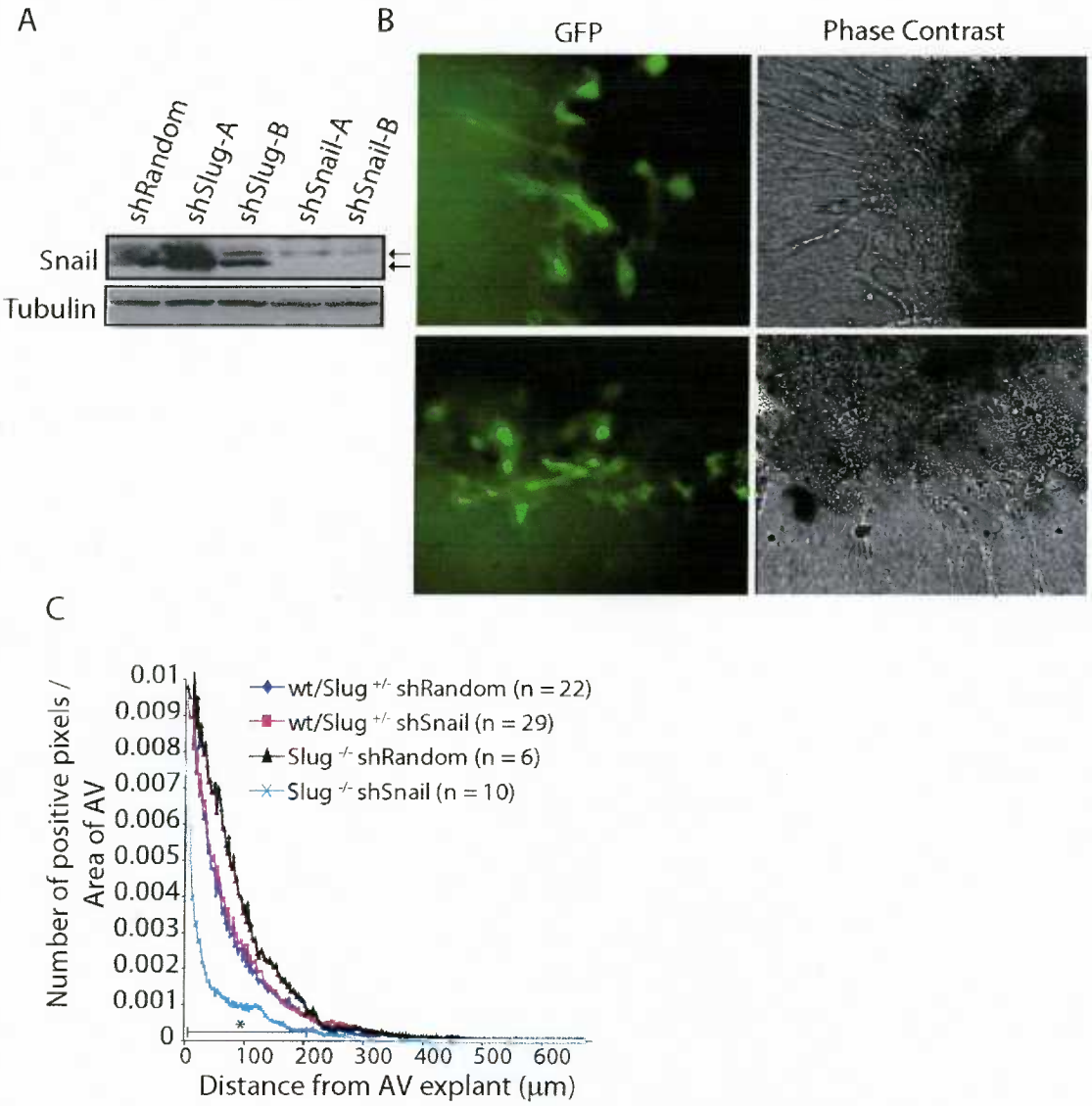


**Figure 5.8 Increased Snail expression compensates for Slug-deficiency.**
(A) Efficient knock down of Snail protein expression in SVEC by a lentiviral shRNA technique by two different shRNAs. Upper arrow indicates nonspecific band, lower arrow indicates Snail. (B) GFP fluorescence and phase contrast images of an AV canal explant transduced with the shSnail construct. (C) Quantitation of EndMT in AV canal explants for E10.5 wild-type (wt) and Slug-heterozygous ($Slug^{+/-}$) or Slug-deficient ($Slug^{-/-}$) embryos that have been transduced with shRandom or shSnail. Note that when Snail is knocked down in Slug-deficient AV canal explants there is a reduction in the number of migrating cells.

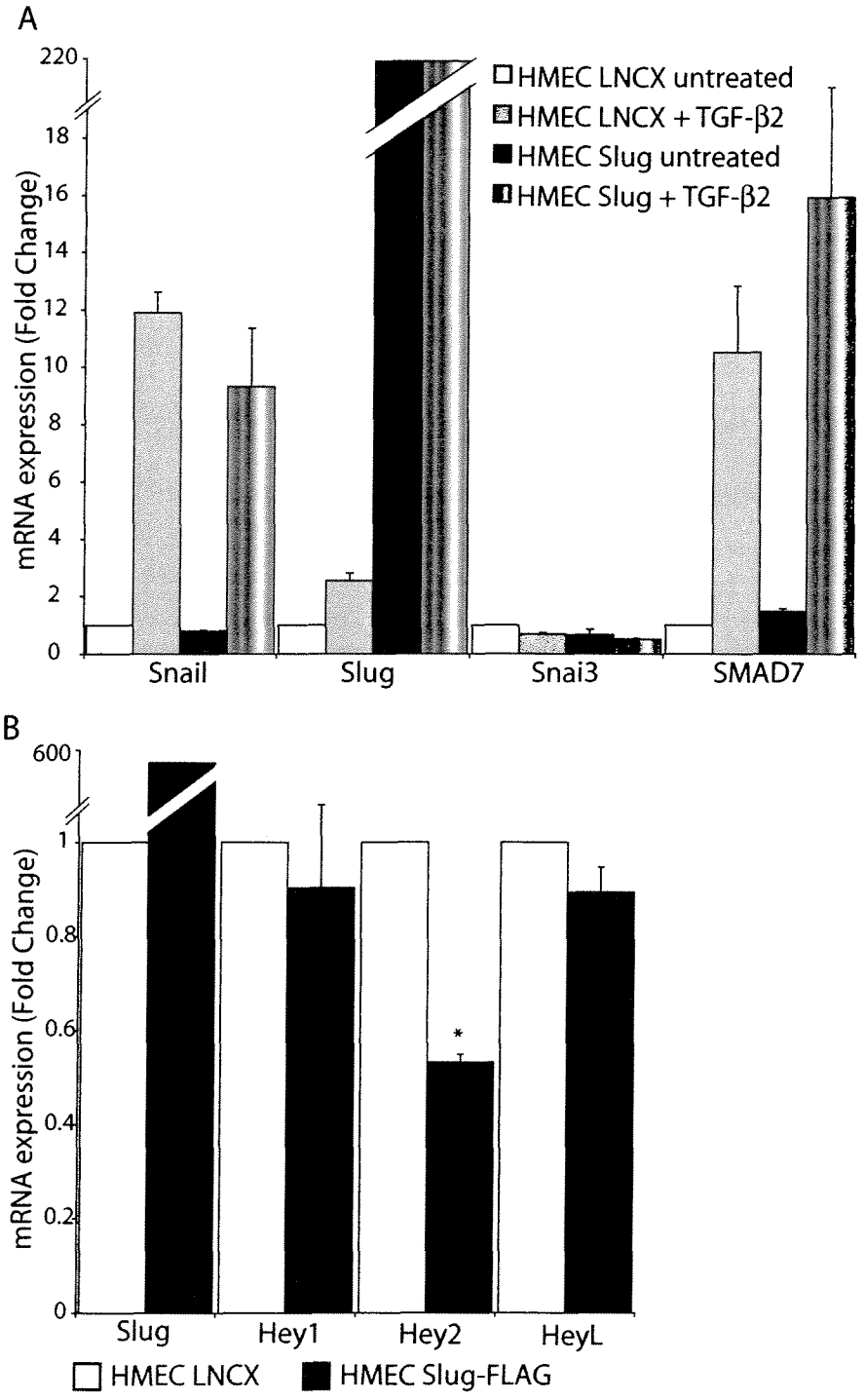


**Figure 5.9 Slug does not affect Snail expression.**
(A) qRT-PCR analysis for mRNA expression in vector control or Slug ectopically expressing HMEC untreated (UT) or treated with TGFβ2 for 2 hours. Notice the overexpression of Slug does not repress Snail expression or affect the ability of TGFβ2 to induce Snail expression. (B) qRT-PCR analysis for mRNA expression in vector control or Slug-expressing HMEC. Note that the overexpression of Slug represses Hey2 but not Hey1 or HeyL expression.

# *Chapter 6*

## SUMMARY, PERSPECTIVES, AND FUTURE DIRECTIONS

Data presented in this thesis reveal several important findings during mammalian heart development. First, we clarified the signaling cascades initiated by the Notch and TGFβ pathways during cardiac cushion EndMT. We demonstrated that the Notch pathway regulates *Slug* but not *Snail* expression in endothelial cells. In comparison, TGFβ regulates *Snail* but not *Slug* expression and combined activation of Notch and TGFβ pathways synergistically upregulates *Snail* expression. We further demonstrated that *Slug* is a direct binding target of CSL, showing that *Slug* belongs to the growing list of direct targets of the Notch pathway. In addition, the synergistic induction of *Snail* expression was possibly due to increased *Smad3* levels and hyperactivation of the TGFβ pathway caused by Notch signaling. It has previously been demonstrated that in *Notch1*- or *CSL*-deficient embryos there is reduced expression of *TGFβ2*, *TGFβRII*, and *Snail* suggesting Notch may regulate the TGFβ pathway upstream of the activation of the Smad proteins. These data and others have demonstrated complex crosstalk between the Notch and TGFβ pathway components. Not only do the Notch and TGFβ pathways regulate expression of each others' components but also key downstream components physically interact to co-regulate target gene expression. This makes dissecting the precise mechanism by which *Snail* is synergistically upregulated by the Notch and TGFβ pathways a very challenging task.

It should be noted that in *Notch1*-deficient and *CSL*-deficient embryos, the heart is severely underdeveloped and the reduced expression of *TGFβ2* and *TGFβRII* observed may represent a developmental delay and not a regulation by the Notch pathway (Timmerman et al. 2004). As Notch signaling controls several other aspects of heart development, blocking Notch signaling specifically in the AV canal endocardium would be required to dissect the relationship between the Notch signaling and *TGFβ2*, *TGFβRII*, *Smad3,* and other TGFβ components in the AV canal endocardium. Furthermore, the reduced expression of *Snail*, or of any mesenchymal marker, in the *Notch1*-deficient and *CSL*-deficient embryos is not surprising as EndMT is not initiated in these embryos and *Snail* expression is only found in the mesenchymal cells (Timmerman et al. 2004). To clarify the regulation of the Snail family members by the Notch and TGFβ pathways, expression of Snail family members in the AV canal endocardium would need to be analyzed when the Notch pathway is ectopically activated and the TGFβ pathway is blocked concurrently, and when the Notch pathway is blocked and the TGFβ pathway is concurrently activated.

The data presented in Chapter 4 and previously published results reveal that the induction of Snail and Slug converge on the endothelial adherens junction protein *VE-cadherin* (Timmerman et al. 2004). It was further demonstrated that Slug directly binds and regulates the *VE-cadherin* promoter via two E2-box elements. Additionally, Slug expression represses endothelial phenotype but does not induce a mesenchymal phenotype, in comparison to epithelial cells where *Slug* expression results in full EMT. In addition to the regulation of endothelial phenotype, Slug was demonstrated to be involved in ensuring the

survival of Notch-transdifferentiated endothelial cells and for the migration of Notch-transdifferentiated cells.

The second area that was investigated was the *in vivo* role of *Slug* during cardiac cushion EndMT. We demonstrated that *Slug* is expressed in the mesenchymal cells and a subset of endothelial cells of the AV canal and OFT beginning at the initiation of EndMT at E9.5 in the mouse. Additionally, we demonstrated that *Slug* and *Snail* are expressed in the EndMT derived structures including the mitral and tricuspid valves and the atrioventricular septum at later stages of human heart development. The expression pattern suggests a critical role for *Slug* in initiating EndMT in the cardiac cushions. It also contradicts previous results that suggested that *Slug* is not expressed in the heart at E9.5 (Timmerman et al. 2004).

Of interest, in the AV canal, *Slug* expression is unique among known Notch target genes. Expression of active Notch1, *Hey1*, and *Hey2* reveal that Notch signaling is active in the majority of endocardial cells but is not active in the mesenchymal cells in the cardiac cushions (Del Monte et al. 2007). However, the restricted *Slug* expression to the mesenchymal cells and a small percentage of endocardial cells, suggests that Notch, in cooperation with other signaling pathways, may initiate the induction of *Slug* expression in the endocardium but that the maintained expression of *Slug* in the mesenchyme is independent of Notch signaling (Figure 6.1).

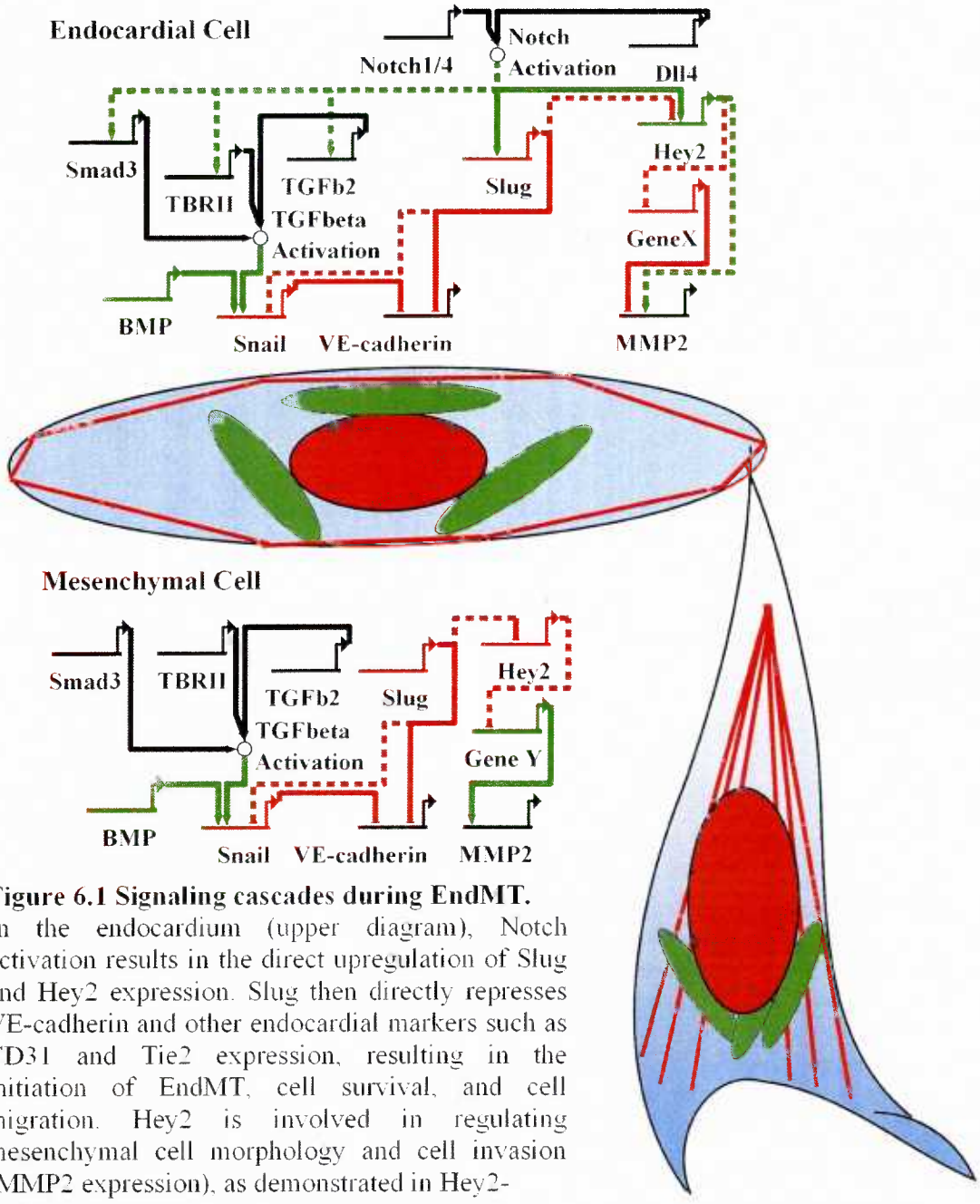


**Figure 6.1 Signaling cascades during EndMT.**
In the endocardium (upper diagram), Notch activation results in the direct upregulation of Slug and Hey2 expression. Slug then directly represses VE-cadherin and other endocardial markers such as CD31 and Tie2 expression, resulting in the initiation of EndMT, cell survival, and cell migration. Hey2 is involved in regulating mesenchymal cell morphology and cell invasion (MMP2 expression), as demonstrated in Hey2-deficient embryos. Concurrently, the Notch pathway modulates the TGFβ pathway, possibly by regulating Smad3, TGFβRII, or TGFβ2 expression. Notch mediated regulation of the TGFβ pathway results in of the TGFβ pathway and synergistic induction of Snail expression. BMP2 can also induce Snail expression, but independently of Notch signaling. Snail also participates in the process of EndMT. In Slug-deficient embryos there is increased Snail expression, suggesting Slug negatively regulates Snail expression through unknown mechanisms. In the mesenchyme (lower diagram), Notch signaling is not active and Slug, Smad3, TGFβRII, TGFβII expression must be regulated through other unknown mechanisms. Expression of Slug and Snail in a mesenchymal cell maintains the repression of endothelial phenotype (VE-cadherin, CD31, Tie2) and promotes migration and survival of transdifferentiated cells. As Hey2 is not expressed in the mesenchymal cells, possibly due to Slug expression, the mesenchymal morphology and invasive phenotype must be regulated by other mechanisms.

The expression pattern and regulation of endothelial phenotype *in vitro* by *Slug* suggest an important role during heart development; however, *Slug*-deficient mice are viable with no obvious heart defects. To more closely investigate the role of *Slug* during cardiac EndMT the AV canal explant assay was utilized, which measures the amount of EndMT occurring in the cardiac cushions. Using this assay we demonstrated that there was a significant reduction in EndMT in *Slug*-deficient embryos at E9.5, the stage when EndMT is initiated. In addition, the *Slug*-deficient AV canal explants displayed either large endothelial outgrowths or migrating cells with a rounded morphology. The rounded morphology is suggestive of a cell expressing both endothelial and mesenchymal markers, consistent with a defect in the activation of the endothelial cell to undergo EndMT. Furthermore, analysis of the cardiac cushion cellularity at E9.5 also revealed reduced numbers of mesenchymal cells. These data suggest that both *in vivo* and *ex vivo* Slug-deficiency results in cardiac cushion cellularity defects that are likely due to reduced EndMT.

In contrast to the AV canal explant results at E9.5, at E10.5 *Slug*-deficiency had no effect on the amount of EndMT occurring, suggesting a compensation or rescue of the *Slug*-deficient phenotype between E9.5 and E10.5. Further analysis of cardiac cushion morphology at E10.5 in wild-type and *Slug*-deficient embryos demonstrated EndMT appeared relatively normal but a defect in the remodeling of the cardiac cushions was evident. As fusion of the cardiac cushions is dependent upon EndMT it further suggested that there was compensation for *Slug*-deficiency. Because of the proposed compensation between Snail family members in other tissues and the co-expression of *Snail* and *Slug* during heart development we investigated whether *Snail* was compensating for *Slug*-deficiency

(Timmerman et al. 2004; Murray et al. 2007). Analysis of mRNA expression in *Slug*-deficient heart revealed that both *Snail* and *Hey2* expression were increased at E10.5 and E11.5, while there was no consistent change in *Hey1*. Interestingly, in wild-type hearts *Slug* expression increased from E9.5 through E11.5 while *Snail* expression remained constant or even decreased. Either the analysis of *Snail* expression missed the induction of *Snail* expression or Slug and the Notch pathway may play a more dominant role in regulating EndMT in wild-type embryos. *Snail* expression in the E10.5 and E11.5 heart was confirmed by *in situ* hybridization, which demonstrated that the expression pattern of *Snail* was unchanged in *Slug*-deficient hearts. These results suggest that *Snail* was expressed in the same cells but at a higher level in the *Slug*-deficient hearts. As Slug is a transcription factor it is possible that it directly regulates *Snail* expression and to test this hypothesis *Snail* expression was analyzed in cells ectopically expressing *Slug*. These results demonstrated that Slug-overexpression does not change *Snail* or *Hey1* expression, which is consistent with published reports that demonstrate Slug does not regulate *Snail* expression (Peiro et al. 2006). In comparison, *Hey2* expression was reduced by Slug-overexpression, which agrees with the increased *Hey2* expression in *Slug*-deficient hearts. Increased *Hey2* expression may suggest an increase in Notch activity and through the co-operation with the TGFβ pathway could synergistically upregulate *Snail* expression. However, as discussed above Notch signaling is only active in the endocardium and therefore the synergistic upregulation of *Snail* would occur in the endocardium and increased expression of *Snail* would need to be maintained by other mechanisms in the mesenchyme. In addition, the *Hey2* expression pattern needs to be further investigated as *Hey2* is highly expressed in the ventricular

myocardium at E10.5 and E11.5 and may not correspond to increased Notch activity in the cardiac cushions.

To investigate whether the increased *Snail* expression functionally rescues the EndMT defect observed in the *Slug*-deficient embryos at E9.5, exogenous TGFβ2 was added to the medium in the AV canal explant assay to activate the TGFβ pathway and induce *Snail* expression. These results demonstrated that TGFβ2 treatment completely rescued the EndMT defect in *Slug*-deficient embryos; however, it does not conclusively demonstrate that *Snail* was involved. To directly demonstrate the involvement of Snail in the compensation of *Slug*-deficiency, a lentiviral shRNA technique to knock down *Snail* expression in *Slug*-deficient AV canal explants was employed. These results demonstrated that knock down of *Snail* in wild-type or *Slug*-heterozygous embryos had no effect on EndMT, while knock down of *Snail* in *Slug*-deficient embryos resulted in significantly decreased EndMT.

One caveat that should be recognized with our studies is that the AV canal explant assay is an *ex vivo* assay and may not represent what is occurring *in vivo*. The use of a *Snail*-deficient mouse would have provided a better understanding of the compensation between the Snail family members. However, *Snail*-deficient embryos are lethal prior to cardiac development and an endocardial specific *Snail*-knockout would be required (Carver et al. 2001). With an endocardial-specific *Snail*-knockout, the effect of *Snail*-heterozygosity or *Snail*-deficiency in combination with *Slug*-deficiency on cardiac cushion cellularity could directly be analyzed *in vivo*. In addition, whether Slug compensates for *Snail*-deficiency could also be examined.

The results presented in this thesis lead to a model in which Notch activation in the developing cardiac cushions results in the upregulation of *Slug*, whereas TGFβ activation results in the upregulation of *Snail*. In cells where there is combined Notch and TGFβ activation there is a synergistic induction of *Snail* expression. When the Notch pathway is disrupted, there is an associated decrease in both *Snail* and *Slug* resulting in reduced EndMT and heart defects. In *Slug*-deficient embryos there is a compensatory increase in Snail expression, possibly through increased Notch activation, and a rescue of EndMT (Figure 6.2). Collectively, these suggest that a minimal dose of *Slug* and *Snail* are required for the initiation of EndMT and that *Snail* and *Slug* are redundantly required for cardiac EndMT.

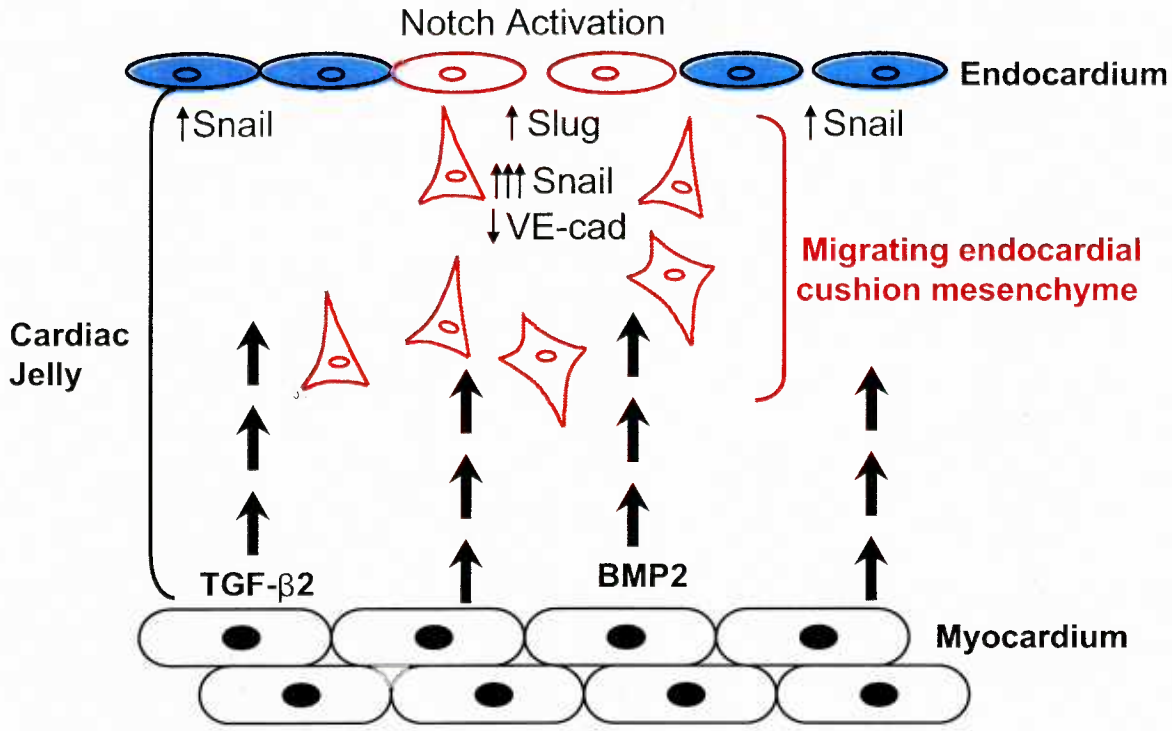


**Figure 6.2 Model of Notch mediated induction of EndMT during heart development.** Prior to EndMT at E9.5 the acellular cardiac cushions of the AV canal consists of the outer myocardial and inner endocardial layer separated by a layer of extracellular matrix protein the cardiac jelly. In response to activation of the Notch pathway in the endocardium there is an induction of Slug expression. At the same time, TGFβ2 expressed by the myocardium induces Snail expression in the endocardium. Furthermore, in cells where there is active Notch signaling there is a synergistic induction of Snail expression. In cells where sufficient levels of Slug and Snail are expressed there is downregulation of VE-cadherin and induction of EndMT.

# REFERENCES


Abe, M., Oda, N., and Sato, Y. 1998. Cell-associated activation of latent transforming growth factor-beta by calpain. *J Cell Physiol* **174**(2): 186-193.

Armstrong, E.J. and Bischoff, J. 2004. Heart valve development: endothelial cell signaling and differentiation. *Circ Res* **95**(5): 459-470.

Artavanis-Tsakonas, S., Rand, M.D., and Lake, R.J. 1999. Notch signaling: cell fate control and signal integration in development. *Science* **284**(5415): 770-776.

Ascano, J.M., Beverly, L.J., and Capobianco, A.J. 2003. The C-terminal PDZ-ligand of JAGGED1 is essential for cellular transformation. *J Biol Chem* **278**(10): 8771-8779.

Attisano, L., Wrana, J.L., Cheifetz, S., and Massague, J. 1992. Novel activin receptors: distinct genes and alternative mRNA splicing generate a repertoire of serine/threonine kinase receptors. *Cell* **68**(1): 97-108.

Azhar, M., Schultz Jel, J., Grupp, I., Dorn, G.W., 2nd, Meneton, P., Molin, D.G., Gittenberger-de Groot, A.C., and Doetschman, T. 2003. Transforming growth factor beta in cardiovascular development and function. *Cytokine Growth Factor Rev* **14**(5): 391-407.

Baarends, W.M., van Helmond, M.J., Post, M., van der Schoot, P.J., Hoogerbrugge, J.W., de Winter, J.P., Uilenbroek, J.T., Karels, B., Wilming, L.G., Meijers, J.H., and et al. 1994. A novel member of the transmembrane serine/threonine kinase receptor family is specifically expressed in the gonads and in mesenchymal cells adjacent to the mullerian duct. *Development* **120**(1): 189-197.

Bachelder, R.E., Yoon, S.O., Franci, C., de Herreros, A.G., and Mercurio, A.M. 2005. Glycogen synthase kinase-3 is an endogenous inhibitor of Snail transcription: implications for the epithelial-mesenchymal transition. *J Cell Biol* **168**(1): 29-33.

Baker, J.C. and Harland, R.M. 1996. A novel mesoderm inducer, Madr2, functions in the activin signal transduction pathway. *Genes Dev* **10**(15): 1880-1889.

Baladron, V., Ruiz-Hidalgo, M.J., Nueda, M.L., Diaz-Guerra, M.J., Garcia-Ramirez, J.J., Bonvini, E., Gubina, E., and Laborda, J. 2005. dlk acts as a negative regulator of Notch1 activation through interactions with specific EGF-like repeats. *Exp Cell Res* **303**(2): 343-359.

Banerjee, A.K. 1986. Waardenburg's syndrome associated with ostium secundum atrial septal defect. *J R Soc Med* **79**(11): 677-678.

Barrallo-Gimeno, A. and Nieto, M.A. 2005. The Snail genes as inducers of cell movement and survival: implications in development and cancer. *Development* **132**(14): 3151-3161.

Bartram, U., Molin, D.G., Wisse, L.J., Mohamad, A., Sanford, L.P., Doetschman, T., Speer, C.P., Poelmann, R.E., and Gittenberger-de Groot, A.C. 2001. Double-outlet right ventricle and overriding tricuspid valve reflect disturbances of looping, myocardialization, endocardial cushion differentiation, and apoptosis in TGF-beta(2)-knockout mice. *Circulation* **103**(22): 2745-2752.

Beatus, P., Lundkvist, J., Oberg, C., Pedersen, K., and Lendahl, U. 2001. The origin of the ankyrin repeat region in Notch intracellular domains is critical for regulation of HES promoter activity. *Mech Dev* **104**(1-2): 3-20.

Benedito, R. and Duarte, A. 2005. Expression of Dll4 during mouse embryogenesis suggests multiple developmental roles. *Gene Expr Patterns* **5**(6): 750-755.

Bettenhausen, B., Hrabe de Angelis, M., Simon, D., Guenet, J.L., and Gossler, A. 1995. Transient and restricted expression during mouse embryogenesis of Dll1, a murine gene closely related to Drosophila Delta. *Development* **121**(8): 2407-2418.

Blaumueller, C.M., Qi, H., Zagouras, P., and Artavanis-Tsakonas, S. 1997. Intracellular cleavage of Notch leads to a heterodimeric receptor on the plasma membrane. *Cell* **90**(2): 281-291.

Blokzijl, A., Dahlqvist, C., Reissmann, E., Falk, A., Moliner, A., Lendahl, U., and Ibanez, C.F. 2003. Cross-talk between the Notch and TGF-beta signaling pathways mediated by interaction of the Notch intracellular domain with Smad3. *J Cell Biol* **163**(4): 723-728.

Brand, T. 2003. Heart development: molecular insights into cardiac specification and early morphogenesis. *Dev Biol* **258**(1): 1-19.

Brou, C., Logeat, F., Gupta, N., Bessia, C., LeBail, O., Doedens, J.R., Cumano, A., Roux, P., Black, R.A., and Israel, A. 2000. A novel proteolytic cleavage involved in Notch signaling: the role of the disintegrin-metalloprotease TACE. *Mol Cell* **5**(2): 207-216.

Brown, C.B., Boyer, A.S., Runyan, R.B., and Barnett, J.V. 1999. Requirement of type III TGF-beta receptor for endocardial cell transformation in the heart. *Science* **283**(5410): 2080-2082.

Bush, G., diSibio, G., Miyamoto, A., Denault, J.B., Leduc, R., and Weinmaster, G. 2001. Ligand-induced signaling in the absence of furin processing of Notch1. *Dev Biol* **229**(2): 494-502.

Camenisch, T.D., Molin, D.G., Person, A., Runyan, R.B., Gittenberger-de Groot, A.C., McDonald, J.A., and Klewer, S.E. 2002a. Temporal and distinct TGFbeta ligand requirements during mouse and avian endocardial cushion morphogenesis. *Dev Biol* **248**(1): 170-181.

Camenisch, T.D., Schroeder, J.A., Bradley, J., Klewer, S.E., and McDonald, J.A. 2002b. Heart-valve mesenchyme formation is dependent on hyaluronan-augmented activation of ErbB2-ErbB3 receptors. *Nat Med* **8**(8): 850-855.

Camenisch, T.D., Spicer, A.P., Brehm-Gibson, T., Biesterfeldt, J., Augustine, M.L., Calabro, A., Jr., Kubalak, S., Klewer, S.E., and McDonald, J.A. 2000. Disruption of hyaluronan synthase-2 abrogates normal cardiac morphogenesis and hyaluronan-mediated transformation of epithelium to mesenchyme. *J Clin Invest* **106**(3): 349-360.

Cano, A., Perez-Moreno, M.A., Rodrigo, I., Locascio, A., Blanco, M.J., del Barrio, M.G., Portillo, F., and Nieto, M.A. 2000. The transcription factor snail controls epithelial-mesenchymal transitions by repressing E-cadherin expression. *Nat Cell Biol* **2**(2): 76-83.

Carmeliet, P., Lampugnani, M.G., Moons, L., Breviario, F., Compernolle, V., Bono, F., Balconi, G., Spagnuolo, R., Oostuyse, B., Dewerchin, M., Zanetti, A., Angellilo, A., Mattot, V., Nuyens, D., Lutgens, E., Clotman, F., de Ruiter, M.C., Gittenberger-de Groot, A., Poelmann, R., Lupu, F., Herbert, J.M., Collen, D., and Dejana, E. 1999. Targeted deficiency or cytosolic truncation of the VE-cadherin gene in mice impairs VEGF-mediated endothelial survival and angiogenesis. *Cell* **98**(2): 147-157.

Carver, E.A., Jiang, R., Lan, Y., Oram, K.F., and Gridley, T. 2001. The mouse snail gene encodes a key regulator of the epithelial-mesenchymal transition. *Mol Cell Biol* **21**(23): 8184-8188.

Castro Alves, C., Rosivatz, E., Schott, C., Hollweck, R., Becker, I., Sarbia, M., Carneiro, F., and Becker, K.F. 2007. Slug is overexpressed in gastric carcinomas and may act synergistically with SIP1 and Snail in the down-regulation of E-cadherin. *J Pathol* **211**(5): 507-515.

Cayouette, M. and Raff, M. 2002. Asymmetric segregation of Numb: a mechanism for neural specification from Drosophila to mammals. *Nat Neurosci* **5**(12): 1265-1269.

Chabriat, H., Vahedi, K., Iba-Zizen, M.T., Joutel, A., Nibbio, A., Nagy, T.G., Krebs, M.O., Julien, J., Dubois, B., Ducrocq, X., and et al. 1995. Clinical spectrum of CADASIL: a study of 7 families. Cerebral autosomal dominant arteriopathy with subcortical infarcts and leukoencephalopathy. *Lancet* **346**(8980): 934-939.

Chan, W.Y., Cheung, C.S., Yung, K.M., and Copp, A.J. 2004. Cardiac neural crest of the mouse embryo: axial level of origin, migratory pathway and cell autonomy of the splotch (Sp2H) mutant effect. *Development* **131**(14): 3367-3379.

Cheifetz, S., Bellon, T., Cales, C., Vera, S., Bernabeu, C., Massague, J., and Letarte, M. 1992. Endoglin is a component of the transforming growth factor-beta receptor system in human endothelial cells. *J Biol Chem* **267**(27): 19027-19030.

Chen, C.R., Kang, Y., Siegel, P.M., and Massague, J. 2002. E2F4/5 and p107 as Smad cofactors linking the TGFbeta receptor to c-myc repression. *Cell* **110**(1): 19-32.

Chen, X., Weisberg, E., Fridmacher, V., Watanabe, M., Naco, G., and Whitman, M. 1997. Smad4 and FAST-1 in the assembly of activin-responsive factor. *Nature* **389**(6646): 85-89.

Chen, Y., Lebrun, J.J., and Vale, W. 1996. Regulation of transforming growth factor beta- and activin-induced transcription by mammalian Mad proteins. *Proc Natl Acad Sci U S A* **93**(23): 12992-12997.

Chin, M.T., Maemura, K., Fukumoto, S., Jain, M.K., Layne, M.D., Watanabe, M., Hsieh, C.M., and Lee, M.E. 2000. Cardiovascular basic helix loop helix factor 1, a novel transcriptional repressor expressed preferentially in the developing and adult cardiovascular system. *J Biol Chem* **275**(9): 6381-6387.

Ciruna, B. and Rossant, J. 2001. FGF signaling regulates mesoderm cell fate specification and morphogenetic movement at the primitive streak. *Dev Cell* **1**(1): 37-49.

Crosby, C.V., Fleming, P.A., Argraves, W.S., Corada, M., Zanetta, L., Dejana, E., and Drake, C.J. 2005. VE-cadherin is not required for the formation of nascent blood vessels but acts to prevent their disassembly. *Blood* **105**(7): 2771-2776.

Dahlqvist, C., Blokzijl, A., Chapman, G., Falk, A., Dannaeus, K., Ibanez, C.F., and Lendahl, U. 2003. Functional Notch signaling is required for BMP4-induced inhibition of myogenic differentiation. *Development* **130**(24): 6089-6099.

Davis, R.L. and Turner, D.L. 2001. Vertebrate hairy and Enhancer of split related proteins: transcriptional repressors regulating cellular differentiation and embryonic patterning. *Oncogene* **20**(58): 8342-8357.

Day, A.J. and Prestwich, G.D. 2002. Hyaluronan-binding proteins: tying up the giant. *J Biol Chem* **277**(7): 4585-4588.

de la Cruz, M.V., Sanchez Gomez, C., Arteaga, M.M., and Arguello, C. 1977. Experimental study of the development of the truncus and the conus in the chick embryo. *J Anat* **123**(Pt 3): 661-686.

De Strooper, B., Annaert, W., Cupers, P., Saftig, P., Craessaerts, K., Mumm, J.S., Schroeter, E.H., Schrijvers, V., Wolfe, M.S., Ray, W.J., Goate, A., and Kopan, R. 1999. A presenilin-1-dependent gamma-secretase-like protease mediates release of Notch intracellular domain. *Nature* **398**(6727): 518-522.

del Barrio, M.G. and Nieto, M.A. 2002. Overexpression of Snail family members highlights their ability to promote chick neural crest formation. *Development* **129**(7): 1583-1593.

Del Monte, G., Grego-Bessa, J., Gonzalez-Rajal, A., Bolos, V., and De La Pompa, J.L. 2007. Monitoring Notch1 activity in development: Evidence for a feedback regulatory loop. *Dev Dyn* **236**(9): 2594-2614.

Di Guglielmo, G.M., Le Roy, C., Goodfellow, A.F., and Wrana, J.L. 2003. Distinct endocytic pathways regulate TGF-beta receptor signalling and turnover. *Nat Cell Biol* **5**(5): 410-421.

Dichgans, M., Ludwig, H., Muller-Hocker, J., Messerschmidt, A., and Gasser, T. 2000. Small in-frame deletions and missense mutations in CADASIL: 3D models predict misfolding of Notch3 EGF-like repeat domains. *Eur J Hum Genet* **8**(4): 280-285.

Dickson, M.C., Slager, H.G., Duffie, E., Mummery, C.L., and Akhurst, R.J. 1993. RNA and protein localisations of TGF beta 2 in the early mouse embryo suggest an involvement in cardiac development. *Development* **117**(2): 625-639.

Donovan, J., Kordylewska, A., Jan, Y.N., and Utset, M.F. 2002. Tetralogy of Fallot and other congenital heart defects in Hey2 mutant mice. *Curr Biol* **12**(18): 1605-1610.

Dor, Y., Camenisch, T.D., Itin, A., Fishman, G.I., McDonald, J.A., Carmeliet, P., and Keshet, E. 2001. A novel role for VEGF in endocardial cushion formation and its potential contribution to congenital heart defects. *Development* **128**(9): 1531-1538.

Drake, C.J. and Fleming, P.A. 2000. Vasculogenesis in the day 6.5 to 9.5 mouse embryo. *Blood* **95**(5): 1671-1679.

Duarte, A., Hirashima, M., Benedito, R., Trindade, A., Diniz, P., Bekman, E., Costa, L., Henrique, D., and Rossant, J. 2004. Dosage-sensitive requirement for mouse Dll4 in artery development. *Genes Dev* **18**(20): 2474-2478.

Ducy, P., Zhang, R., Geoffroy, V., Ridall, A.L., and Karsenty, G. 1997. Osf2/Cbfa1: a transcriptional activator of osteoblast differentiation. *Cell* **89**(5): 747-754.

Dudley, A.T., Lyons, K.M., and Robertson, E.J. 1995. A requirement for bone morphogenetic protein-7 during development of the mammalian kidney and eye. *Genes Dev* **9**(22): 2795-2807.

Dudley, A.T. and Robertson, E.J. 1997. Overlapping expression domains of bone morphogenetic protein family members potentially account for limited tissue defects in BMP7 deficient embryos. *Dev Dyn* **208**(3): 349-362.

Edery, P., Attie, T., Amiel, J., Pelet, A., Eng, C., Hofstra, R.M., Martelli, H., Bidaud, C., Munnich, A., and Lyonnet, S. 1996. Mutation of the endothelin-3 gene in the Waardenburg-Hirschsprung disease (Shah-Waardenburg syndrome). *Nat Genet* **12**(4): 442-444.

Ehebauer, M.T., Chirgadze, D.Y., Hayward, P., Martinez Arias, A., and Blundell, T.L. 2005. High-resolution crystal structure of the human Notch 1 ankyrin domain. *Biochem J* **392**(Pt 1): 13-20.

Eisenberg, L.M. and Markwald, R.R. 1995. Molecular regulation of atrioventricular valvuloseptal morphogenesis. *Circ Res* **77**(1): 1-6.

Eldadah, Z.A., Hamosh, A., Biery, N.J., Montgomery, R.A., Duke, M., Elkins, R., and Dietz, H.C. 2001. Familial Tetralogy of Fallot caused by mutation in the jagged1 gene. *Hum Mol Genet* **10**(2): 163-169.

Eppert, K., Scherer, S.W., Ozcelik, H., Pirone, R., Hoodless, P., Kim, H., Tsui, L.C., Bapat, B., Gallinger, S., Andrulis, I.L., Thomsen, G.H., Wrana, J.L., and Attisano, L. 1996. MADR2 maps to 18q21 and encodes a TGFbeta-regulated MAD-related protein that is functionally mutated in colorectal carcinoma. *Cell* **86**(4): 543-552.

Espinosa, L., Ingles-Esteve, J., Aguilera, C., and Bigas, A. 2003. Phosphorylation by glycogen synthase kinase-3 beta down-regulates Notch activity, a link for Notch and Wnt pathways. *J Biol Chem* **278**(34): 32227-32235.

Evin, G., Cappai, R., Li, Q.X., Culvenor, J.G., Small, D.H., Beyreuther, K., and Masters, C.L. 1995. Candidate gamma-secretases in the generation of the carboxyl terminus of the Alzheimer's disease beta A4 amyloid: possible involvement of cathepsin D. *Biochemistry* **34**(43): 14185-14192.

Feng, X.H. and Derynck, R. 2005. Specificity and versatility in tgf-beta signaling through Smads. *Annu Rev Cell Dev Biol* **21**: 659-693.

Feng, X.H., Zhang, Y., Wu, R.Y., and Derynck, R. 1998. The tumor suppressor Smad4/DPC4 and transcriptional adaptor CBP/p300 are coactivators for smad3 in TGF-beta-induced transcriptional activation. *Genes Dev* **12**(14): 2153-2163.

Fischer, A., Schumacher, N., Maier, M., Sendtner, M., and Gessler, M. 2004. The Notch target genes Hey1 and Hey2 are required for embryonic vascular development. *Genes Dev* **18**(8): 901-911.

Fischer, A., Steidl, C., Wagner, T.U., Lang, E., Jakob, P.M., Friedl, P., Knobeloch, K.P., and Gessler, M. 2007a. Combined loss of Hey1 and HeyL causes congenital heart defects because of impaired epithelial to mesenchymal transition. *Circ Res* **100**(6): 856-863.

Fleming, R.J. 1998. Structural conservation of Notch receptors and ligands. *Semin Cell Dev Biol* **9**(6): 599-607.

Foltz, D.R., Santiago, M.C., Berechid, B.E., and Nye, J.S. 2002. Glycogen synthase kinase-3beta modulates notch signaling and stability. *Curr Biol* **12**(12): 1006-1011.

Francis, R., McGrath, G., Zhang, J., Ruddy, D.A., Sym, M., Apfeld, J., Nicoll, M., Maxwell, M., Hai, B., Ellis, M.C., Parks, A.L., Xu, W., Li, J., Gurney, M., Myers, R.L., Himes, C.S., Hiebsch, R., Ruble, C., Nye, J.S., and Curtis, D. 2002. aph-1 and pen-2 are required for Notch pathway signaling, gamma-secretase cleavage of betaAPP, and presenilin protein accumulation. *Dev Cell* **3**(1): 85-97.

Fryer, C.J., Lamar, E., Turbachova, I., Kintner, C., and Jones, K.A. 2002. Mastermind mediates chromatin-specific transcription and turnover of the Notch enhancer complex. *Genes Dev* **16**(11): 1397-1411.

Fryer, C.J., White, J.B., and Jones, K.A. 2004. Mastermind recruits CycC:CDK8 to phosphorylate the Notch ICD and coordinate activation with turnover. *Mol Cell* **16**(4): 509-520.

Galvin, K.M., Donovan, M.J., Lynch, C.A., Meyer, R.I., Paul, R.J., Lorenz, J.N., Fairchild-Huntress, V., Dixon, K.L., Dunmore, J.H., Gimbrone, M.A., Jr., Falb, D., and Huszar, D. 2000. A role for smad6 in development and homeostasis of the cardiovascular system. *Nat Genet* **24**(2): 171-174.

Garg, V., Muth, A.N., Ransom, J.F., Schluterman, M.K., Barnes, R., King, I.N., Grossfeld, P.D., and Srivastava, D. 2005. Mutations in NOTCH1 cause aortic valve disease. *Nature* **437**(7056): 270-274.

Gaussin, V., Van de Putte, T., Mishina, Y., Hanks, M.C., Zwijsen, A., Huylebroeck, D., Behringer, R.R., and Schneider, M.D. 2002. Endocardial cushion and myocardial defects after cardiac myocyte-specific conditional deletion of the bone morphogenetic protein receptor ALK3. *Proc Natl Acad Sci U S A* **99**(5): 2878-2883.

Ge, W., Martinowich, K., Wu, X., He, F., Miyamoto, A., Fan, G., Weinmaster, G., and Sun, Y.E. 2002. Notch signaling promotes astrogliogenesis via direct CSL-mediated glial gene activation. *J Neurosci Res* **69**(6): 848-860.

Gessler, M., Knobeloch, K.P., Helisch, A., Amann, K., Schumacher, N., Rohde, E., Fischer, A., and Leimeister, C. 2002. Mouse gridlock: no aortic coarctation or deficiency, but fatal cardiac defects in Hey2 -/- mice. *Curr Biol* **12**(18): 1601-1604.

Glittenberg, M., Pitsouli, C., Garvey, C., Delidakis, C., and Bray, S. 2006. Role of conserved intracellular motifs in Serrate signalling, cis-inhibition and endocytosis. *Embo J* **25**(20): 4697-4706.

Grau, Y., Carteret, C., and Simpson, P. 1984. Mutations and Chromosomal Rearrangements Affecting the Expression of Snail, a Gene Involved in Embryonic Patterning in DROSOPHILA MELANOGASTER. *Genetics* **108**(2): 347-360.

Greenwald, I. and Seydoux, G. 1990. Analysis of gain-of-function mutations of the lin-12 gene of Caenorhabditis elegans. *Nature* **346**(6280): 197-199.

Grego-Bessa, J., Luna-Zurita, L., Del Monte, G., Bolos, V., Melgar, P., Arandilla, A., Garratt, A.N., Zang, H., Mukouyama, Y.S., Chen, H., Shou, W., Ballestar, E., Esteller, M., Rojas, A., Perez-Pomares, J.M., and de la Pompa, J.L. 2007. Notch signaling is essential for ventricular chamber development. *Dev Cell* **12**(3): 415-429.

Gu, Z., Reynolds, E.M., Song, J., Lei, H., Feijen, A., Yu, L., He, W., MacLaughlin, D.T., van den Eijnden-van Raaij, J., Donahoe, P.K., and Li, E. 1999. The type I serine/threonine kinase receptor ActRIA (ALK2) is required for gastrulation of the mouse embryo. *Development* **126**(11): 2551-2561.

Hajra, K.M., Chen, D.Y., and Fearon, E.R. 2002. The SLUG zinc-finger protein represses E-cadherin in breast cancer. *Cancer Res* **62**(6): 1613-1618.

Haltiwanger, R.S. 2002. Regulation of signal transduction pathways in development by glycosylation. *Curr Opin Struct Biol* **12**(5): 593-598.

Hamada, Y., Kadokawa, Y., Okabe, M., Ikawa, M., Coleman, J.R., and Tsujimoto, Y. 1999. Mutation in ankyrin repeats of the mouse Notch2 gene induces early embryonic lethality. *Development* **126**(15): 3415-3424.

Hansson, E.M., Lendahl, U., and Chapman, G. 2004. Notch signaling in development and disease. *Semin Cancer Biol* **14**(5): 320-328.

Haritunians, T., Boulter, J., Hicks, C., Buhrman, J., DiSibio, G., Shawber, C., Weinmaster, G., Nofziger, D., and Schanen, C. 2002. CADASIL Notch3 mutant proteins localize to the cell surface and bind ligand. *Circ Res* **90**(5): 506-508.

Harrelson, Z., Kelly, R.G., Goldin, S.N., Gibson-Brown, J.J., Bollag, R.J., Silver, L.M., and Papaioannou, V.E. 2004. Tbx2 is essential for patterning the atrioventricular canal and for morphogenesis of the outflow tract during heart development. *Development* **131**(20): 5041-5052.

Hay, E.D. 2005. The mesenchymal cell, its role in the embryo, and the remarkable signaling mechanisms that create it. *Dev Dyn* **233**(3): 706-720.

Hicks, C., Johnston, S.H., diSibio, G., Collazo, A., Vogt, T.F., and Weinmaster, G. 2000. Fringe differentially modulates Jagged1 and Delta1 signalling through Notch1 and Notch2. *Nat Cell Biol* **2**(8): 515-520.

Hiratochi, M., Nagase, H., Kuramochi, Y., Koh, C.S., Ohkawara, T., and Nakayama, K. 2007. The Delta intracellular domain mediates TGF-{beta}/Activin signaling through binding to Smads and has an important bi-directional function in the Notch-Delta signaling pathway. *Nucleic Acids Res.*

Hoffman, J.I. and Kaplan, S. 2002. The incidence of congenital heart disease. *J Am Coll Cardiol* **39**(12): 1890-1900.

Hoodless, P.A., Haerry, T., Abdollah, S., Stapleton, M., O'Connor, M.B., Attisano, L., and Wrana, J.L. 1996. MADR1, a MAD-related protein that functions in BMP2 signaling pathways. *Cell* **85**(4): 489-500.

Hori, K., Fostier, M., Ito, M., Fuwa, T.J., Go, M.J., Okano, H., Baron, M., and Matsuno, K. 2004. Drosophila deltex mediates suppressor of Hairless-independent and late-endosomal activation of Notch signaling. *Development* **131**(22): 5527-5537.

Hsieh, J.J., Henkel, T., Salmon, P., Robey, E., Peterson, M.G., and Hayward, S.D. 1996. Truncated mammalian Notch1 activates CBF1/RBPJk-repressed genes by a mechanism resembling that of Epstein-Barr virus EBNA2. *Mol Cell Biol* **16**(3): 952-959.

Hsieh, J.J., Zhou, S., Chen, L., Young, D.B., and Hayward, S.D. 1999. CIR, a corepressor linking the DNA binding factor CBF1 to the histone deacetylase complex. *Proc Natl Acad Sci U S A* **96**(1): 23-28.

Hu, Q.D., Ang, B.T., Karsak, M., Hu, W.P., Cui, X.Y., Duka, T., Takeda, Y., Chia, W., Sankar, N., Ng, Y.K., Ling, E.A., Maciag, T., Small, D., Trifonova, R., Kopan, R., Okano, H., Nakafuku, M., Chiba, S., Hirai, H., Aster, J.C., Schachner, M., Pallen, C.J., Watanabe, K., and Xiao, Z.C. 2003. F3/contactin acts as a functional ligand for Notch during oligodendrocyte maturation. *Cell* **115**(2): 163-175.

Hu, T., Yamagishi, H., Maeda, J., McAnally, J., Yamagishi, C., and Srivastava, D. 2004. Tbx1 regulates fibroblast growth factors in the anterior heart field through a reinforcing autoregulatory loop involving forkhead transcription factors. *Development* **131**(21): 5491-5502.

Hu, Y., Ye, Y., and Fortini, M.E. 2002. Nicastrin is required for gamma-secretase cleavage of the Drosophila Notch receptor. *Dev Cell* **2**(1): 69-78.

Imamura, T., Takase, M., Nishihara, A., Oeda, E., Hanai, J., Kawabata, M., and Miyazono, K. 1997. Smad6 inhibits signalling by the TGF-beta superfamily. *Nature* **389**(6651): 622-626.

Inagaki, T., Garcia-Martinez, V., and Schoenwolf, G.C. 1993. Regulative ability of the prospective cardiogenic and vasculogenic areas of the primitive streak during avian gastrulation. *Dev Dyn* **197**(1): 57-68.

Inman, G.J. and Hill, C.S. 2002. Stoichiometry of active smad-transcription factor complexes on DNA. *J Biol Chem* **277**(52): 51008-51016.

Inoue, A., Seidel, M.G., Wu, W., Kamizono, S., Ferrando, A.A., Bronson, R.T., Iwasaki, H., Akashi, K., Morimoto, A., Hitzler, J.K., Pestina, T.I., Jackson, C.W., Tanaka, R., Chong, M.J., McKinnon, P.J., Inukai, T., Grosveld, G.C., and Look, A.T. 2002. Slug, a highly conserved zinc finger transcriptional repressor, protects hematopoietic progenitor cells from radiation-induced apoptosis in vivo. *Cancer Cell* **2**(4): 279-288.

Inukai, T., Inoue, A., Kurosawa, H., Goi, K., Shinjyo, T., Ozawa, K., Mao, M., Inaba, T., and Look, A.T. 1999. SLUG, a ces-1-related zinc finger transcription factor gene with antiapoptotic activity, is a downstream target of the E2A-HLF oncoprotein. *Mol Cell* **4**(3): 343-352.

Iso, T., Chung, G., Hamamori, Y., and Kedes, L. 2002. HERP1 is a cell type-specific primary target of Notch. *J Biol Chem* **277**(8): 6598-6607.

Iso, T., Maeno, T., Oike, Y., Yamazaki, M., Doi, H., Arai, M., and Kurabayashi, M. 2006. Dll4-selective Notch signaling induces ephrinB2 gene expression in endothelial cells. *Biochem Biophys Res Commun* **341**(3): 708-714.

Itoh, F., Itoh, S., Goumans, M.J., Valdimarsdottir, G., Iso, T., Dotto, G.P., Hamamori, Y., Kedes, L., Kato, M., and ten Dijke Pt, P. 2004. Synergy and antagonism between Notch and BMP receptor signaling pathways in endothelial cells. *Embo J* **23**(3): 541-551.

Itoh, S., Ericsson, J., Nishikawa, J., Heldin, C.H., and ten Dijke, P. 2000. The transcriptional co-activator P/CAF potentiates TGF-beta/Smad signaling. *Nucleic Acids Res* **28**(21): 4291-4298.

Izon, D.J., Aster, J.C., He, Y., Weng, A., Karnell, F.G., Patriub, V., Xu, L., Bakkour, S., Rodriguez, C., Allman, D., and Pear, W.S. 2002. Deltex1 redirects lymphoid progenitors to the B cell lineage by antagonizing Notch1. *Immunity* **16**(2): 231-243.

Jehn, B.M., Dittert, I., Beyer, S., von der Mark, K., and Bielke, W. 2002. c-Cbl binding and ubiquitin-dependent lysosomal degradation of membrane-associated Notch1. *J Biol Chem* **277**(10): 8033-8040.

Jiang, R., Lan, Y., Norton, C.R., Sundberg, J.P., and Gridley, T. 1998. The Slug gene is not essential for mesoderm or neural crest development in mice. *Dev Biol* **198**(2): 277-285.

Jones, C.M., Lyons, K.M., and Hogan, B.L. 1991. Involvement of Bone Morphogenetic Protein-4 (BMP-4) and Vgr-1 in morphogenesis and neurogenesis in the mouse. *Development* **111**(2): 531-542.

Joutel, A., Andreux, F., Gaulis, S., Domenga, V., Cecillon, M., Battail, N., Piga, N., Chapon, F., Godfrain, C., and Tournier-Lasserve, E. 2000. The ectodomain of the Notch3 receptor accumulates within the cerebrovasculature of CADASIL patients. *J Clin Invest* **105**(5): 597-605.

Joutel, A., Corpechot, C., Ducros, A., Vahedi, K., Chabriat, H., Mouton, P., Alamowitch, S., Domenga, V., Cecillion, M., Marechal, E., Maciazek, J., Vayssiere, C., Cruaud, C., Cabanis, E.A., Ruchoux, M.M., Weissenbach, J., Bach, J.F., Bousser, M.G., and Tournier-Lasserve, E. 1996. Notch3 mutations in CADASIL, a hereditary adult-onset condition causing stroke and dementia. *Nature* **383**(6602): 707-710.

Joutel, A. and Tournier-Lasserve, E. 1998. Notch signalling pathway and human diseases. *Semin Cell Dev Biol* **9**(6): 619-625.

Joutel, A., Vahedi, K., Corpechot, C., Troesch, A., Chabriat, H., Vayssiere, C., Cruaud, C., Maciazek, J., Weissenbach, J., Bousser, M.G., Bach, J.F., and Tournier-Lasserve, E. 1997. Strong clustering and stereotyped nature of Notch3 mutations in CADASIL patients. *Lancet* **350**(9090): 1511-1515.

Kaartinen, V., Dudas, M., Nagy, A., Sridurongrit, S., Lu, M.M., and Epstein, J.A. 2004. Cardiac outflow tract defects in mice lacking ALK2 in neural crest cells. *Development* **131**(14): 3481-3490.

Kadesch, T. 2000. Notch signaling: a dance of proteins changing partners. *Exp Cell Res* **260**(1): 1-8.

Kajita, M., McClinic, K.N., and Wade, P.A. 2004. Aberrant expression of the transcription factors snail and slug alters the response to genotoxic stress. *Mol Cell Biol* **24**(17): 7559-7566.

Kamath, B.M., Spinner, N.B., Emerick, K.M., Chudley, A.E., Booth, C., Piccoli, D.A., and Krantz, I.D. 2004. Vascular anomalies in Alagille syndrome: a significant cause of morbidity and mortality. *Circulation* **109**(11): 1354-1358.

Kao, H.Y., Ordentlich, P., Koyano-Nakagawa, N., Tang, Z., Downes, M., Kintner, C.R., Evans, R.M., and Kadesch, T. 1998. A histone deacetylase corepressor complex regulates the Notch signal transduction pathway. *Genes Dev* **12**(15): 2269-2277.

Karsan, A., Yee, E., and Harlan, J.M. 1996. Endothelial cell death induced by tumor necrosis factor-alpha is inhibited by the Bcl-2 family member, A1. *J Biol Chem* **271**(44): 27201-27204.

Karsan, A., Yee, E., Poirier, G.G., Zhou, P., Craig, R., and Harlan, J.M. 1997. Fibroblast growth factor-2 inhibits endothelial cell apoptosis by Bcl-2-dependent and independent mechanisms. *Am J Pathol* **151**(6): 1775-1784.

Katoh, M. and Katoh, M. 2003. Identification and characterization of human SNAIL3 (SNAI3) gene in silico. *Int J Mol Med* **11**(3): 383-388.

Kawabata, M., Chytil, A., and Moses, H.L. 1995. Cloning of a novel type II serine/threonine kinase receptor through interaction with the type I transforming growth factor-beta receptor. *J Biol Chem* **270**(10): 5625-5630.

Kelly, R.G., Brown, N.A., and Buckingham, M.E. 2001. The arterial pole of the mouse heart forms from Fgf10-expressing cells in pharyngeal mesoderm. *Dev Cell* **1**(3): 435-440.

Kelly, R.G. and Buckingham, M.E. 2002. The anterior heart-forming field: voyage to the arterial pole of the heart. *Trends Genet* **18**(4): 210-216.

Kim, R.Y., Robertson, E.J., and Solloway, M.J. 2001. Bmp6 and Bmp7 are required for cushion formation and septation in the developing mouse heart. *Dev Biol* **235**(2): 449-466.

Kingsley, D.M., Bland, A.E., Grubber, J.M., Marker, P.C., Russell, L.B., Copeland, N.G., and Jenkins, N.A. 1992. The mouse short ear skeletal morphogenesis locus is associated with defects in a bone morphogenetic member of the TGF beta superfamily. *Cell* **71**(3): 399-410.

Kitajima, S., Takagi, A., Inoue, T., and Saga, Y. 2000. MesP1 and MesP2 are essential for the development of cardiac mesoderm. *Development* **127**(15): 3215-3226.

Klinakis, A., Szabolcs, M., Politi, K., Kiaris, H., Artavanis-Tsakonas, S., and Efstratiadis, A. 2006. Myc is a Notch1 transcriptional target and a requisite for Notch1-induced mammary tumorigenesis in mice. *Proc Natl Acad Sci U S A*.

Kokubo, H., Miyagawa-Tomita, S., Tomimatsu, H., Nakashima, Y., Nakazawa, M., Saga, Y., and Johnson, R.L. 2004. Targeted disruption of hesr2 results in atrioventricular valve anomalies that lead to heart dysfunction. *Circ Res* **95**(5): 540-547.

Kokubo, H., Tomita-Miyagawa, S., Hamada, Y., and Saga, Y. 2007. Hesr1 and Hesr2 regulate atrioventricular boundary formation in the developing heart through the repression of Tbx2. *Development* **134**(4): 747-755.

Komiyama, M., Ito, K., and Shimada, Y. 1987. Origin and development of the epicardium in the mouse embryo. *Anat Embryol (Berl)* **176**(2): 183-189.

Krantz, I.D., Smith, R., Colliton, R.P., Tinkel, H., Zackai, E.H., Piccoli, D.A., Goldmuntz, E., and Spinner, N.B. 1999. Jagged1 mutations in patients ascertained with isolated congenital heart defects. *Am J Med Genet* **84**(1): 56-60.

Krebs, L.T., Iwai, N., Nonaka, S., Welsh, I.C., Lan, Y., Jiang, R., Saijoh, Y., O'Brien, T.P., Hamada, H., and Gridley, T. 2003a. Notch signaling regulates left-right asymmetry determination by inducing Nodal expression. *Genes Dev* **17**(10): 1207-1212.

Krebs, L.T., Xue, Y., Norton, C.R., Sundberg, J.P., Beatus, P., Lendahl, U., Joutel, A., and Gridley, T. 2003b. Characterization of Notch3-deficient mice: normal embryonic development and absence of genetic interactions with a Notch1 mutation. *Genesis* **37**(3): 139-143.

Kretzschmar, M., Liu, F., Hata, A., Doody, J., and Massague, J. 1997. The TGF-beta family mediator Smad1 is phosphorylated directly and activated functionally by the BMP receptor kinase. *Genes Dev* **11**(8): 984-995.

Kurooka, H., Kuroda, K., and Honjo, T. 1998. Roles of the ankyrin repeats and C-terminal region of the mouse notch1 intracellular region. *Nucleic Acids Res* **26**(23): 5448-5455.

Lagna, G., Hata, A., Hemmati-Brivanlou, A., and Massague, J. 1996. Partnership between DPC4 and SMAD proteins in TGF-beta signalling pathways. *Nature* **383**(6603): 832-836.

Lechleider, R.J., de Caestecker, M.P., Dehejia, A., Polymeropoulos, M.H., and Roberts, A.B. 1996. Serine phosphorylation, chromosomal localization, and transforming growth factor-beta signal transduction by human bsp-1. *J Biol Chem* **271**(30): 17617-17620.

Leimeister, C., Externbrink, A., Klamt, B., and Gessler, M. 1999. Hey genes: a novel subfamily of hairy- and Enhancer of split related genes specifically expressed during mouse embryogenesis. *Mech Dev* **85**(1-2): 173-177.

Leimeister, C., Schumacher, N., Steidl, C., and Gessler, M. 2000. Analysis of HeyL expression in wild-type and Notch pathway mutant mouse embryos. *Mech Dev* **98**(1-2): 175-178.

Lelievre, E., Mattot, V., Huber, P., Vandenbunder, B., and Soncin, F. 2000. ETS1 lowers capillary endothelial cell density at confluence and induces the expression of VE-cadherin. *Oncogene* **19**(20): 2438-2446.

Leong, G.M., Subramaniam, N., Issa, L.L., Barry, J.B., Kino, T., Driggers, P.H., Hayman, M.J., Eisman, J.A., and Gardiner, E.M. 2004. Ski-interacting protein, a bifunctional nuclear receptor coregulator that interacts with N-CoR/SMRT and p300. *Biochem Biophys Res Commun* **315**(4): 1070-1076.

Li, Y. and Baker, N.E. 2004. The roles of cis-inactivation by Notch ligands and of neuralized during eye and bristle patterning in Drosophila. *BMC Dev Biol* **4**: 5.

Lin, H.Y., Wang, X.F., Ng-Eaton, E., Weinberg, R.A., and Lodish, H.F. 1992. Expression cloning of the TGF-beta type II receptor, a functional transmembrane serine/threonine kinase. *Cell* **68**(4): 775-785.

Lin, S.J., Lerch, T.F., Cook, R.W., Jardetzky, T.S., and Woodruff, T.K. 2006a. The structural basis of TGF-beta, bone morphogenetic protein, and activin ligand binding. *Reproduction* **132**(2): 179-190.

Lin, X., Duan, X., Liang, Y.Y., Su, Y., Wrighton, K.H., Long, J., Hu, M., Davis, C.M., Wang, J., Brunicardi, F.C., Shi, Y., Chen, Y.G., Meng, A., and Feng, X.H. 2006b. PPM1A functions as a Smad phosphatase to terminate TGFbeta signaling. *Cell* **125**(5): 915-928.

Liu, F., Hata, A., Baker, J.C., Doody, J., Carcamo, J., Harland, R.M., and Massague, J. 1996. A human Mad protein acting as a BMP-regulated transcriptional activator. *Nature* **381**(6583): 620-623.

Locascio, A., Manzanares, M., Blanco, M.J., and Nieto, M.A. 2002. Modularity and reshuffling of Snail and Slug expression during vertebrate evolution. *Proc Natl Acad Sci U S A* **99**(26): 16841-16846.

Logeat, F., Bessia, C., Brou, C., LeBail, O., Jarriault, S., Seidah, N.G., and Israel, A. 1998. The Notch1 receptor is cleaved constitutively by a furin-like convertase. *Proc Natl Acad Sci U S A* **95**(14): 8108-8112.

Loomes, K.M., Taichman, D.B., Glover, C.L., Williams, P.T., Markowitz, J.E., Piccoli, D.A., Baldwin, H.S., and Oakey, R.J. 2002. Characterization of Notch receptor expression in the developing mammalian heart and liver. *Am J Med Genet* **112**(2): 181-189.

Loomes, K.M., Underkoffler, L.A., Morabito, J., Gottlieb, S., Piccoli, D.A., Spinner, N.B., Baldwin, H.S., and Oakey, R.J. 1999. The expression of Jagged1 in the developing mammalian heart correlates with cardiovascular disease in Alagille syndrome. *Hum Mol Genet* **8**(13): 2443-2449.

Lopez-Casillas, F., Cheifetz, S., Doody, J., Andres, J.L., Lane, W.S., and Massague, J. 1991. Structure and expression of the membrane proteoglycan betaglycan, a component of the TGF-beta receptor system. *Cell* **67**(4): 785-795.

Lyons, K.M., Pelton, R.W., and Hogan, B.L. 1990a. Organogenesis and pattern formation in the mouse: RNA distribution patterns suggest a role for bone morphogenetic protein-2A (BMP-2A). *Development* **109**(4): 833-844.

Lyons, R.M., Gentry, L.E., Purchio, A.F., and Moses, H.L. 1990b. Mechanism of activation of latent recombinant transforming growth factor beta 1 by plasmin. *J Cell Biol* **110**(4): 1361-1367.

Ma, L., Lu, M.F., Schwartz, R.J., and Martin, J.F. 2005. Bmp2 is essential for cardiac cushion epithelial-mesenchymal transition and myocardial patterning. *Development* **132**(24): 5601-5611.

MacKenzie, F., Duriez, P., Larrivee, B., Chang, L., Pollet, I., Wong, F., Yip, C., and Karsan, A. 2004a. Notch4-induced inhibition of endothelial sprouting requires the ankyrin repeats and involves signaling through RBP-Jkappa. *Blood* **104**(6): 1760-1768.

MacKenzie, F., Duriez, P., Wong, F., Noseda, M., and Karsan, A. 2004b. Notch4 inhibits endothelial apoptosis via RBP-Jkappa-dependent and -independent pathways. *J Biol Chem* **279**(12): 11657-11663.

Marambaud, P., Shioi, J., Serban, G., Georgakopoulos, A., Sarner, S., Nagy, V., Baki, L., Wen, P., Efthimiopoulos, S., Shao, Z., Wisniewski, T., and Robakis, N.K. 2002. A presenilin-1/gamma-secretase cleavage releases the E-cadherin intracellular domain and regulates disassembly of adherens junctions. *Embo J* **21**(8): 1948-1956.

Marguerie, A., Bajolle, F., Zaffran, S., Brown, N.A., Dickson, C., Buckingham, M.E., and Kelly, R.G. 2006. Congenital heart defects in Fgfr2-IIIb and Fgf10 mutant mice. *Cardiovasc Res* **71**(1): 50-60.

Massague, J. and Gomis, R.R. 2006. The logic of TGFbeta signaling. *FEBS Lett* **580**(12): 2811-2820.

Massague, J., Seoane, J., and Wotton, D. 2005. Smad transcription factors. *Genes Dev* **19**(23): 2783-2810.

Mathews, L.S. and Vale, W.W. 1991. Expression cloning of an activin receptor, a predicted transmembrane serine kinase. *Cell* **65**(6): 973-982.

Matsuno, K., Ito, M., Hori, K., Miyashita, F., Suzuki, S., Kishi, N., Artavanis-Tsakonas, S., and Okano, H. 2002. Involvement of a proline-rich motif and RING-H2 finger of Deltex in the regulation of Notch signaling. *Development* **129**(4): 1049-1059.

Mauhin, V., Lutz, Y., Dennefeld, C., and Alberga, A. 1993. Definition of the DNA-binding site repertoire for the Drosophila transcription factor SNAIL. *Nucleic Acids Res* **21**(17): 3951-3957.

Mayer, M., Straube, A., Bruening, R., Uttner, I., Pongratz, D., Gasser, T., Dichgans, M., and Muller-Hocker, J. 1999. Muscle and skin biopsies are a sensitive diagnostic tool in the diagnosis of CADASIL. *J Neurol* **246**(7): 526-532.

McCright, B., Gao, X., Shen, L., Lozier, J., Lan, Y., Maguire, M., Herzlinger, D., Weinmaster, G., Jiang, R., and Gridley, T. 2001. Defects in development of the kidney, heart and eye vasculature in mice homozygous for a hypomorphic Notch2 mutation. *Development* **128**(4): 491-502.

McCright, B., Lozier, J., and Gridley, T. 2002. A mouse model of Alagille syndrome: Notch2 as a genetic modifier of Jag1 haploinsufficiency. *Development* **129**(4): 1075-1082.

McDaniell, R., Warthen, D.M., Sanchez-Lara, P.A., Pai, A., Krantz, I.D., Piccoli, D.A., and Spinner, N.B. 2006. NOTCH2 Mutations Cause Alagille Syndrome, a Heterogeneous Disorder of the Notch Signaling Pathway. *Am J Hum Genet* **79**(1): 169-173.

McDonald, J.A. and Camenisch, T.D. 2002. Hyaluronan: genetic insights into the complex biology of a simple polysaccharide. *Glycoconj J* **19**(4-5): 331-339.

McElhinney, D.B., Krantz, I.D., Bason, L., Piccoli, D.A., Emerick, K.M., Spinner, N.B., and Goldmuntz, E. 2002. Analysis of cardiovascular phenotype and genotype-phenotype correlation in individuals with a JAG1 mutation and/or Alagille syndrome. *Circulation* **106**(20): 2567-2574.

Miquerol, L., Gertsenstein, M., Harpal, K., Rossant, J., and Nagy, A. 1999. Multiple developmental roles of VEGF suggested by a LacZ-tagged allele. *Dev Biol* **212**(2): 307-322.

Miquerol, L., Langille, B.L., and Nagy, A. 2000. Embryonic development is disrupted by modest increases in vascular endothelial growth factor gene expression. *Development* **127**(18): 3941-3946.

Molin, D.G., Bartram, U., Van der Heiden, K., Van Iperen, L., Speer, C.P., Hierck, B.P., Poelmann, R.E., and Gittenberger-de-Groot, A.C. 2003. Expression patterns of Tgfbeta1-3 associate with myocardialisation of the outflow tract and the development of the epicardium and the fibrous heart skeleton. *Dev Dyn* **227**(3): 431-444.

Molin, D.G., DeRuiter, M.C., Wisse, L.J., Azhar, M., Doetschman, T., Poelmann, R.E., and Gittenberger-de Groot, A.C. 2002. Altered apoptosis pattern during pharyngeal arch artery remodelling is associated with aortic arch malformations in Tgfbeta2 knock-out mice. *Cardiovasc Res* **56**(2): 312-322.

Monet, M., Domenga, V., Lemaire, B., Souilhol, C., Langa, F., Babinet, C., Gridley, T., Tournier-Lasserve, E., Cohen-Tannoudji, M., and Joutel, A. 2007. The archetypal R90C CADASIL-NOTCH3 mutation retains NOTCH3 function in vivo. *Hum Mol Genet* **16**(8): 982-992.

Muller, N., Reinacher-Schick, A., Baldus, S., van Hengel, J., Berx, G., Baar, A., van Roy, F., Schmiegel, W., and Schwarte-Waldhoff, I. 2002. Smad4 induces the tumor suppressor E-cadherin and P-cadherin in colon carcinoma cells. *Oncogene* **21**(39): 6049-6058.

Mumm, J.S. and Kopan, R. 2000. Notch signaling: from the outside in. *Dev Biol* **228**(2): 151-165.

Murakami, D., Okamoto, I., Nagano, O., Kawano, Y., Tomita, T., Iwatsubo, T., De Strooper, B., Yumoto, E., and Saya, H. 2003. Presenilin-dependent gamma-secretase activity mediates the intramembranous cleavage of CD44. *Oncogene* **22**(10): 1511-1516.

Murray, S.A., Oram, K.F., and Gridley, T. 2007. Multiple functions of Snail family genes during palate development in mice. *Development* **134**(9): 1789-1797.

Nakagawa, O., Nakagawa, M., Richardson, J.A., Olson, E.N., and Srivastava, D. 1999. HRT1, HRT2, and HRT3: a new subclass of bHLH transcription factors marking specific cardiac, somitic, and pharyngeal arch segments. *Dev Biol* **216**(1): 72-84.

Nakao, A., Afrakhte, M., Moren, A., Nakayama, T., Christian, J.L., Heuchel, R., Itoh, S., Kawabata, M., Heldin, N.E., Heldin, C.H., and ten Dijke, P. 1997a. Identification of Smad7, a TGFbeta-inducible antagonist of TGF-beta signalling. *Nature* **389**(6651): 631-635.

Nakao, A., Imamura, T., Souchelnytskyi, S., Kawabata, M., Ishisaki, A., Oeda, E., Tamaki, K., Hanai, J., Heldin, C.H., Miyazono, K., and ten Dijke, P. 1997b. TGF-beta receptor-mediated signalling through Smad2, Smad3 and Smad4. *Embo J* **16**(17): 5353-5362.

Nakao, A., Roijer, E., Imamura, T., Souchelnytskyi, S., Stenman, G., Heldin, C.H., and ten Dijke, P. 1997c. Identification of Smad2, a human Mad-related protein in the transforming growth factor beta signaling pathway. *J Biol Chem* **272**(5): 2896-2900.

Nam, Y., Sliz, P., Song, L., Aster, J.C., and Blacklow, S.C. 2006. Structural basis for cooperativity in recruitment of MAML coactivators to Notch transcription complexes. *Cell* **124**(5): 973-983.

Nam, Y., Weng, A.P., Aster, J.C., and Blacklow, S.C. 2003. Structural requirements for assembly of the CSL.intracellular Notch1.Mastermind-like 1 transcriptional activation complex. *J Biol Chem* **278**(23): 21232-21239.

Ni, C.Y., Murphy, M.P., Golde, T.E., and Carpenter, G. 2001. gamma -Secretase cleavage and nuclear localization of ErbB-4 receptor tyrosine kinase. *Science* **294**(5549): 2179-2181.

Nickoloff, B.J., Osborne, B.A., and Miele, L. 2003. Notch signaling as a therapeutic target in cancer: a new approach to the development of cell fate modifying agents. *Oncogene* **22**(42): 6598-6608.

Nieto, M.A. 2002. The snail superfamily of zinc-finger transcription factors. *Nat Rev Mol Cell Biol* **3**(3): 155-166.

Nieto, M.A., Sargent, M.G., Wilkinson, D.G., and Cooke, J. 1994. Control of cell behavior during vertebrate development by Slug, a zinc finger gene. *Science* **264**(5160): 835-839.

Noseda, M., Fu, Y., Niessen, K., Wong, F., Chang, L., McLean, G., and Karsan, A. 2006. Smooth Muscle {alpha}-Actin Is a Direct Target of Notch/CSL. *Circ Res*.

Noseda, M., McLean, G., Niessen, K., Chang, L., Pollet, I., Montpetit, R., Shahidi, R., Dorovini-Zis, K., Li, L., Beckstead, B., Durand, R.E., Hoodless, P.A., and Karsan, A. 2004. Notch activation results in phenotypic and functional changes consistent with endothelial-to-mesenchymal transformation. *Circ Res* **94**(7): 910-917.

Novak, A., Hsu, S.C., Leung-Hagesteijn, C., Radeva, G., Papkoff, J., Montesano, R., Roskelley, C., Grosschedl, R., and Dedhar, S. 1998. Cell adhesion and the integrin-linked kinase regulate the LEF-1 and beta-catenin signaling pathways. *Proc Natl Acad Sci U S A* **95**(8): 4374-4379.

Nueda, M.L., Baladron, V., Sanchez-Solana, B., Ballesteros, M.A., and Laborda, J. 2007. The EGF-like protein dlk1 inhibits notch signaling and potentiates adipogenesis of mesenchymal cells. *J Mol Biol* **367**(5): 1281-1293.

Oberg, C., Li, J., Pauley, A., Wolf, E., Gurney, M., and Lendahl, U. 2001. The Notch intracellular domain is ubiquitinated and negatively regulated by the mammalian Sel-10 homolog. *J Biol Chem* **276**(38): 35847-35853.

Oka, C., Nakano, T., Wakeham, A., de la Pompa, J.L., Mori, C., Sakai, T., Okazaki, S., Kawaichi, M., Shiota, K., Mak, T.W., and Honjo, T. 1995. Disruption of the mouse RBP-J kappa gene results in early embryonic death. *Development* **121**(10): 3291-3301.

Okochi, M., Steiner, H., Fukumori, A., Tanii, H., Tomita, T., Tanaka, T., Iwatsubo, T., Kudo, T., Takeda, M., and Haass, C. 2002. Presenilins mediate a dual intramembranous gamma-secretase cleavage of Notch-1. *Embo J* **21**(20): 5408-5416.

Ong, C.T., Cheng, H.T., Chang, L.W., Ohtsuka, T., Kageyama, R., Stormo, G.D., and Kopan, R. 2006. Target selectivity of vertebrate notch proteins. Collaboration between discrete domains and CSL-binding site architecture determines activation probability. *J Biol Chem* **281**(8): 5106-5119.

Oram, K.F., Carver, E.A., and Gridley, T. 2003. Slug expression during organogenesis in mice. *Anat Rec A Discov Mol Cell Evol Biol* **271**(1): 189-191.

Peinado, H., Ballestar, E., Esteller, M., and Cano, A. 2004. Snail mediates E-cadherin repression by the recruitment of the Sin3A/histone deacetylase 1 (HDAC1)/HDAC2 complex. *Mol Cell Biol* **24**(1): 306-319.

Peiro, S., Escriva, M., Puig, I., Barbera, M.J., Dave, N., Herranz, N., Larriba, M.J., Takkunen, M., Franci, C., Munoz, A., Virtanen, I., Baulida, J., and Garcia de Herreros, A. 2006. Snail1 transcriptional repressor binds to its own promoter and controls its expression. *Nucleic Acids Res* **34**(7): 2077-2084.

Perez-Moreno, M.A., Locascio, A., Rodrigo, I., Dhondt, G., Portillo, F., Nieto, M.A., and Cano, A. 2001. A new role for E12/E47 in the repression of E-cadherin expression and epithelial-mesenchymal transitions. *J Biol Chem* **276**(29): 27424-27431.

Person, A.D., Klewer, S.E., and Runyan, R.B. 2005. Cell biology of cardiac cushion development. *Int Rev Cytol* **243**: 287-335.

Petcherski, A.G. and Kimble, J. 2000. Mastermind is a putative activator for Notch. *Curr Biol* **10**(13): R471-473.

Pierreux, C.E., Nicolas, F.J., and Hill, C.S. 2000. Transforming growth factor beta-independent shuttling of Smad4 between the cytoplasm and nucleus. *Mol Cell Biol* **20**(23): 9041-9054.

Pingault, V., Bondurand, N., Kuhlbrodt, K., Goerich, D.E., Prehu, M.O., Puliti, A., Herbarth, B., Hermans-Borgmeyer, I., Legius, E., Matthijs, G., Amiel, J., Lyonnet, S., Ceccherini, I., Romeo, G., Smith, J.C., Read, A.P., Wegner, M., and Goossens, M. 1998. SOX10 mutations in patients with Waardenburg-Hirschsprung disease. *Nat Genet* **18**(2): 171-173.

Prandini, M.H., Dreher, I., Bouillot, S., Benkerri, S., Moll, T., and Huber, P. 2005. The human VE-cadherin promoter is subjected to organ-specific regulation and is activated in tumour angiogenesis. *Oncogene* **24**(18): 2992-3001.

Przemeck, G.K., Heinzmann, U., Beckers, J., and Hrabe de Angelis, M. 2003. Node and midline defects are associated with left-right development in Delta1 mutant embryos. *Development* **130**(1): 3-13.

Puffenberger, E.G., Hosoda, K., Washington, S.S., Nakao, K., deWit, D., Yanagisawa, M., and Chakravart, A. 1994. A missense mutation of the endothelin-B receptor gene in multigenic Hirschsprung's disease. *Cell* **79**(7): 1257-1266.

Pursglove, S.E. and Mackay, J.P. 2005. CSL: a notch above the rest. *Int J Biochem Cell Biol* **37**(12): 2472-2477.

Qiu, L., Joazeiro, C., Fang, N., Wang, H.Y., Elly, C., Altman, Y., Fang, D., Hunter, T., and Liu, Y.C. 2000. Recognition and ubiquitination of Notch by Itch, a hect-type E3 ubiquitin ligase. *J Biol Chem* **275**(46): 35734-35737.

Raffin, M., Leong, L.M., Rones, M.S., Sparrow, D., Mohun, T., and Mercola, M. 2000. Subdivision of the cardiac Nkx2.5 expression domain into myogenic and nonmyogenic compartments. *Dev Biol* **218**(2): 326-340.

Ramain, P., Khechumian, K., Seugnet, L., Arbogast, N., Ackermann, C., and Heitzler, P. 2001. Novel Notch alleles reveal a Deltex-dependent pathway repressing neural fate. *Curr Biol* **11**(22): 1729-1738.

Rand, M.D., Grimm, L.M., Artavanis-Tsakonas, S., Patriub, V., Blacklow, S.C., Sklar, J., and Aster, J.C. 2000. Calcium depletion dissociates and activates heterodimeric notch receptors. *Mol Cell Biol* **20**(5): 1825-1835.

Rangarajan, A., Talora, C., Okuyama, R., Nicolas, M., Mammucari, C., Oh, H., Aster, J.C., Krishna, S., Metzger, D., Chambon, P., Miele, L., Aguet, M., Radtke, F., and Dotto, G.P. 2001. Notch signaling is a direct determinant of keratinocyte growth arrest and entry into differentiation. *Embo J* **20**(13): 3427-3436.

Raya, A., Kawakami, Y., Rodriguez-Esteban, C., Buscher, D., Koth, C.M., Itoh, T., Morita, M., Raya, R.M., Dubova, I., Bessa, J.G., de la Pompa, J.L., and Belmonte, J.C. 2003. Notch activity induces Nodal expression and mediates the establishment of left-right asymmetry in vertebrate embryos. *Genes Dev* **17**(10): 1213-1218.

Read, A.P. and Newton, V.E. 1997. Waardenburg syndrome. *J Med Genet* **34**(8): 656-665.

Rebay, I., Fleming, R.J., Fehon, R.G., Cherbas, L., Cherbas, P., and Artavanis-Tsakonas, S. 1991. Specific EGF repeats of Notch mediate interactions with Delta and Serrate: implications for Notch as a multifunctional receptor. *Cell* **67**(4): 687-699.

Redkar, A., Montgomery, M., and Litvin, J. 2001. Fate map of early avian cardiac progenitor cells. *Development* **128**(12): 2269-2279.

Reese, D.E., Mikawa, T., and Bader, D.M. 2002. Development of the coronary vessel system. *Circ Res* **91**(9): 761-768.

Roelen, B.A., Goumans, M.J., van Rooijen, M.A., and Mummery, C.L. 1997a. Differential expression of BMP receptors in early mouse development. *Int J Dev Biol* **41**(4): 541-549.

Roelen, B.A., van Rooijen, M.A., and Mummery, C.L. 1997b. Expression of ALK-1, a type 1 serine/threonine kinase receptor, coincides with sites of vasculogenesis and angiogenesis in early mouse development. *Dev Dyn* **209**(4): 418-430.

Romano, L.A. and Runyan, R.B. 2000. Slug is an essential target of TGFbeta2 signaling in the developing chicken heart. *Dev Biol* **223**(1): 91-102.

Ronchini, C. and Capobianco, A.J. 2001. Induction of cyclin D1 transcription and CDK2 activity by Notch(ic): implication for cell cycle disruption in transformation by Notch(ic). *Mol Cell Biol* **21**(17): 5925-5934.

Rones, M.S., McLaughlin, K.A., Raffin, M., and Mercola, M. 2000. Serrate and Notch specify cell fates in the heart field by suppressing cardiomyogenesis. *Development* **127**(17): 3865-3876.

Rubinson, D.A., Dillon, C.P., Kwiatkowski, A.V., Sievers, C., Yang, L., Kopinja, J., Rooney, D.L., Ihrig, M.M., McManus, M.T., Gertler, F.B., Scott, M.L., and Van Parijs, L. 2003. A lentivirus-based system to functionally silence genes in primary mammalian cells, stem cells and transgenic mice by RNA interference. *Nat Genet* **33**(3): 401-406.

Ruchoux, M.M., Chabriat, H., Bousser, M.G., Baudrimont, M., and Tournier-Lasserve, E. 1994. Presence of ultrastructural arterial lesions in muscle and skin vessels of patients with CADASIL. *Stroke* **25**(11): 2291-2292.

Ruchoux, M.M., Domenga, V., Brulin, P., Maciazek, J., Limol, S., Tournier-Lasserve, E., and Joutel, A. 2003. Transgenic mice expressing mutant Notch3 develop vascular alterations characteristic of cerebral autosomal dominant arteriopathy with subcortical infarcts and leukoencephalopathy. *Am J Pathol* **162**(1): 329-342.

Ruchoux, M.M., Guerouaou, D., Vandenhaute, B., Pruvo, J.P., Vermersch, P., and Leys, D. 1995. Systemic vascular smooth muscle cell impairment in cerebral autosomal dominant arteriopathy with subcortical infarcts and leukoencephalopathy. *Acta Neuropathol (Berl)* **89**(6): 500-512.

Runyan, R.B. and Markwald, R.R. 1983. Invasion of mesenchyme into three-dimensional collagen gels: a regional and temporal analysis of interaction in embryonic heart tissue. *Dev Biol* **95**(1): 108-114.

Rutenberg, J.B., Fischer, A., Jia, H., Gessler, M., Zhong, T.P., and Mercola, M. 2006. Developmental patterning of the cardiac atrioventricular canal by Notch and Hairy-related transcription factors. *Development.*

Saga, Y., Kitajima, S., and Miyagawa-Tomita, S. 2000. Mesp1 expression is the earliest sign of cardiovascular development. *Trends Cardiovasc Med* **10**(8): 345-352.

Saga, Y., Miyagawa-Tomita, S., Takagi, A., Kitajima, S., Miyazaki, J., and Inoue, T. 1999. MesP1 is expressed in the heart precursor cells and required for the formation of a single heart tube. *Development* **126**(15): 3437-3447.

Sakai, D., Suzuki, T., Osumi, N., and Wakamatsu, Y. 2006. Cooperative action of Sox9, Snail2 and PKA signaling in early neural crest development. *Development* **133**(7): 1323-1333.

Sakata, Y., Kamei, C.N., Nakagami, H., Bronson, R., Liao, J.K., and Chin, M.T. 2002. Ventricular septal defect and cardiomyopathy in mice lacking the transcription factor CHF1/Hey2. *Proc Natl Acad Sci U S A* **99**(25): 16197-16202.

Salghetti, S.E., Muratani, M., Wijnen, H., Futcher, B., and Tansey, W.P. 2000. Functional overlap of sequences that activate transcription and signal ubiquitin-mediated proteolysis. *Proc Natl Acad Sci U S A* **97**(7): 3118-3123.

Sanchez-Irizarry, C., Carpenter, A.C., Weng, A.P., Pear, W.S., Aster, J.C., and Blacklow, S.C. 2004. Notch subunit heterodimerization and prevention of ligand-independent proteolytic activation depend, respectively, on a novel domain and the LNR repeats. *Mol Cell Biol* **24**(21): 9265-9273.

Sanchez-Martin, M., Rodriguez-Garcia, A., Perez-Losada, J., Sagrera, A., Read, A.P., and Sanchez-Garcia, I. 2002. SLUG (SNAI2) deletions in patients with Waardenburg disease. *Hum Mol Genet* **11**(25): 3231-3236.

Sanford, L.P., Ormsby, I., Gittenberger-de Groot, A.C., Sariola, H., Friedman, R., Boivin, G.P., Cardell, E.L., and Doetschman, T. 1997. TGFbeta2 knockout mice have multiple developmental defects that are non-overlapping with other TGFbeta knockout phenotypes. *Development* **124**(13): 2659-2670.

Savagner, P., Yamada, K.M., and Thiery, J.P. 1997. The zinc-finger protein slug causes desmosome dissociation, an initial and necessary step for growth factor-induced epithelial-mesenchymal transition. *J Cell Biol* **137**(6): 1403-1419.

Schlange, T., Andree, B., Arnold, H., and Brand, T. 2000. Expression analysis of the chicken homologue of CITED2 during early stages of embryonic development. *Mech Dev* **98**(1-2): 157-160.

Schneider, A., Brand, T., Zweigerdt, R., and Arnold, H. 2000. Targeted disruption of the Nkx3.1 gene in mice results in morphogenetic defects of minor salivary glands: parallels to glandular duct morphogenesis in prostate. *Mech Dev* **95**(1-2): 163-174.

Schroeter, E.H., Kisslinger, J.A., and Kopan, R. 1998. Notch-1 signalling requires ligand-induced proteolytic release of intracellular domain. *Nature* **393**(6683): 382-386.

Schultz-Cherry, S. and Murphy-Ullrich, J.E. 1993. Thrombospondin causes activation of latent transforming growth factor-beta secreted by endothelial cells by a novel mechanism. *J Cell Biol* **122**(4): 923-932.

Sefton, M., Sanchez, S., and Nieto, M.A. 1998. Conserved and divergent roles for members of the Snail family of transcription factors in the chick and mouse embryo. *Development* **125**(16): 3111-3121.

Seki, K., Fujimori, T., Savagner, P., Hata, A., Aikawa, T., Ogata, N., Nabeshima, Y., and Kaechoong, L. 2003. Mouse Snail family transcription repressors regulate chondrocyte, extracellular matrix, type II collagen, and aggrecan. *J Biol Chem* **278**(43): 41862-41870.

Seoane, J., Le, H.V., Shen, L., Anderson, S.A., and Massague, J. 2004. Integration of Smad and forkhead pathways in the control of neuroepithelial and glioblastoma cell proliferation. *Cell* **117**(2): 211-223.

Shi, Y. and Massague, J. 2003. Mechanisms of TGF-beta signaling from cell membrane to the nucleus. *Cell* **113**(6): 685-700.

Shi, Y., Wang, Y.F., Jayaraman, L., Yang, H., Massague, J., and Pavletich, N.P. 1998. Crystal structure of a Smad MH1 domain bound to DNA: insights on DNA binding in TGF-beta signaling. *Cell* **94**(5): 585-594.

Shull, M.M., Ormsby, I., Kier, A.B., Pawlowski, S., Diebold, R.J., Yin, M., Allen, R., Sidman, C., Proetzel, G., Calvin, D., and et al. 1992. Targeted disruption of the mouse transforming growth factor-beta 1 gene results in multifocal inflammatory disease. *Nature* **359**(6397): 693-699.

Singh, M.K., Christoffels, V.M., Dias, J.M., Trowe, M.O., Petry, M., Schuster-Gossler, K., Burger, A., Ericson, J., and Kispert, A. 2005. Tbx20 is essential for cardiac chamber differentiation and repression of Tbx2. *Development* **132**(12): 2697-2707.

Sissman, N.J. 1970. Developmental landmarks in cardiac morphogenesis: comparative chronology. *Am J Cardiol* **25**(2): 141-148.

Six, E., Ndiaye, D., Laabi, Y., Brou, C., Gupta-Rossi, N., Israel, A., and Logeat, F. 2003. The Notch ligand Delta1 is sequentially cleaved by an ADAM protease and gamma-secretase. *Proc Natl Acad Sci U S A* **100**(13): 7638-7643.

Solloway, M.J., Dudley, A.T., Bikoff, E.K., Lyons, K.M., Hogan, B.L., and Robertson, E.J. 1998. Mice lacking Bmp6 function. *Dev Genet* **22**(4): 321-339.

Solloway, M.J. and Robertson, E.J. 1999. Early embryonic lethality in Bmp5;Bmp7 double mutant mice suggests functional redundancy within the 60A subgroup. *Development* **126**(8): 1753-1768.

Souilhol, C., Cormier, S., Tanigaki, K., Babinet, C., and Cohen-Tannoudji, M. 2006. RBP-Jkappa-dependent notch signaling is dispensable for mouse early embryonic development. *Mol Cell Biol* **26**(13): 4769-4774.

Spagnoli, F.M., Cicchini, C., Tripodi, M., and Weiss, M.C. 2000. Inhibition of MMH (Met murine hepatocyte) cell differentiation by TGF(beta) is abrogated by pre-treatment with the heritable differentiation effector FGF1. *J Cell Sci* **113 ( Pt 20)**: 3639-3647.

Spinner, N.B., Colliton, R.P., Crosnier, C., Krantz, I.D., Hadchouel, M., and Meunier-Rotival, M. 2001. Jagged1 mutations in alagille syndrome. *Hum Mutat* **17**(1): 18-33.

Struhl, G. and Greenwald, I. 2001. Presenilin-mediated transmembrane cleavage is required for Notch signal transduction in Drosophila. *Proc Natl Acad Sci U S A* **98**(1): 229-234.

Tam, B.Y. and Philip, A. 1998. Transforming growth factor-beta receptor expression on human skin fibroblasts: dimeric complex formation of type I and type II receptors and identification of glycosyl phosphatidylinositol-anchored transforming growth factor-beta binding proteins. *J Cell Physiol* **176**(3): 553-564.

Tamura, K., Taniguchi, Y., Minoguchi, S., Sakai, T., Tun, T., Furukawa, T., and Honjo, T. 1995. Physical interaction between a novel domain of the receptor Notch and the transcription factor RBP-J kappa/Su(H). *Curr Biol* **5**(12): 1416-1423.

Tan, C., Costello, P., Sanghera, J., Dominguez, D., Baulida, J., de Herreros, A.G., and Dedhar, S. 2001. Inhibition of integrin linked kinase (ILK) suppresses beta-catenin-Lef/Tcf-dependent transcription and expression of the E-cadherin repressor, snail, in APC-/- human colon carcinoma cells. *Oncogene* **20**(1): 133-140.

Tani, S., Kurooka, H., Aoki, T., Hashimoto, N., and Honjo, T. 2001. The N- and C-terminal regions of RBP-J interact with the ankyrin repeats of Notch1 RAMIC to activate transcription. *Nucleic Acids Res* **29**(6): 1373-1380.

Tassabehji, M., Newton, V.E., and Read, A.P. 1994. Waardenburg syndrome type 2 caused by mutations in the human microphthalmia (MITF) gene. *Nat Genet* **8**(3): 251-255.

Tassabehji, M., Read, A.P., Newton, V.E., Harris, R., Balling, R., Gruss, P., and Strachan, T. 1992. Waardenburg's syndrome patients have mutations in the human homologue of the Pax-3 paired box gene. *Nature* **355**(6361): 635-636.

ten Dijke, P., Ichijo, H., Franzen, P., Schulz, P., Saras, J., Toyoshima, H., Heldin, C.H., and Miyazono, K. 1993. Activin receptor-like kinases: a novel subclass of cell-surface receptors with predicted serine/threonine kinase activity. *Oncogene* **8**(10): 2879-2887.

ten Dijke, P., Yamashita, H., Sampath, T.K., Reddi, A.H., Estevez, M., Riddle, D.L., Ichijo, H., Heldin, C.H., and Miyazono, K. 1994. Identification of type I receptors for osteogenic protein-1 and bone morphogenetic protein-4. *J Biol Chem* **269**(25): 16985-16988.

Thomsen, G.H. 1996. Xenopus mothers against decapentaplegic is an embryonic ventralizing agent that acts downstream of the BMP-2/4 receptor. *Development* **122**(8): 2359-2366.

Timmerman, L.A., Grego-Bessa, J., Raya, A., Bertran, E., Perez-Pomares, J.M., Diez, J., Aranda, S., Palomo, S., McCormick, F., Izpisua-Belmonte, J.C., and de la Pompa, J.L. 2004. Notch promotes epithelial-mesenchymal transition during cardiac development and oncogenic transformation. *Genes Dev* **18**(1): 99-115.

Tomita, T., Tanaka, S., Morohashi, Y., and Iwatsubo, T. 2006. Presenilin-dependent intramembrane cleavage of ephrin-B1. *Mol Neurodegener* **1**: 2.

Tsuchida, K., Mathews, L.S., and Vale, W.W. 1993. Cloning and characterization of a transmembrane serine kinase that acts as an activin type I receptor. *Proc Natl Acad Sci U S A* **90**(23): 11242-11246.

Tsuchida, K., Sawchenko, P.E., Nishikawa, S., and Vale, W.W. 1996. Molecular cloning of a novel type I receptor serine/threonine kinase for the TGF beta superfamily from rat brain. *Mol Cell Neurosci* **7**(6): 467-478.

Tsukazaki, T., Chiang, T.A., Davison, A.F., Attisano, L., and Wrana, J.L. 1998. SARA, a FYVE domain protein that recruits Smad2 to the TGFbeta receptor. *Cell* **95**(6): 779-791.

Van Den Akker, N.M., Lie-Venema, H., Maas, S., Eralp, I., DeRuiter, M.C., Poelmann, R.E., and Gittenberger-De Groot, A.C. 2005. Platelet-derived growth factors in the developing avian heart and maturating coronary vasculature. *Dev Dyn* **233**(4): 1579-1588.

Vandewalle, C., Comijn, J., De Craene, B., Vermassen, P., Bruyneel, E., Andersen, H., Tulchinsky, E., Van Roy, F., and Berx, G. 2005. SIP1/ZEB2 induces EMT by repressing genes of different epithelial cell-cell junctions. *Nucleic Acids Res* **33**(20): 6566-6578.

Villa, N., Walker, L., Lindsell, C.E., Gasson, J., Iruela-Arispe, M.L., and Weinmaster, G. 2001. Vascular expression of Notch pathway receptors and ligands is restricted to arterial vessels. *Mech Dev* **108**(1-2): 161-164.

Viragh, S. and Challice, C.E. 1981. The origin of the epicardium and the embryonic myocardial circulation in the mouse. *Anat Rec* **201**(1): 157-168.

Vittet, D., Buchou, T., Schweitzer, A., Dejana, E., and Huber, P. 1997. Targeted null-mutation in the vascular endothelial-cadherin gene impairs the organization of vascular-like structures in embryoid bodies. *Proc Natl Acad Sci U S A* **94**(12): 6273-6278.

Waldo, K.L., Kumiski, D.H., Wallis, K.T., Stadt, H.A., Hutson, M.R., Platt, D.H., and Kirby, M.L. 2001. Conotruncal myocardium arises from a secondary heart field. *Development* **128**(16): 3179-3188.

Wallez, Y., Vilgrain, I., and Huber, P. 2006. Angiogenesis: the VE-cadherin switch. *Trends Cardiovasc Med* **16**(2): 55-59.

Wang, J., Sridurongrit, S., Dudas, M., Thomas, P., Nagy, A., Schneider, M.D., Epstein, J.A., and Kaartinen, V. 2005. Atrioventricular cushion transformation is mediated by ALK2 in the developing mouse heart. *Dev Biol* **286**(1): 299-310.

Wang, W., Prince, C.Z., Mou, Y., and Pollman, M.J. 2002. Notch3 signaling in vascular smooth muscle cells induces c-FLIP expression via ERK/MAPK activation. Resistance to Fas ligand-induced apoptosis. *J Biol Chem* **277**(24): 21723-21729.

Wang, X.F., Lin, H.Y., Ng-Eaton, E., Downward, J., Lodish, H.F., and Weinberg, R.A. 1991. Expression cloning and characterization of the TGF-beta type III receptor. *Cell* **67**(4): 797-805.

Warthen, D.M., Moore, E.C., Kamath, B.M., Morrissette, J.J., Sanchez, P., Piccoli, D.A., Krantz, I.D., and Spinner, N.B. 2006. Jagged1 (JAG1) mutations in Alagille syndrome: increasing the mutation detection rate. *Hum Mutat* **27**(5): 436-443.

Watanabe, Y., Kokubo, H., Miyagawa-Tomita, S., Endo, M., Igarashi, K., Aisaki, K.I., Kanno, J., and Saga, Y. 2006. Activation of Notch1 signaling in cardiogenic mesoderm induces abnormal heart morphogenesis in mouse. *Development* **133**(9): 1625-1634.

Wells, R.G., Gilboa, L., Sun, Y., Liu, X., Henis, Y.I., and Lodish, H.F. 1999. Transforming growth factor-beta induces formation of a dithiothreitol-resistant type I/Type II receptor complex in live cells. *J Biol Chem* **274**(9): 5716-5722.

Wharton, K.A., Johansen, K.M., Xu, T., and Artavanis-Tsakonas, S. 1985. Nucleotide sequence from the neurogenic locus notch implies a gene product that shares homology with proteins containing EGF-like repeats. *Cell* **43**(3 Pt 2): 567-581.

Whelan, J.T., Forbes, S.L., and Bertrand, F.E. 2007. CBF-1 (RBP-Jkappa) binds to the PTEN promoter and regulates PTEN gene expression. *Cell Cycle* **6**(1): 80-84.

Wilkinson, D.G. 1992. *Whole mount in situ hybridization of vertebrate embryos. in situ hybridization: a practical approach* Oxford University Press.

Williams, R., Lendahl, U., and Lardelli, M. 1995. Complementary and combinatorial patterns of Notch gene family expression during early mouse development. *Mech Dev* **53**(3): 357-368.

Willis, S.A., Zimmerman, C.M., Li, L.I., and Mathews, L.S. 1996. Formation and activation by phosphorylation of activin receptor complexes. *Mol Endocrinol* **10**(4): 367-379.

Winnier, G., Blessing, M., Labosky, P.A., and Hogan, B.L. 1995. Bone morphogenetic protein-4 is required for mesoderm formation and patterning in the mouse. *Genes Dev* **9**(17): 2105-2116.

Wu, J.W., Hu, M., Chai, J., Seoane, J., Huse, M., Li, C., Rigotti, D.J., Kyin, S., Muir, T.W., Fairman, R., Massague, J., and Shi, Y. 2001. Crystal structure of a phosphorylated Smad2. Recognition of phosphoserine by the MH2 domain and insights on Smad function in TGF-beta signaling. *Mol Cell* **8**(6): 1277-1289.

Wu, W.S., Heinrichs, S., Xu, D., Garrison, S.P., Zambetti, G.P., Adams, J.M., and Look, A.T. 2005. Slug antagonizes p53-mediated apoptosis of hematopoietic progenitors by repressing puma. *Cell* **123**(4): 641-653.

Xue, Y., Gao, X., Lindsell, C.E., Norton, C.R., Chang, B., Hicks, C., Gendron-Maguire, M., Rand, E.B., Weinmaster, G., and Gridley, T. 1999. Embryonic lethality and vascular defects in mice lacking the Notch ligand Jagged1. *Hum Mol Genet* **8**(5): 723-730.

Yamada, M., Revelli, J.P., Eichele, G., Barron, M., and Schwartz, R.J. 2000. Expression of chick Tbx-2, Tbx-3, and Tbx-5 genes during early heart development: evidence for BMP2 induction of Tbx2. *Dev Biol* **228**(1): 95-105.

Yang, Z., Rayala, S., Nguyen, D., Vadlamudi, R.K., Chen, S., and Kumar, R. 2005. Pak1 phosphorylation of snail, a master regulator of epithelial-to-mesenchyme transition, modulates snail's subcellular localization and functions. *Cancer Res* **65**(8): 3179-3184.

Yingling, J.M., Das, P., Savage, C., Zhang, M., Padgett, R.W., and Wang, X.F. 1996. Mammalian dwarfins are phosphorylated in response to transforming growth factor beta and are implicated in control of cell growth. *Proc Natl Acad Sci U S A* **93**(17): 8940-8944.

Yook, J.I., Li, X.Y., Ota, I., Fearon, E.R., and Weiss, S.J. 2005. Wnt-dependent regulation of the E-cadherin repressor snail. *J Biol Chem* **280**(12): 11740-11748.

Yu, Q. and Stamenkovic, I. 2000. Cell surface-localized matrix metalloproteinase-9 proteolytically activates TGF-beta and promotes tumor invasion and angiogenesis. *Genes Dev* **14**(2): 163-176.

Zavadil, J. and Bottinger, E.P. 2005. TGF-beta and epithelial-to-mesenchymal transitions. *Oncogene* **24**(37): 5764-5774.

Zavadil, J., Cermak, L., Soto-Nieves, N., and Bottinger, E.P. 2004. Integration of TGF-beta/Smad and Jagged1/Notch signalling in epithelial-to-mesenchymal transition. *Embo J* **23**(5): 1155-1165.

Zhang, H. and Bradley, A. 1996. Mice deficient for BMP2 are nonviable and have defects in amnion/chorion and cardiac development. *Development* **122**(10): 2977-2986.

Zhang, Y., Feng, X., We, R., and Derynck, R. 1996. Receptor-associated Mad homologues synergize as effectors of the TGF-beta response. *Nature* **383**(6596): 168-172.

Zhou, B.P., Deng, J., Xia, W., Xu, J., Li, Y.M., Gunduz, M., and Hung, M.C. 2004. Dual regulation of Snail by GSK-3beta-mediated phosphorylation in control of epithelial-mesenchymal transition. *Nat Cell Biol* **6**(10): 931-940.

Zhou, S., Fujimuro, M., Hsieh, J.J., Chen, L., Miyamoto, A., Weinmaster, G., and Hayward, S.D. 2000. SKIP, a CBF1-associated protein, interacts with the ankyrin repeat domain of NotchIC To facilitate NotchIC function. *Mol Cell Biol* **20**(7): 2400-2410.

Zweifel, M.E., Leahy, D.J., Hughson, F.M., and Barrick, D. 2003. Structure and stability of the ankyrin domain of the Drosophila Notch receptor. *Protein Sci* **12**(11): 2622-2632.

APPENDIX

The following are the animal care certificates and human ethical approvals required during this thesis, copyright approvals, and a list of publications I have achieved during my graduate school career. For each publication, I have summarized the major finding and have indicated my contribution to the published data.

Leong KG*, **Niessen K*** (co-first author), Kulic I*, Raouf A, Eaves C, Pollet I, Karsan A. Jagged1-mediated Notch activation induces epithelial-to-mesenchymal transition through Slug-induced repression of E-cadherin. J. Exp. Medicine. In Press.

- This peer-reviewed article identifies Slug and a novel Notch target gene in breast cancer.
- In collaboration with the other two co-first authors, I was involved in generating data for almost every figure in this manuscript. Furthermore this manuscript uses data that was established in this thesis.

**Niessen K**, Karsan A. Notch signaling in the developing cardiovascular system. Am J Physiol Cell Physiol. 2007 Jul;293(1):C1-11. Epub 2007 Mar 21. Review. PMID: 17376817

- This review summarizes the role of the Notch pathway during heart development.
- I wrote this review.

Noseda M*, McLean G*, **Niessen K**, Chang L, Pollet I, Montpetit R, Shahidi R, Dorovini-Zis K, Li L, Beckstead B, Durand RE, Hoodless PA, Karsan A. Notch activation results in phenotypic and functional changes consistent with endothelial-to-mesenchymal transformation. Circ Res. 2004 Apr 16;94(7):910-7. Epub 2004 Feb 26. PMID: 14988227

- This peer-reviewed article demonstrates that Notch induces EndMT, which is the foundation for this thesis.
- I was involved in generated the following data:
  Figure 1C. Activation of the Notch pathway induces EndMT
  Figure 5C and 5D. Notch activates the SMA promoter

Noseda M, **Niessen K**, McLean G, Chang L, Karsan A. Notch-dependent cell cycle arrest is associated with downregulation of minichromosome maintenance proteins. Circ Res. 2005 Jul 22;97(2):102-4. Epub 2005 Jun 23. PMID: 15976316

- This peer-reviewed article demonstrates that Notch induces cell cycle arrest by downregulating the minichromosome maintenance proteins.
- I was involved in generated the following data:
  Figure 1A, 1B, 1C. Activation of the Notch pathway downregualtes MCM2/6

Noseda M, Fu Y, **Niessen K**, Wong F, Chang L, McLean G, Karsan A. Smooth Muscle alpha-actin is a direct target of Notch/CSL. Circ Res. 2006 Jun 23;98(12):1468-70. Epub 2006 Jun 1. PMID: 16741155

- This peer-reviewed article identifies SMA and a novel Notch target gene.
- I was involved in generated the following data:
  Figure 2D. CSL is required for Notch upregulation of SMA

Larrivee B, **Niessen K**, Pollet I, Corbel SY, Long M, Rossi FM, Olive PL, Karsan A. Minimal contribution of marrow-derived endothelial precursors to tumor vasculature. J Immunol. 2005 Sep 1;175(5):2890-9. PMID: 16116175

- This peer-reviewed demonstrates there is minimal contribution of bone marrow-derived cells to tumor vasculature.
- I was mainly involved in unpublished data but did contribute to several of the figures by making cell lines that were used in tumor assays.

*The University of British Columbia*
*Office of Research Services*
*Clinical Research Ethics Board – Room 210, 828 West 10th Avenue, Vancouver, BC V5Z 1L8*

# ETHICS CERTIFICATE OF EXPEDITED APPROVAL: RENEWAL

| PRINCIPAL INVESTIGATOR: | DEPARTMENT: | UBC CREB NUMBER: |
|---|---|---|
| Aly Karsan | | H05-70417 |

**INSTITUTION(S) WHERE RESEARCH WILL BE CARRIED OUT:**

| Institution | Site |
|---|---|
| Children's and Women's Health Centre of BC (incl. Sunny Hill) | Children's and Women's Health Centre of BC (incl. Sunny Hill) |

**Other locations where the research will be conducted:**
N/A

**CO-INVESTIGATOR(S):**
Kyle S. Niessen

**SPONSORING AGENCIES:**
Canadian Institutes of Health Research - "Endothelial to Mesenchymal Transformation"

**PROJECT TITLE:**
Endothelial to Mesenchymal Transformation

**EXPIRY DATE OF THIS APPROVAL: November 6, 2007**

**APPROVAL DATE: November 3, 2006**

CERTIFICATION:
**In respect of clinical trials:**
1. The membership of this Research Ethics Board complies with the membership requirements for Research Ethics Boards defined in Division 5 of the Food and Drug Regulations.
2. The Research Ethics Board carries out its functions in a manner consistent with Good Clinical Practices.
3. This Research Ethics Board has reviewed and approved the clinical trial protocol and informed consent form for the trial which is to be conducted by the qualified investigator named above at the specified clinical trial site. This approval and the views of this Research Ethics Board have been documented in writing.

The Chair of the UBC Clinical Research Ethics Board has reviewed the documentation for the above named project. The research study, as presented in the documentation, was found to be acceptable on ethical grounds for research involving human subjects and was approved for renewal by the UBC Clinical Research Ethics Board.

*Approval of the Clinical Research Ethics Board by one of:*

**Dr. James McCormack,**
**Associate Chair**

| | |
|---|---|
| **Funding Title:** | Breeding: Endothelial to Mesenchymal Transformation |
| **Unfunded title:** | n/a |

The Animal Care Committee has examined and approved the use of animals for the above breeding program.

This certificate is valid for one year from the above approval date provided there is no change in the experimental procedures. Annual review is required by the CCAC and some granting agencies.

**A copy of this certificate must be displayed in your animal facility.**

Office of Research Services and Administration
102, 6190 Agronomy Road, Vancouver, BC V6T 1Z3
Phone: 604-827-5111 Fax: 604-822-5093

THE UNIVERSITY OF BRITISH COLUMBIA

# ANIMAL CARE CERTIFICATE
## BREEDING PROGRAMS

**Application Number:** A06-1559

**Investigator or Course Director:** Aly Karsan

**Department:** Medical Biophysics (BCCA)

**Animals:**

| |
|---|
| Mice Tie1-tTA 200 |
| Mice C57Bl/6J 12 |
| Mice 129 12 |
| Mice Slug-LacZ 440 |
| Mice TetOS-DNMAML-GFP 160 |
| Mice VE-tTA 150 |
| Mice TetOS-LacZ 160 |
| Mice CD1 24 |

**Approval Date: February 9, 2007**

**Funding Sources:**

| | |
|---|---|
| **Funding Agency:** | Canadian Institutes of Health Research |
| **Funding Title:** | Role of Notch Signaling in Endothelial to Mesenchymal Transformation |
| **Funding Agency:** | Heart and Stroke Foundation of B.C. & Yukon |
| **Funding Title:** | Arteriogenesis in Ischemia |
| **Funding Agency:** | Canadian Institutes of Health Research |

THE UNIVERSITY OF BRITISH COLUMBIA

# ANIMAL CARE CERTIFICATE

**Application Number:** A03-0229

**Investigator or Course Director:** Aly Karsan

**Department:** Pathology & Laboratory Medicine

**Animals:** Mice Slug-LacZ +/- 251
Mice 676
Mice C57Bl/6J 127

**Start Date:** **October 1, 2003** **Approval Date:** **December 14, 2006**

**Funding Sources:**

**Funding Agency:** Canadian Institutes of Health Research
**Funding Title:** Endothelial to mesenchymal transformation

**Funding Agency:** Canadian Institutes of Health Research
**Funding Title:** Endothelial to Mesenchymal Transformation

**Unfunded title:** n/a

**The Animal Care Committee has examined and approved the use of animals for the above experimental project.**

**This certificate is valid for one year from the above start or approval date (whichever is later) provided there is no change in the experimental procedures. Annual review is required by the CCAC and some granting agencies.**